



3D printed drug delivery and testing systems – a passing fad or the future?

Seng Han Lim^a, Himanshu Kathuria^a, Justin Jia Yao Tan^a, Lifeng Kang^{b,*}

^a Department of Pharmacy, National University of Singapore, 18 Science Drive 4, Block S4A, Level 3, 117543, Singapore

^b School of Pharmacy, University of Sydney, Pharmacy and Bank Building A15, NSW 2006, Australia

ARTICLE INFO

Article history:

Received 16 December 2017

Received in revised form 12 April 2018

Accepted 12 May 2018

Available online 18 May 2018

Keywords:

Drug delivery system

Dosage form

3D printing

Additive manufacturing

Personalised medicine

in vitro drug testing

ABSTRACT

The US Food and Drug Administration approval of the first 3D printed tablet in 2015 has ignited growing interest in 3D printing, or additive manufacturing (AM), for drug delivery and testing systems. Beyond just a novel method for rapid prototyping, AM provides key advantages over traditional manufacturing of drug delivery and testing systems. These include the ability to fabricate complex geometries to achieve variable drug release kinetics; ease of personalising pharmacotherapy for patient and lowering the cost for fabricating personalised dosages. Furthermore, AM allows fabrication of complex and micron-sized tissue scaffolds and models for drug testing systems that closely resemble *in vivo* conditions. However, there are several limitations such as regulatory concerns that may impede the progression to market. Here, we provide an overview of the advantages of AM drug delivery and testing, as compared to traditional manufacturing techniques. Also, we discuss the key challenges and future directions for AM enabled pharmaceutical applications.

© 2018 Elsevier B.V. All rights reserved.

Contents

1. Introduction	140
2. Classification of AM technologies	140
3. AM for drug delivery systems	142
3.1. Oral solid dosage forms	142
3.1.1. Rapid prototyping and formulation optimisation	142
3.1.2. Improved bioavailability/zero order kinetics	143
3.1.3. Immediate release and intestinal targeted delivery	145
3.1.4. Personalised medicine/multi-drug/multi-function tablet	145
3.1.5. Ease of swallowing	147
3.2. Transdermal patches	149
3.3. Rectal and vaginal delivery	149

Abbreviations: 2PP, 2-photon polymerisation; 3D, 3-dimensional; 4-ASA, 4-amino-salicylic acid; 5-ASA, 5-amino-salicylic acid; ABS, Acrylonitrile butadiene styrene; AM, Additive manufacturing; Apo2L/TRAIL, Tumour necrosis factor related apoptosis-inducing ligand; BCP, Biphasic calcium phosphate; B-Ink™, 52% mPDC, 2.2% Irgacure 819, 0.2% Sudan I & 46% diethyl fumarate; BJ, Binder Jetting; BMP-2, bone morphogenic protein-2; Brushite, dicalcium phosphate dehydrate (CaHPO₄·2H₂O); CAD, Computer aided design; CL, Contact lenses; CLIP, Continuous liquid interface production; CPC paste, 60 wt% α-TCP, 26 wt% calcium hydrogen phosphate, 10 wt% calcium carbonate and 4 wt% precipitated HA, the carrier liquid was prepared from Miglyol 812, Tween 80 and Amphisol A.; Cu₂O, Copper I oxide; CuAAC, Copper-catalyzed azide alkyne cycloaddition; DED, Direct energy deposition; DLP, Digital light processing; DMOG, Dimethylallyl glycine; EHD, Electrohydrodynamic; EVA, Ethylene vinyl acetate; FDM, Fused-deposition-modelling; HA, Hyaluronic acid; HACC, Hydroxypropyltrimethyl ammonium chloride chitosan; HME, Hot melt extrusion; HPC, Hydroxy propyl cellulose; HPMC, Hydroxy propyl methyl cellulose; HPMCAS, Hypromellose acetate succinate; hydroxyapatite, (HA, Ca₅(PO₄)₃OH); INH, Isoniazid; IORT, Intraoperative radiation therapy; IUS, Intrauterine systems; LFX, Levofloxacin; MBG, Mesoporous bioactive glass; MCC, Micro crystalline cellulose; MHDS, Multi-head deposition system; microCLIP, micro-continuous liquid interface production system; MJ, Material Jetting; MN, Microneedles; Monetite, dicalcium phosphate anhydrous (CaHPO₄); MoO₃, Molybdenum trioxide; mPDC, Methacrylated poly(1,12-dodecamethylene citrate); MPS, Microphysiological systems; N3, Azide; OGP, Osteogenic growth peptide; OoC, Organ-on-a-Chip; P25, Anatase; PBF, Powder bed fusion; PCL, Polycaprolactone; PDLA, Poly D-lactic acid; PDLA, Poly D,L-lactic acid; PE, Pneumatic Extrusion; PEG, Poly(ethylene glycol); PEGDA, Poly(ethylene glycol) diacrylate; PEO, Polyethylene oxide; PET, Polyethylene terephthalate; PEU, Poly(ester urea); PG, Propylene glycol; PHBHHx, Poly(3-hydroxybutyrate-co-3-hydroxyhexanoate); PLA, Poly-lactic acid; PLGA, Poly(lactic-co-glycolic acid); PLLA, Poly-L-Lactic acid; PMMA, Poly(methyl methacrylate); PPF, Poly(propylene fumarate); PU, Polyurethane; PVA, Poly vinyl alcohol; PVP, Polyvinylpyrrolidone; RFP, Rifampicin; rhBMP-2, Recombinant-human bone morphogenetic protein 2; SE, Syringe Extrusion; SLA, Stereolithographic apparatus; SLS, Selective laser sintering; SR, Sustained release; Sr-MBG, Strontium-containing mesoporous bioactive glass; TB, Tuberculosis; TCP, Tricalcium phosphate; Ti6Al4V, Titanium Alloy; TiO₂, Titanium dioxide; UV, Ultraviolet; VNC, Vancomycin; α-TCP, Alpha tricalcium phosphate; β-TCP, Beta tricalcium phosphate.

* Corresponding author at: School of Pharmacy, University of Sydney, Pharmacy and Bank Building A15, NSW 2006, Australia.

E-mail address: lifeng.kang@sydney.edu.au (L. Kang).

3.4.	Drug delivery implants	152
3.4.1.	Discs, filaments and surgical patches	152
3.4.2.	Stents	152
3.4.3.	Implants for bone regeneration	153
3.4.4.	Custom brachytherapy applicator	155
4.	AM for drug testing systems	156
4.1.	Ocular	156
4.2.	Nasal	156
4.3.	Respiratory	158
4.4.	Cardiovascular	159
4.5.	Chemotherapy	159
4.6.	Drug transport	159
4.7.	Antimicrobial	159
4.8.	Bioprinting for <i>in vitro</i> drug testing.	159
4.8.1.	Bioprinted organ-on-a-chip models for <i>in vitro</i> drug testing.	161
4.8.2.	Bioprinted cell-laden models for <i>in vitro</i> drug testing.	161
5.	Future directions and challenges	162
5.1.	Material/safety	162
5.2.	Scalability of AM technology.	162
5.3.	AM ecosystem	162
5.4.	Regulatory challenges.	163
5.5.	Cost effectiveness.	163
6.	Conclusion	163
	References.	164

1. Introduction

Unlike traditional manufacturing of subtractive and formative nature, 3-Dimensional (3D) printing, also known as additive manufacturing (AM), fabricates a structure *via* deposition, binding or polymerisation of materials in successive layers until the complete object is created [1]. Since its inception in mid 1980s, the technology has found applications in numerous fields, such as automotive, consumer electronics and healthcare (or medical) industries [2]. While it was first developed for rapid prototyping, the advances in usable material, speed, accuracy and precision of AM has led experts to believe that AM can one day be used for large scale manufacturing [3]. Over the last 15 years, there have been over 100 publications on AM of drug delivery and testing systems, with an increasing amount of research especially in recent years, mainly from United States (US), United Kingdom and China (Fig. 1). The efforts and advances of AM technology in the field of pharmaceuticals has recently culminated with the US Food and Drug Administration (FDA) approval of the world's first AM orodispersible tablet SPRITAM® (Levetiracetam) [4], further supporting the capabilities of AM to improve upon current pharmaceutical dosage forms through complex and customised dosage forms which are not cost-effective or otherwise impossible with traditional manufacturing [5].

There are several differences between traditional manufacturing and AM for pharmaceutical applications. These differences were largely the motivation behind the increased hype in AM and the amount of research for it. As illustrated by Norman et al. [6], some of the key motivations of AM for pharmaceutical applications are product complexity, personalisation and on-demand manufacturing. Firstly, AM is able to fabricate complex geometries to give pharmaceutical products their multiple functions such as a polypill with different drug release kinetics, with a single tablet [7]. Secondly, AM provides an avenue for personalisation, such as the printing of drug eluting implants that contour to the patient's anatomical parts [8], or personalised dosing of narrow therapeutic window medications, e.g., theophylline [9]. Thirdly, the rapid prototyping nature of AM and relatively ease of use meant that fabrication can be performed onsite as proposed by Lim et al. [10] in personalising patient's pharmacotherapy in pharmacy, where pharmacists fabricate the personalised tablets on the spot and dispense them to the patients. Furthermore, AM has been known for its cost efficiency, owing to its potential for low-cost production of small quantities of personalised products (Fig. 2A). The cost of AM is also becoming increasingly competitive, especially for small production runs such as small-sized standard implants, prosthetics

or personalised dosing tablets *etc.* [11]. This low cost is further compounded by the expiry of several key patents of AM technologies. Among them includes stereolithography, fused deposition modelling and selective laser sintering [12].

Despite these key advantages of AM over traditional pharmaceutical manufacturing, the question remains whether AM of pharmaceutical dosage forms and *in vitro* drug testing devices is here to stay in our daily life. Based on Gartner's Hype Cycle, there are 5 different stages for a trend as illustrated in Fig. 2B, with stage 5 the closest to mainstream adoption and stage 1 the furthest. Among all, AM drugs are evaluated as trends on the rise that tend to gather a lot of interest, but mostly only proof of concept or research exists, not usable technology, requiring >10 years before it gets mainstream adoption [13]. Yet, this is hardly surprising as AM drugs can be expected to come under heavy scrutiny by the regulatory authorities [5,11,14–16]. FDA has recently released its Technical Considerations for AM Medical Devices on December 5, 2017, to provide the Agency's initial technical considerations specific to devices using AM technologies [17].

The aim of this review is to firstly, provide a summary and simple classification to the latest AM technologies available. The subsequent 2 sections summarize the potential benefit of AM in drug delivery and testing systems. We also evaluated if the benefits are essential or simply add-ons for the current drug delivery systems and testing devices. Unlike most other reviews that approach this evaluation from the perspective of AM technologies, we have approached this evaluation from the perspective of drug delivery and testing, by first identifying the limitations of current manufacturing or delivery systems and subsequently, evaluating how AM has resolved or mitigated these limitations. The final section delves into future directions and challenges for AM in pharmaceutical applications.

2. Classification of AM technologies

AM was first introduced in the year 1986 by Charles Hull, when he developed and later commercialised the first 3D printer for photo-polymerisation of light sensitive liquid polymers using ultraviolet (UV) laser source [1]. This technology came to be known as Stereolithography Apparatus or (SLA). Subsequently, many other AM technologies came about quickly and in abundance. By the end of 2016, there are >10 different AM technologies in the market and many others are still in development.

In general, the commonly available AM technologies may be classified into 5 broad categories, as illustrated in Fig. 3 [18]. This classification is based, in part, upon the baseline technology, type of machine architecture

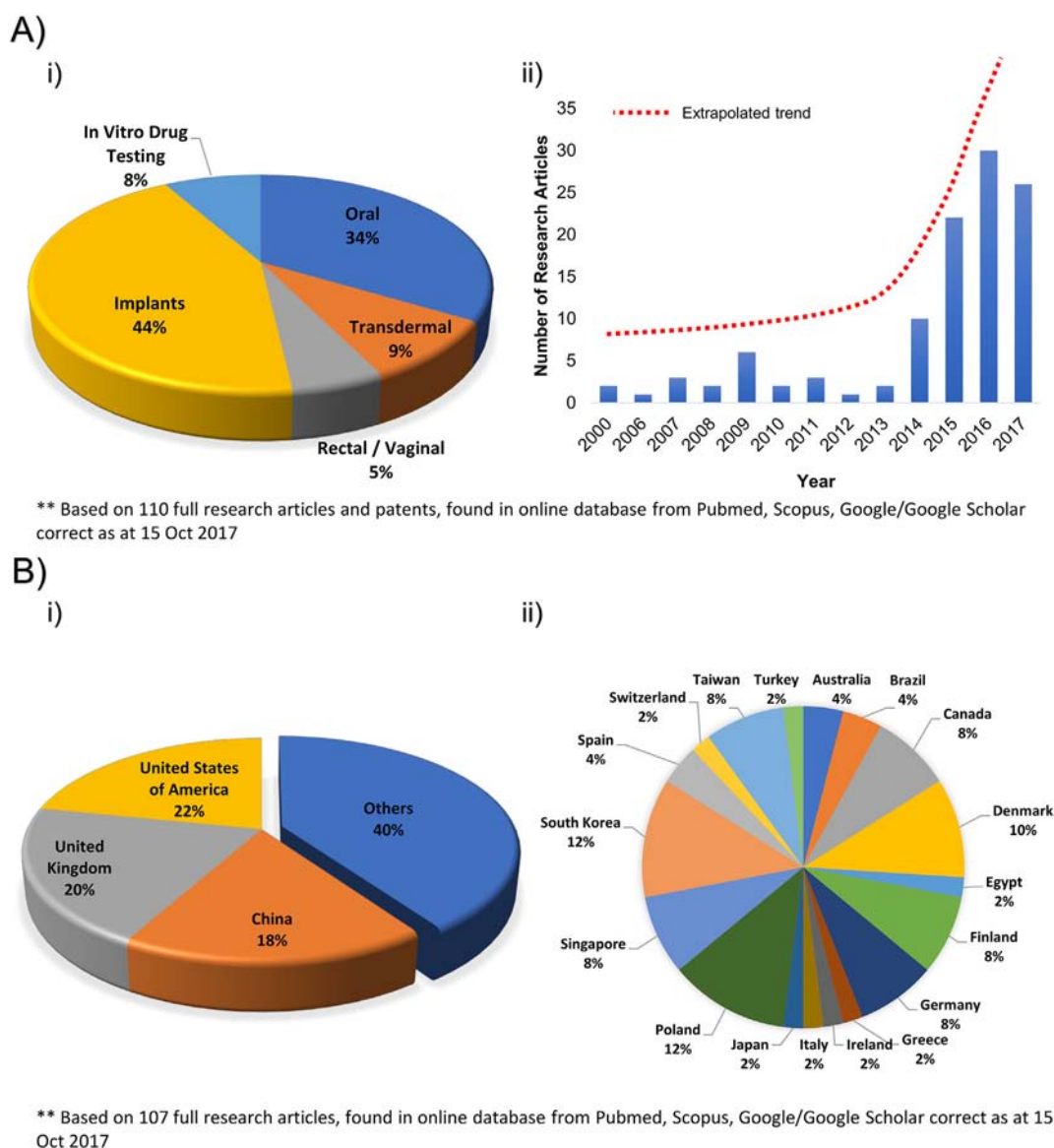


Fig. 1. Trends of AM research for pharmaceutical applications in recent years. Ai) The trend of AM by drug delivery or non-cellular *in vitro* drug testing systems. The largest amount of research in AM drugs come from drug eluting implants and oral solid dosage forms, followed by transdermal, rectal/vaginal dosage forms and lastly, *in vitro* drug testing systems; Aii) Number of research publications in AM for pharmaceutical applications with time. There is an increasing amount of publications for AM drugs, especially in recent years, after the approval of Spritam® by FDA; Bi) Major players in AM research by countries; Bii) Other players in AM research by countries.

and the material transformation physics. The ones with a green tick are those technologies that have been reported for pharmaceutical applications.

Vat polymerisation (VP) in general, is regarded as one of the highest resolution 3D printers, especially for 2-photon polymerisation (2PP) which boast of a resolution in the nanometer range [19]. This high resolution allows fabrication of highly personalised organic shapes critical for implants and transdermal delivery systems, or other complex geometries necessary for controlling drug release kinetics. The drug of interest, depending on its solubility, can be loaded directly into the liquid pre-polymer solution. Depending on the polymer used, various extended or immediate release drug delivery systems can be fabricated. However, the usable material for this technology may be limited due to a requirement for the starting solution to be photo-reactive and photocurable. Furthermore, the use of free radical polymerisation also has a perpetual concern over its safety profile due to potential residual free radicals or monomers and the technique may not be suitable for medications with anti-oxidant properties such as Vitamin A, C and E. In this aspect, biocompatible photo-initiators such as (2-hydroxy-1-[4-(2-hydroxyethoxy)phenyl]-2-methyl-1-propanone (Irgacure® 2959) or monomers such as

methacrylated gelatin (GelMA) have been developed and tested for its safety [20]. Finally, vat polymerisation may also require multiple post curing steps to render it biocompatible. This may result in a loss of drug loaded and subsequent imprecise dosing.

Material extrusion (ME) uses either a high melting point thermoplastic polymer, as in the case of fused-deposition-modelling (FDM) or with a low melting point paste or gel, as in the case of pneumatic or syringe extrusion (PE/SE). Due to the relatively low cost of FDM printers, many researches on oral dosage forms have been conducted using them. However, the key disadvantage of FDM lies in the use of heat which is unsuitable for thermal labile drugs and excipients [21]. Also, the drug loading process may be tedious, either through hot melt extrusion (HME) to extrude both the drug and polymer into a single filament, or through passive loading by submerging the final printed drug delivery system into a drug solution. Pneumatic or syringe extrusions, on the other hand, have been utilised in a series of bioprinters to print cellular materials, critical for organ on a chip or cell laden drug testing systems. It is considered as one of the most biocompatible AM technology for cellular work, as it does not use elevated temperature. Finally, pneumatic or syringe

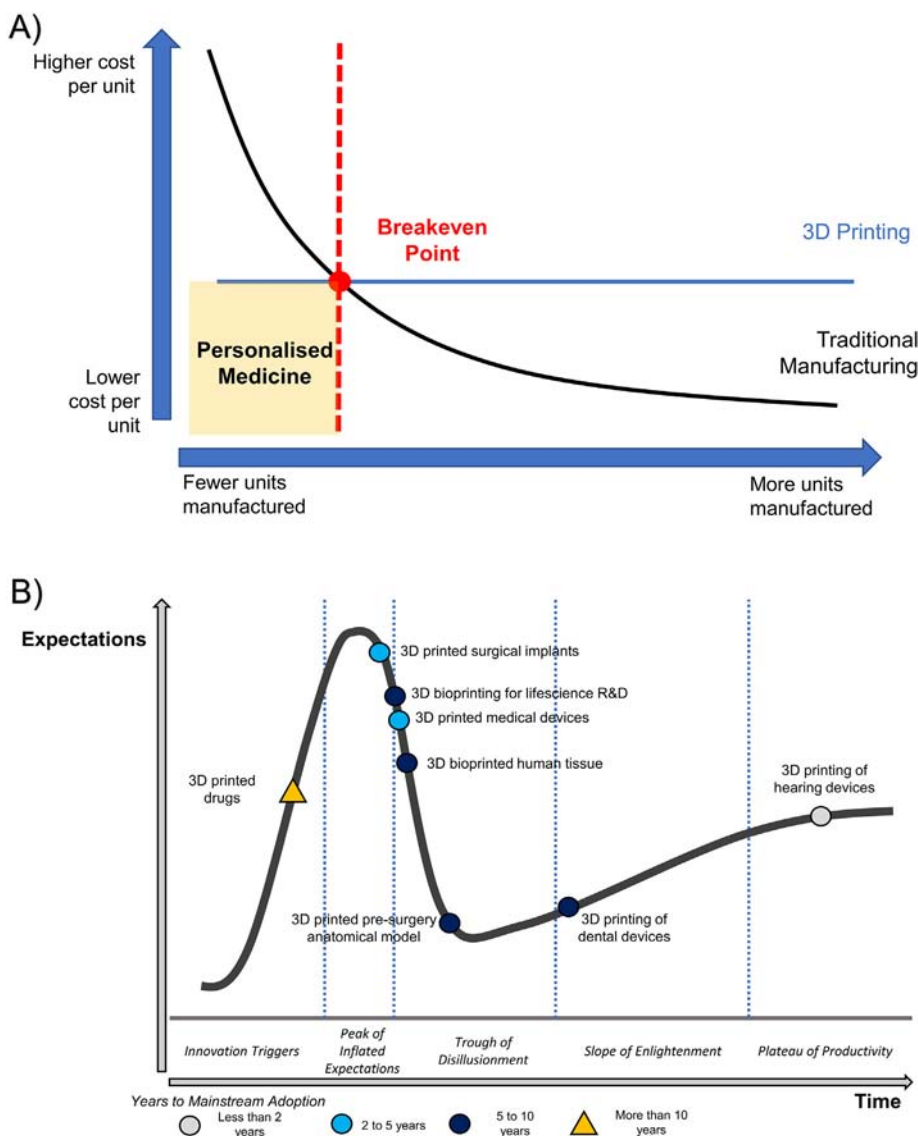


Fig. 2. Current state of AM of drug delivery & testing systems. A) The breakeven analysis comparing traditional manufacturing and AM. AM plays an important role in propelling personalised medicine for public acceptance due to its lower cost, compared to traditional manufacturing. B) A simplified Gartner's Hype Curve for AM, specifically for biomedical related applications. AM drugs are estimated to take >10 years to reach public acceptance and widespread usage. One of the key challenges will be that from the regulatory authorities.

extrusions often uses only a small amount of sample, in the range of 3 to 5 mL, as compared to a few hundred grams for other technologies. This may be helpful especially for the fabrication of drug delivery or testing systems due to the shortage and cost of the key components.

Material jetting (MJ) pushes either the binder liquid or building material at high speed, through very tiny nozzles and deposit them onto a substrate in accordance to the CAD model. The jetting process is controlled by well-established technologies such as thermal jetting or piezoelectric jetting [22]. The nature of the material jetting process allows for different materials to be printed into the same object, depending on the number of print heads available. The jetting of material in specific proportion can be a potential for tuning of the drug composition during the printing process. In the case of binder jetting (BJ), instead of the building material that is jetted, a liquid with binding power is being jetted onto a bed of powder. This forms the basis of numerous research in tablet printing and it is also the only AM technology that has been used in an FDA approved drug product, Spritam®. However, there is a requirement for optimisation of the jetting fluid in terms of drop formation velocity and the fluid viscosity, thereby increasing the complexity of the technology [22].

Powder bed fusion (PBF) and direct energy deposition (DED) are largely similar where both apply a source of high energy onto a powder

bed of building material to join the particles together, in the image defined by the CAD model. PBF utilises a thermal source to induce fusion between powder particles, while DED creates parts by melting material as it is deposited. Both technologies deal primarily with metal material and are therefore less used in pharmaceutical applications.

Typically, the choice of AM technologies depends on the printing materials. For pharmaceutical applications, the product needs to have biocompatibility, safe degradation by-product, good degradation kinetics, sufficient printing resolution and appropriate mechanical strength [23]. Taking these factors together allows one to select the most appropriate material and accordingly, the AM technology.

3. AM for drug delivery systems

3.1. Oral solid dosage forms

3.1.1. Rapid prototyping and formulation optimisation

One of the huge advantages in using AM for oral solid dosage form fabrication, over traditional manufacturing, is the ability for rapid prototyping and quick optimisation of different parameters (Table 1). Many research groups have produced tablets of varying release profiles,

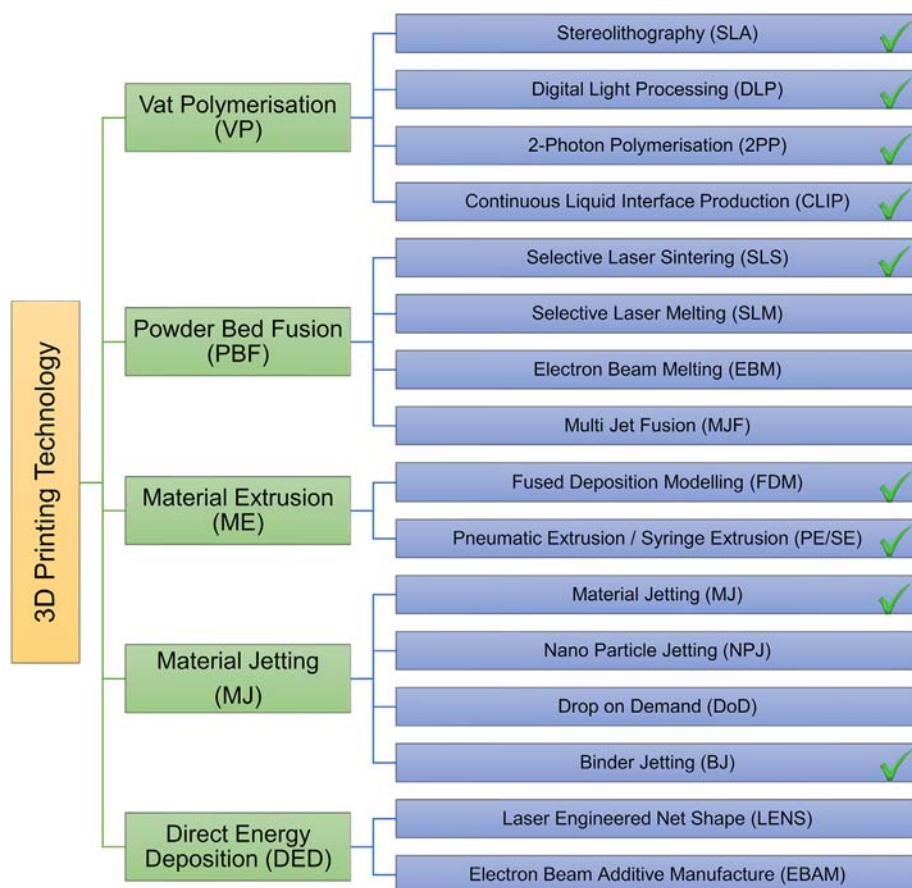


Fig. 3. Different classes of AM technologies. There are 5 main classes of AM technologies beginning with the vat polymerisation, following by powder bed fusion, material extrusion, material jetting and finally direct energy deposition. Each has its unique working principles that may sometimes restrict the type of material available for use in that technology. The green ticks refer to technologies that have been used for pharmaceutical applications either in actual product or in research.

i.e., immediate or sustained or delayed release by varying polymer compositions [24–28], tablet shapes [29], tablet infill densities [30,31] or printing substrates [32]. The ability to fabricate and change complex shapes with a simple amendment in CAD model and the flexibility to change formulation rapidly proved to be an advantage for product development and optimisation (Fig. 4A). This is especially important in personalised medicine, where a specific dosage or formulation may be required in small amounts and the turnover of production line may be swift.

3.1.2. Improved bioavailability/zero order kinetics

Oral solid dosage form such as tablets, capsules, pills, lozenges, troches, pellets or films is the most widely accepted form of medication due to its convenience and the resulting improved patient compliance [33]. However, oral drug delivery can be particularly challenging when considering the variations that occur in the absorption of drug molecules due to potential interactions with the contents/secretions of the gastric intestinal tract, membrane permeability of drug, intestinal transit and gastric emptying [34]. These interactions result in poor bioavailability of oral drugs [35] and variations of the serum/plasma drug level. Often, these fluctuations in drug serum level are the cause of either increased incidences in adverse effects due to supra-therapeutic levels [36]; or loss in efficacy of the drug due to sub-therapeutic levels [37].

One effective way to improve the bioavailability of oral drugs is to increase the gastric residence time of the drug and thereby, improving the absorption [38]. Two of the most common ways of achieving this are the bio/mucoadhesive systems and floating systems [39]. However, the efficiency of bio/mucoadhesive systems can be impaired by constant turnover of the mucus and the system may be adhered to other mucous

membrane such as the oesophagus. In the case of floating system, traditional production either have tedious production or they involve multiple polymers which makes optimisation effort difficult and taxing. Chai et al. [40] illustrated the use of FDM printers to fabricate hydroxypropyl cellulose (HPC) tablets for intragastric floating delivery of domperidone in a low cost and simple method (Table 2). The floating capabilities of tablet was achieved by varying the infill density of the printed tablet. The optimized formulation (contain 10% domperidone, with 2 shells and 0% infill) exhibited a sustained release profile and could float for about 10 h *in vitro* and >8 h *in vivo* (rabbits). The relative bioavailability of the printed tablet was $222.49 \pm 62.85\%$ as compared to the commercial tablet.

Other than improving bioavailability, one of the more common applications of AM in pharmaceuticals is the fabrication of sustained or zero-order release kinetics tablets (Table 2). In previous studies, sustained release or uniform delivery of drug has been shown to improve tolerability or reduce incidences of adverse event [41,42]. Yet, as the tablet dissolves into the gastric-intestinal fluid, the surface area to volume ratio changes, resulting in nonlinear drug release kinetics. Utilising the capability of AM to produce complex geometries, Yu et al. [43] and Wang et al. [44] fabricated complex donut shape tablets using BJ and SLA. The donut shape tablet provides a stable, sustained release rate of drug by keeping a constant effective drug release surface area to volume ratio. In a similar attempt by Lim et al. [10], an acrylonitrile butadiene styrene (ABS) scaffold containing carbamazepine was fabricated through FDM (Fig. 4B). Each of the scaffolds contains small holes for drug release, while the remaining of the scaffold remains impermeable to the drug release. As the ABS remains relatively stable throughout the dissolution, the effective surface area for drug release

Table 1
AM oral dosage forms for rapid prototyping and optimisation.

Application	Drug	Drug loading	3D printer	Material	Author
Free form ability demonstrates effectiveness for rapid prototyping & optimisation					
Photocurable bioink for AM of hydrophilic active drugs, for accurate dosing. Ink was jetted to a preformed tablet	Ropinirole hydro-chloride	Drug mixed in pre-polymer solution	MJ/BJ (MJ-ABP-01-080, MicroFab Technologies)	Norbornene Functionalized Hyaluronic Acid	Acosta-Velez et al., 2017 [27]
UV inkjetted tablet for possible large scale manufacturing	Ropinirole hydro-chloride	Drug mixed in pre-polymer solution	Piezo-activated MJ with UV (Dimatix DMP 2830 inkjet printer)	PEGDA	Clark et al., 2017 [28]
Relationship study between heat and infill densities on drug release for oral tablet	Curcumin	PVA filament was soaked in drug solution	FDM (NinjaBot)	PVA	Tagami et al., 2016 [30]
Novel shapes of tablet for varied drug release (Cube; pyramid; torus; cylinder; sphere)	Paracetamol	Drug mixed with PVA during HME	FDM (MakerBot Replicator 2X Desktop)	PVA	Goyanes et al., 2015 [29]
Customisable release kinetics based on drug loading and composition	Paracetamol/caffeine	Drug mixed with PVA during HME	FDM (MakerBot Replicator 2X)	PVA	Goyanes et al., 2016 [24]
Fully customisable release profile tablet	Orange G (model drug)	Added into pre-polymer	FDM (UP), reverse molding	Polyanhydride (surface eroding); PLA (impermeable protective layer)	Soh & Sun, 2015 [25]
Varying release profile with changes to infill percentages of AM tablets	Fluorescein (Model drug)	PVA filament was soaked in drug solution	FDM (MakerBot Replicator 2 Desktop);	PVA	Goyanes et al., 2014 [31]
Precision patterning of low dose drug with individualised dosing and automated fabrication of medicines	Paracetamol; Theophylline; Caffeine	Drug dissolved in PG-purified water (30:70%)	MJ (Dimatix DMP 2800 inkjet printer)	Drug dissolved in propylene glycol (PG)-purified water (30:70%). 3 different substrate of uncoated paper, coated paper and PET film	Sandler et al., 2011 [32]
Customisable release kinetics based on binder or polymer used for oral tablet	Chlor-pheniramine/Fluorescein	Drug mixed with powder polymer	BJ (Not disclosed)	1) Avicel PH301; Eudragit E-100 2) Avicel PH301; Eudragit RLPO 3) Pharmatose DCL 11; PVP + Tween20	Katstra et al., 2000 [26]
pH based release mechanism tablet; Immediate-extended; Breakaway; Enteric dual pulsatory; Dual pulsatory tablet	Diclofenac	Drug mixed with powder polymer	BJ (Not disclosed)	Multiple pharmaceutical grade polymers	Rowe et al., 2000 [26]

* MJ: Material Jetting; BJ: Binder Jetting; FDM: Fused Deposition Modelling; HME: Hot Melt Extrusion; PVA: Poly Vinyl Alcohol; PEGDA: Polyethylene glycol diacrylate; PLA: Poly Lactic Acid; PET: Poly Ethylene Terephthalate; PVP: Poly Vinyl Pyrrolidone

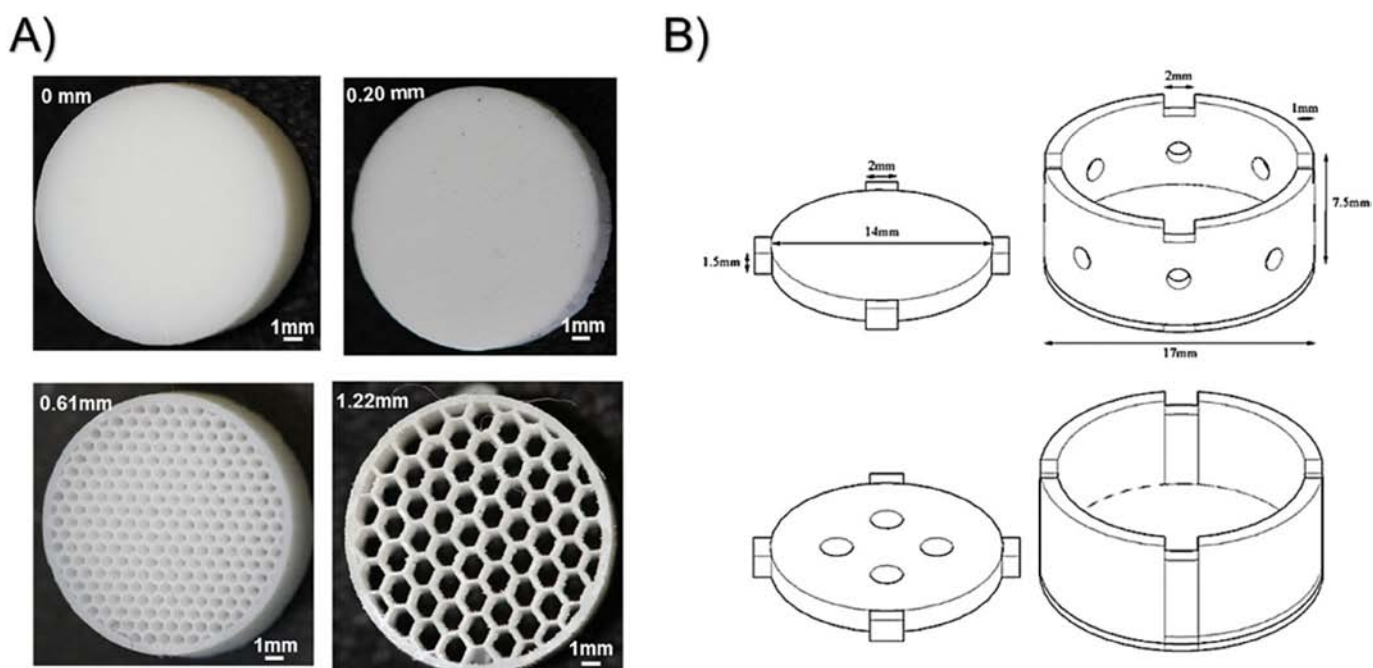


Fig. 4. Rapid prototyping ability of AM to fabricate complex geometries for oral tablets. A) The use of AM to quickly varying the degree of infills of a tablet to achieve controlled and tunable drug release. B) The use of AM to fabricate tablet scaffold with small holes in the body of the tablet to achieve zero order drug release. Adapted from [10,48] with permission.

remains constant and zero-order release kinetics was achieved. Furthermore, the ability to place components at specific location allowed 3D printers to achieve a material gradient in the case of Yu et al. [45]. The matrix tablet, fabricated via a BJ printer, exhibited material gradient in a radial direction coupled with a drug-free release-barrier layer on both the top and bottom layer of the tablet. Using this method, 98% of the drug could be released linearly in 12 h. Poly ethylene glycol (PEG) and poly vinyl alcohol (PVA) can be also be used for sustained drug release, as reported by Hsu et al. [46] and Skowyra et al. [47].

3.1.3. Immediate release and intestinal targeted delivery

Beyond zero order/sustained release kinetics, immediate release oral dosage form is also a common drug release profile (Table 3). This profile is especially suited for medications that require quick onset, such as analgesics. In this aspect, Fina et al. [51], Okwuosa et al. [52] and Sadia et al. [53] fabricated immediate release tablets using selective laser sintering (SLS) and FDM, respectively. For FDM, instead of the commonly available thermoplastics such as polylactic acid (PLA) or ABS, which binds tightly to the active drug, hydrophilic pharmaceutical grade polymers such as polyvinyl pyrrolidone (PVP) and Eudragit EPO were used to allow quick release of the medications upon contact with water.

For drugs which are degraded by gastric acid, an enteric coating is usually applied to the tablet. This allows the tablet to be resistant to acidic pH and will disintegrate and release the drug in alkali environment (Table 3). Using this approach, it also allows a targeted delivery of drugs to the intestinal region, such as the use of budesonide in inflammatory bowel disease, as demonstrated by Goyanes et al. [54]. In a 2-step process, budesonide loaded polyvinyl alcohol caplets were first fabricated using an FDM printer and subsequently coated with a layer of enteric polymer using a bottom

spray fluidised bed coater. This sequential step process produced a modified release budesonide product which demonstrated an absent of drug release in acidic pH and an ~80% of total drug released in alkali pH within 8 h. To simplify this approach further, Goyanes et al. [55] demonstrated the fabrication of paracetamol loaded hypromellose succinate (enteric polymer) tablet in a single step process using FDM. In dissolution, <10% drug release took place in the acidic pH phase; in the intestinal phase, drug release profiles were dependent on the polymer composition of the tablets, the percentage of drug loading and the internal structures. The LG grade of hypromellose succinate generally gave the highest drug release within 8 h in the intestinal phase. Also in a one-step approach using FDM, Okwuosa et al. [56] illustrated the use of a dual nozzle FDM in fabricating an enteric methacrylic polymer shell encapsulating a PVP core, previously loaded with theophylline, budesonide and diclofenac sodium. This shell-core tablet demonstrated sufficient resistant of the tablet in acidic pH and only releasing the drugs in an alkali pH, with total drug release >80% for all 3 drugs within 8 h. All the above studies are clear evidence of the capabilities of AM in fabricating tablets with drug targeted for intestinal release.

3.1.4. Personalised medicine/multi-drug/multi-function tablet

For drug dosing, there will be variations in drug efficacy or adverse events for each individual. These variations could be attributed to inter-individual differences in drug metabolism or absorption profiles [57]. Yet, current mass manufacturing of oral dosage form via traditional powder compaction offers no cost-effective means to meet the challenges of personalised therapeutic regimes for individuals [58]. In addition, with the use of multiple medications to control complex diseases becoming a common phenomenon, the inconvenience of consuming numerous tablets poses a polypharmacy pill burden, leading to an increased risk of

Table 2

AM oral dosage forms for intragastric floating tablet & sustained release tablet.

Application	Drug	Drug loading	3D Printer	Material	Author
Increase bioavailability Intragastric floating tablet, for extended release; Increased bioavailability	Domperidone	HME for preparing drug loaded filament	FDM (MakerBot Replicator 2X)	HPC	Chai et al., 2017 [40]
Reduce fluctuations in drug serum/plasma level Controlled and tunable drug release with bespoke complex geometries tablet	Fenofibrate	Incorporated into melted beeswax at 90 °C with magnetic stirrer	MJ (Dimatix DMP 2800 inkjet printer)	Beeswax	Kyobula et al., 2017 [48]
Scaffold (cap and body) with varying hole sizes on body; zero order release kinetics tablet	Carbamazepine	Commercial tablet was grounded to load into scaffold	FDM (Da Vinci 1.0)	ABS	Lim et al., 2016 [10]
Torus shaped tablet; modified release; Customisable	4-ASA; paracetamol	Drug mixed with pre-polymer solution	SLA (form 1+)	PEGDA; PEG	Wang et al., 2016 [44]
Controlled release tablet	Acetaminophen	HME for preparing drug loaded filament	FDM (Prusa i3)	(HPC; Eudragit L100; HPMC)	Zhang et al., 2016 [49]
Controllable release kinetics tablet	Naproxen	Drug mixed with PEG	MJ (custom made)	PEG	Hsu et al., 2015 [46]
Donut shaped; zero order release kinetics tablet	Paracetamol	Drug mixed with powder polymer	BJ (Shanghai Folichif Co., Ltd)	HPMC; Ethyl cellulose	Yu et al., 2008 [43]
Tablet with material gradient; zero order release kinetics	Paracetamol	Drug mixed with powder polymer	BJ (Shanghai Folichif Co., Ltd)	Ethylcellulose; Sodium lauryl sulfate; Stearic acid; Eudragit RS-100	Yu et al., 2006 [45]
Customisable; extended release tablet	Prednisolone	PVA filament was soaked in drug solution	FDM (MakerBot Replicator 2X Experimental)	PVA	Skowyra et al., 2014 [47]
Modified release tablet (thermal degradation of 4-ASA)	5-ASA; 4-ASA	PVA filament was soaked in drug solution	FDM (MakerBot Replicator 2 Desktop);	PVA	Goyanes et al., 2014 [50]

* MJ: Material Jetting; BJ: Binder Jetting; SLA: Stereolithographic Apparatus; FDM: Fused Deposition Modelling; HME: Hot Melt Extrusion; PVA: Poly Vinyl Alcohol; PEGDA: Poly Ethylene Glycol Diacrylate; PEG: Poly Ethylene Glycol; 4-ASA: 4-amino-salicylic acid; 5-ASA: 5-amino salicylic acid; HPMC: Hydroxy Propyl Methyl Cellulose; HPC: Hydroxy Propyl Cellulose; ABS: Acrylonitrile Butadiene Styrene

Table 3
AM oral dosage forms for immediate/intestinal release of drugs.

Application	Drug	Drug loading	3D printer	Material	Author
Shortens time to onset of action Immediate/modified release tablet	Paracetamol	Drug mixed with powder polymer	SLS (Sintratec Kit)	Kollocoat IR; eudragit L100–55; ethyl acrylate copolymer	Fina et al., 2017 [51]
Immediate release tablet	Di-pyridamole; Theo-phylline	HME for preparing drug loaded filament	FDM, 110 °C, (MakerBot Replicator 2X Experimental)	PVP + talc	Okwuosa et al., 2016 [52]
Immediate release tablet	5-ASA captopril; theo-phylline; pred-nisolone	HME for preparing drug loaded filament	FDM (MakerBot Replicator 2X)	Eudragit EPO; microcrystalline cellulose; talc; tri-calcium phosphate, in various ratio	Sadia et al., 2016 [53]
Prevents degradation of drugs sensitive to acidic pH Enteric coated, controlled release caplet	Budesonide	HME for preparing drug loaded filament; fluid bed processing for enteric coating	FDM (MakerBot Replicator 2X Desktop); Fluid bed for enteric coating	PVA	Goyanes et al., 2015 [54]
Modified release enteric tablet	Paracetamol	HME for preparing drug loaded filament	FDM (MakerBot Replicator 2X)	HPMCAS LG, HPMCAS MG and HPMCAS HG; magnesium stearate; methylparaben NF grade	Goyanes et al., 2017 [55]
Shell-core delayed release tablet targeted for small intestine release	Theophylline; Budesonide; diclofenac sodium	HME for preparing drug loaded filament	FDM (not disclosed), multi-nozzle	Eudragit L (enteric shell); PVP (core)	Okwuosa et al., 2017 [56]

* SLS: Selective laser sintering; FDM: Fused Deposition Modelling; HME: Hot Melt Extrusion; PVA: Poly Vinyl Alcohol; PVP: Poly Vinyl Pyrrolidone; HPMCAS: Hypromellose Acetate Succinate; 5-ASA: 5-Amino Salicylic Acid.

medication errors and poor patient compliance. Therefore, combining multiple medications, with personalised dosing into one single tablet with suitable dosing and release profile will be an attractive alternative for the healthcare systems around the world.

In the aspect of fabricating multi-drug tablet, the capability of AM to produce specific geometries allows the compartmentalisation of incompatible drugs into different regions of a single tablet. Different mixtures of excipients/polymers can be incorporated into specific regions of the tablet to achieve customised drug release profiles (Table 4). Using a pneumatic extrusion (PE) bioprinter, Khaled et al. [59] demonstrated

the combination of multiple drugs in a single tablet (Fig. 5A). Both immediate and sustained release profiles were achieved when 2 different mixtures of excipients were compartmentalised into a single tablet. Similarly, Khaled et al. [60] demonstrated the use of pneumatic extrusion, to fabricate a single guaifenesin drug compartmentalised into 2 different excipients mixture to produce both an immediate and sustained release of guaifenesin in a single tablet, comparable to that of the commercial tablet. Using an inexpensive FDM printer with dual extrusion nozzles, Goyanes et al. [61] and Li et al. [62] separately fabricated a shell and core tablet with either different drugs or varying contents of

Table 4
AM oral dosage forms for multi-functional/multi drug component tablets.

Application	Drug	Drug loading	3DP printer	Material	Author
Multi-functional/multi drug tablet/personalisation					
Multi-functional tablets loaded with Nano sized carriers	Deflazacort	PCL tablets with Eudragit were soaked with nanocapsules suspension	FDM (MakerBot Replicator 2)	PCL; Eudragit RL100; Mannitol (with or without)	Beck et al., 2017 [63]
Multiple drug in 1 tablet (3 in 1); Immediate/sustained release	Captopril; nifedipine; glipizide	Added into paste	PE (Regen HU), multi-nozzle	Cellulose acetate; D-mannitol; PEG 6000	Khaled et al., 2015 [64]
Multiple drug in 1 tablet (5 in 1); Immediate/sustained release	Aspirin; hydro-chloro-thiazide; pravastatin; atenolol; ramipril	Added into paste	PE (Regen HU), multi-nozzle	Cellulose acetate; D-mannitol; PEG 6000	Khaled et al., 2015 [59]
2 compartment caplets (central core with outer shell different drug); 2 compartment caplet (alternating layers with different drug)	Paracetamol; caffeine	HME for preparing drug loaded filament	FDM, Multi-nozzle, (MakerBot Replicator 2X)	PVA	Goyanes et al., 2015 [61]
Controlled release kinetics, with varying content of drug between core and outer shell (DuoTablet)	Glipizide	HME for preparing drug loaded filament	FDM (Clouovo Delta-MK2), Multi-nozzle	PVA	Li et al., 2017 [62]
Fully customisable release profile tablet	Orange G (model drug)	Added into pre-polymer	FDM (UP), reverse molding	Polyanhydride (surface eroding); PLA (impermeable protective layer)	Soh & Sun, 2015 [25]
Bilayer tablet	Guaifenesin	Drug mixed with powder polymer	PE (Fab@Home), multi-nozzle; room temperature	HPMC + Sodium starch glycolate + MCC (Immediate release); HPMC + polyacrylic acid	Khaled et al., 2013 [60]

* FDM: Fused Deposition Modelling; PE: Pneumatic Extrusion; HME: Hot Melt Extrusion; PVA: Poly Vinyl Alcohol; PVP: Poly Vinyl Pyrrolidone; PLA: Poly Lactic Acid; HPMC: Hydroxy Propyl Methyl Cellulose; MCC: Microcrystalline Cellulose; PEG: Poly Ethylene Glycol; PCL: Polycaprolactone

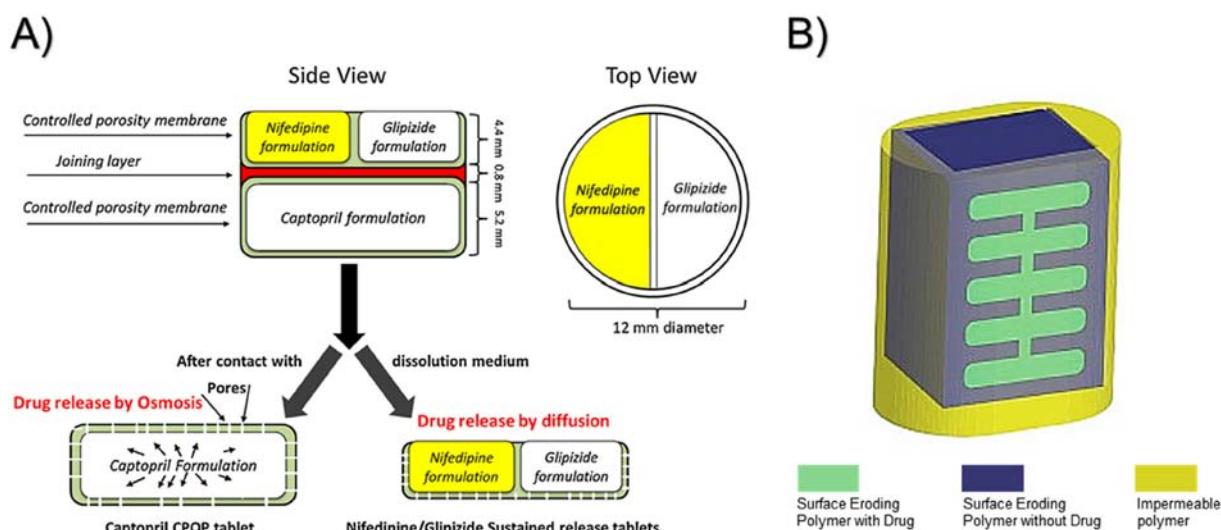


Fig. 5. Schematic structural diagram of multi-drug, multi-function polypill. A) The polypill consists of 3 drugs in 1 tablet. Captopril is embedded within an osmotic formulation for immediate release while nifedipine and glipizide are embedded within the diffusion formulation for sustained release. B) The polypill here illustrates the use of different polymer such as an impermeable polymer to restrict the diffusion surface of drug loaded surface eroding polymer. This helps to control the release profile (pulsating, decreasing release or sustained zero order release) of drugs in the shape as determined by the surface eroding polymer. Adapted from [25,64] with permission.

the same drug between shell and core both made of PVA. Also using FDM, Soh et al. [25] fabricated a series of negative moulds to produce a fully customisable drug release profile tablet using both polyanhydride and PLA (Fig. 5B). Beck et al. [63] combined both AM and nanosized carriers of Deflazacort into a single tablet in a 2-step process to convert nanosuspension into solid drug dosage form for increased stability and improved drug loading.

In addition, Beck et al. [63] also demonstrated the opportunity for tuning of drug composition during the fabrication process. By adjusting the infill density of each printed tablet, the author demonstrated a customisable dose for each of the printed tablet. Alternatively, by changing the size of printed tablet, one can also adjust the dose to be taken. This signify how the dose of a printed tablet can potentially be tuned for personalised dosing, without changing the composition of the starting material and it may be useful for subsequent high throughput development of AM oral solid dosage form.

Together, these evidences have demonstrated the ability of AM to produce multi-functional, multi-drug component oral dosage forms that will be ideal for the aging population and diverse individuals within the healthcare system.

3.1.5. Ease of swallowing

Beyond the technical aspect of pharmaceuticals, in terms of user experience, current oral solid dosage forms can also be difficult to swallow, especially for special populations including the geriatrics [65] and paediatrics [66]. While there are liquid formulations for those who cannot swallow, they have their disadvantages such as strong medicine taste, poor stability of drug, high cost and inconvenience of measuring doses, as compared to oral solid dosage forms. Depending on drug and individual susceptibility, oral liquid dosage form may also cause uncomfortable gastrointestinal irritation and can require frequent dosing [67] as compared to some other dosage forms.

One common way of resolving the difficulties in swallowing is to fabricate tablets that disperses readily in the oral cavity (Table 5). The world's first FDA-approved, AM tablet SPRITAM® was manufactured with the intention of doing so. The mean time to disintegrate in the oral cavity for SPRITAM® was in mere seconds [68], as compared to minutes for traditional orodispersible tablets. This is likely due to the absence of high compression forces in SPRITAM®, as compared to traditional powder compaction tablet press. Yet, this does not compromise the efficacy of SPRITAM® compared to traditional levetiracetam

Table 5
AM oral dosage forms for easy swallowing.

Application	Drug	Drug loading	3D printer	Material	Author
Resolve difficulties in swallowing					
Rapid release of drug from AM orodispersible films	Aripiprazole	HME for preparing drug loaded filament	FDM (ZMorph1 2.0S Personal Fabricator)	PVA	Jamroza et al., 2017 [71]
Fast-melt; porous; quick disintegrating; easy to swallow	Levetiracetam	Patented Formula, FDA approved Spiritam	BJ (Zip Dose® technology)	Patented formula	Boudriau et al., 2016 [69]
Immediate/extended release; easy to swallow design for tablet	Theophylline	HME for preparing drug loaded filament	FDM (MakerBot Replicator 2X Experimental)	Eudragit RL, RS & E; hydroxypropyl cellulose	Pietrzak et al., 2015 [72]
Fast disintegrating tablet	Paracetamol	Drug mixed with powder polymer	BJ (Shanghai Folichif Co., Ltd)	Colloidal silicon dioxide; PVP K30; lactose; D-mannitol; crosslinked PVP	Yu et al., 2009 [70]
Fast disintegrating tablet	Paracetamol	Drug mixed with powder polymer	BJ (Shanghai Folichif Co., Ltd)	Colloidal silicon dioxide; PVP K30; lactose; D-mannitol	Yu et al., 2008 [70]

* FDM: Fused Deposition Modelling; BJ: Binder Jetting; HME: Hot Melt Extrusion; PVA: Poly Vinyl Alcohol; PVP: Poly Vinyl Pyrrolidone

Table 6
AM transdermal patches.

Application	Drug	Drug loading	3D printer	Material	Author
Personalised antimicrobial wound dressing	Copper sulphate; zinc oxide	HME for preparing drug loaded filament	FDM (MakerBot Replicator 2X)	PCL	Muwaffaka et al., 2017 [78]
Acne patch/mask personalised to individual nose	Salicylic acid	Casting/HME for preparing drug loaded filament Drug loaded into pre-polymer solution	FDM (MakerBot Replicator 2X)	PCL	Goyanes et al., 2016 [77]
Microneedle fabricated on a personalised splint for trigger finger	Diclofenac sodium	N/A	SLA (Form 1+) DLP, (Titan 1)	PEGDA 700 and PEG 300 3DM-Cast	Lim et al., 2017 [87]
Varying shape and geometry of microneedle	N/A	N/A	Continuous DLP (custom made)	PEGDA	Ali et al., 2016 [88]
Quick fabrication of mould-independent microneedle; varying geometries	Rhodamine; fluorescein (model drug)	Drug loaded into pre-polymer solution	CLIP (Carbon3D)	PCL trimethacrylate; PEG dimethacrylate; polyacrylic acid	Johnson et al., 2016 [89]
Anticancer agent coated metal microneedle via inkjet printing	5-fluoro-uracil; curcumin; cisplatin	Piezodriven jetting onto microneedle	MJ (Nanoplotter II, with piezodriven dispenser)	Metal microneedle	Uddin et al., 2015 [91]
Antimicrobial coated microneedle	Silver & zinc oxide coating	Pulsed laser deposition	DLP (Perfactory III SXGA +)	Envisiontec GmbH, eShell 200	Gittard et al., 2011 [96]
Antimicrobial loaded microneedle, reverse mould printed	Gentamicin sulfate	Drug loaded into pre-polymer solution	2PP (custom made)	PEGDA 600	Gittard et al., 2010 [93]
AM microneedle for transdermal drug delivery, reverse mould printed	N/A	N/A	2PP (custom made)	Envisiontec GmbH, eShell 200	Gittard et al., 2009 [92]
Extra fine microneedles with tip of nanometer range	N/A	N/A	2PP (custom made)	Ormocer® US-S4	Doraiswamy et al., 2006 [94]

* FDM: Fused Deposition Modelling; SLA: Stereolithographic Apparatus; DLP: Digital Light Processing; 2PP: 2 Photon Polymerisation; MJ: Material Jetting; CLIP: Continuous Liquid Interface Production; PEGDA: Poly Ethylene Glycol Diacrylate; PCL: Polycaprolactone HME: Hot Melt Extrusion; PCL: Polycaprolactone

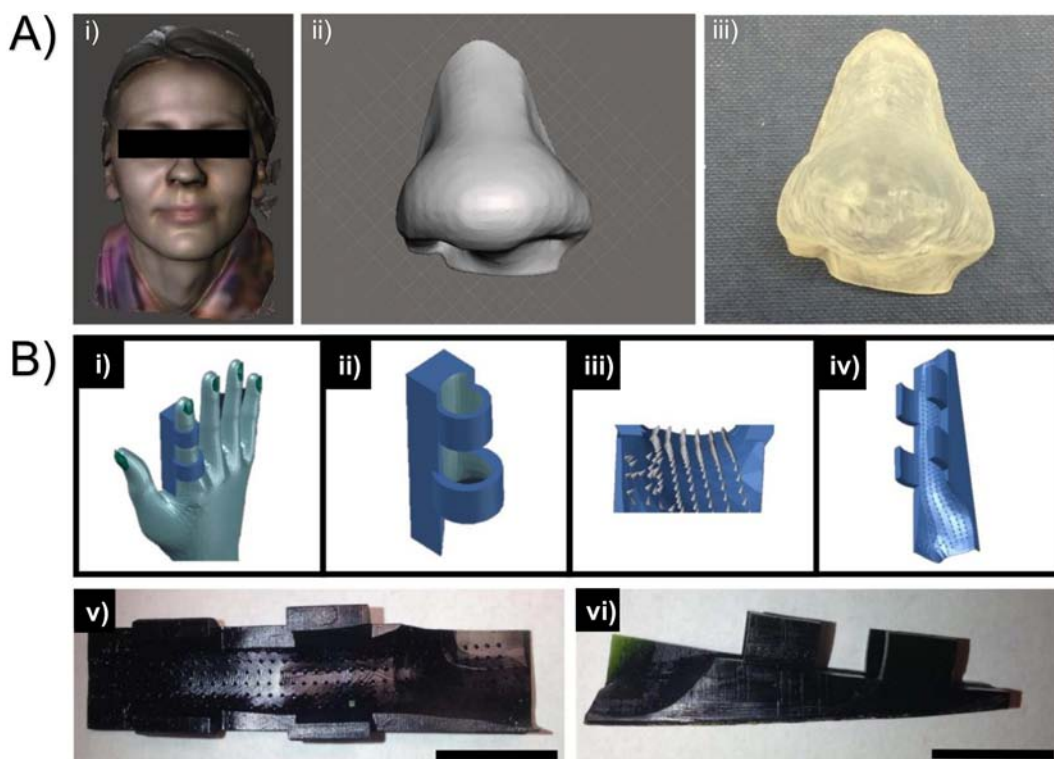


Fig. 6. The Use of 3D scanners for design and fabrication of personalised transdermal drug delivery devices. Ai – iii) images for the design of a personalised transdermal patch with Ai) scanned CAD model of female volunteer, Aii) CAD model of personalised nose patch, Aiii) actual printed nose patch using SLA printer. Bi – vi) images for the design of a personalised, dual- function splint plus microneedle patch. Bi – iv) CAD manipulations to achieve a personalised splint with microneedles placed on the inner surface, Bv – vi) the top and side view of the fabricated microneedle splint using DLP printer. Scale bar = 2 cm.

tablet of the same dose as they both presented with similar pharmacokinetics profiles in human [69]. Similarly, in the case of Yu et al. [70], fast disintegrating paracetamol tablets were fabricated in a similar BJ technology, using a range of pharmaceutical polymers. Other than orodispersible tablet, Jamroza et al. [71] utilised FDM to produce AM orodispersible films. This was achieved using a water soluble thermoplastic PVA that dissolves readily in the oral cavity especially for thin films. Also using FDM, but instead of fabricating orodispersible dosage forms, Pietrzak et al. [72] focused on fabricating capsule-shaped tablet that is usually preferred by patients for the ease of swallow [73]. All these provided evidences on the potential of AM in fabricating easy to swallow tablets or other oral dosage forms.

3.2. Transdermal patches

Delivery of drugs through the skin offers an attractive alternative to oral delivery of drugs due to its advantages such as by-pass of the liver's first pass effect, reduction of pill burden and improved patient compliance [74]. The first transdermal system was developed in 1979, as a 72 h sustained release patch to deliver scopolamine for anti-motion sickness. Between year 2003 and 2007, a new transdermal delivery system is approved every 7.5 months. It is estimated that more than one billion transdermal patches are currently manufactured each year [74].

Most of the current transdermal patches are fabricated as a single layer or multiple layers patch. Several methods of fabrication exist today such as free film or circular Teflon mould-method [75,76]. Yet, these current fabrication methods involve solvent evaporation and multiple steps which are often time consuming. Using SLA, Goyanes et al. [77] fabricated a personalised nose patch containing salicylic acid for acne treatment. While no specific duration was provided in the article, there was no evaporation or long stirring time mentioned and therefore, can be assumed to be of a reasonable duration for the fabrication of the personalised nose patch.

Furthermore, the skin is undulating and curved around the body anatomy such as nose or head. While current transdermal patches are fabricated on a flexible backing layer to allow gentle contouring around the human anatomy, it may not be able to account for precise and complete contouring of the patch around minor contours of the skin. Application of a transdermal patch onto the skin may also require a certain degree of user expertise to ensure no trapped air bubbles between the patch and skin. AM offers an alternative method for fabricating transdermal patch (Table 6). Both Goyanes et al. [77] and Muwaffak et al. [78] utilised a hand-held 3D scanner to obtain a 3D computer aided design (CAD) model of a human volunteer's head and face, before designing a perfectly contouring, patient-specific nose patch. The nose patch was fabricated with either drug loaded polycaprolactone (PCL) using FDM to deliver antimicrobial metal ions such as silver or drug loaded PEGDA using SLA to deliver

anti-acne salicylic acid (Fig. 6A). With a patient specific nose patch, there may potentially be less issues with the application of patch onto skin and may provide a more accurate dosing of drugs through the skin.

In recent years, there is also an increasing interest in the use of microneedles (MN) transdermal patch. MN are three dimensional micromechanical structures which can produce superficial pores in the skin to allow local permeation of big molecules into the skin such as insulin [79–81], melanostatin [82] or erythropoietin [83], which do not usually cross the stratum corneum. Current fabrication techniques of MN, such as etching [84], drawing lithography [85] or micro molding [86] method are unable to fabricate MN onto curved surfaces to account for the undulating skin surfaces. This imperfect contouring of MN patch onto human skin surfaces, may result in improper insertion of MN and potentially a subtherapeutic dosing administered.

To potentially overcome these limitation (Table 6), Lim et al. [87] demonstrated the use of a DLP printer to fabricate a patient specific microneedle patch, using a high resolution castable resin 3DM-Cast (Fig. 6B). The microneedles were fabricated onto a solid substrate, which doubled up as a splint to immobilise the inflamed finger joint or tendons, in the case of trigger finger. Microneedles on a personalised curved surface meant that each microneedle is perpendicular to the skin surface and can fully insert into the skin. The other significant advantage of AM is the ability to change the geometry of microneedle rapidly [88,89]. This allows quick optimisation of material and other parameters of MN which may affect transdermal drug delivery.

Coating of microneedles is also technically challenging especially in terms of depositing a known amount of drug onto the needle [90]. 3D printer with a piezoelectric driven material jetting function allows deposition of specific amount of drug solution onto existing microneedles [91]. Apart from accurate dosing, it also allowed user to retain the superior mechanical strength of existing microneedles such as that of metal microneedles. Using a 2PP printer, which is currently the highest resolution printer, Gittard et al. [92,93] and Doraiswamy et al. [94] demonstrated the fabrication of microneedles, which have extremely fine tip that allows good penetration of skin and potentially cell targeted delivery due to its nanosize [95].

3.3. Rectal and vaginal delivery

In current scenario, various vaginal and rectal delivery systems are used for local as well as systemic delivery. The delivery system includes, but are not limited to, suppositories, pessary, intra uterine devices, surgical meshes, vaginal stents and vaginal dilators. The current approach does not consider the specific anatomy of each patient, patient's medical conditions, age and gender specificity which limit the effective therapy due to poor fit whereas every patient is unique and requires different doses of drugs and hormones. In addition, other factors such as

Table 7
AM vaginal/rectal drug delivery systems (suppositories, pessaries, IUS, surgical).

Delivery device	Drug	Drug loading	3D printer	Material	Author
Suppository & pessary/sustained release, non-dissolving suppository & tunable release.	Lidocaine, ibuprofen sodium, diclofenac sodium, ketoprofen	Mixed with pre-polymer	DLP (Titan 1)	Suppositories/silastic1 Q-4720 & MED-4901 Mould/3DM resin	Sun et al., 2016 [99]
Pessary/patient specific cerclage pessaries	NA	NA	SLA (ProJet 3500 HDMMax)	Silicone (Sylgard 184)	Tudela et al., 2016 [100]
Implants/IUS, surgical meshes, subdermal rod, pessary & extended release (1 week)	Estrogen &/or pro-gesterone	Mixed with PCL for HME	FDM (MakerBot Replicator 5th generation)	PCL	Tappa et al., 2017 [102]
Implants/subcutaneous rods, T-shaped IUS, feedstock material	Indo-methacin	Mixed with EVA for HME	FDM (MakerBot Replicator 2X)	EVA	Genina et al., 2016 [104]
Implants/T-shaped IUS, feedstock material	Indo-methacin	Mixed with PCL for HME	FDM (MakerBot Replicator 2X)	PCL	Hollander et al., 2016 [104,105]

* DLP: Digital Light Processing; SLA: Stereolithography Apparatus; FDM: Fused Deposition Modelling; HME: Hot Melt Extrusion; PCL: Polycaprolactone; EVA: Ethyl Vinyl Acetate; IUS: Intrauterine System

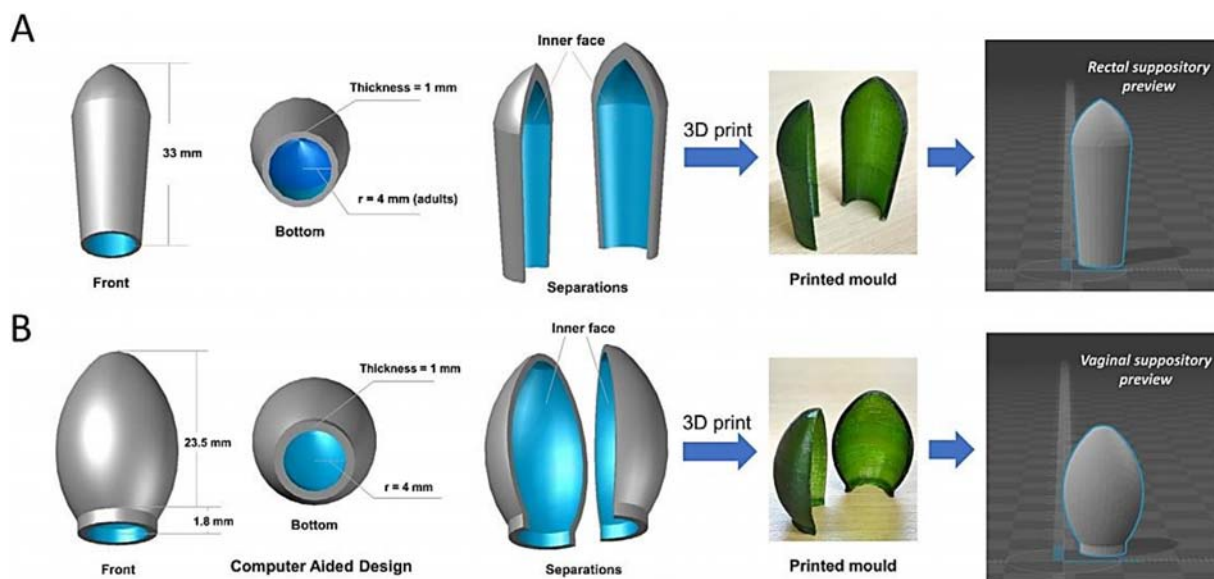


Fig. 7. Computer aided design of suppository moulds. A) Rectal suppository and B) vaginal suppository. Adapted from [99] with permission.

variability in drug absorption related with menstrual cycle, menopause and pregnancy is different among patients. The differences in obstetric and gynaecologic products such as intrauterine devices shapes and dosage concentrations have been known to cause uterine perforations or inflammation due to poor fit of device to patient's vaginal anatomy [97,98]. Therefore, patient-specific/personalised delivery systems are needed to provide personalised shape, size and tailored drug release to improve the efficacy and to increase compliance. The AM delivery system in this regard can provide personalised geometry, snug fit, increase efficacy, improve patient compliance and prevent the post-surgical complications such as hematoma formation after surgery.

Recent developments in AM gave rise to potential solution to the issues pertaining to rectal and vaginal delivery systems. However, to date, very few studies have been reported in this area. The latest development in this field has been briefly summarized in Table 7. Sun et al. has shown the application of DLP 3D printer to prepare moulds of different shape and size made from 3DM Castable resin (Kudo3D Inc., USA) which were later utilised to make non-dissolving suppositories and pessaries of non-dissolving elastic silicone polymer (Silastic Q7-4720 and MED-4901) loaded with anti-inflammatory drugs [99]. The use of elastic polymer can provide a snug fit for rectal or vaginal delivery and allow tailoring of anti-inflammatory drugs release. The use of elastic polymer

Table 8
AM drug delivery implants (bioactive disc and filaments; patch; stents; meshes; discs; catheters).

Delivery device	Drug	Drug loading	3D printer	Material	Author
Drug eluting product/flexible dosing & precision medication.	Nitrofurantoin	Mixed with PLA & metolose for HME	FDM, MakerBot Replicator 2 (USA)	PLA & metolose(R)	Boetker et al., 2016 [111]
Drug-eluting product/drug-loaded feedstock materials	Nitrofurantoin	Mixed with PLA for HME	FDM, MakerBot Replicator 2 (USA)	PLA	Water et al., 2015 [112]
Drug-eluting product/biofilm inhibition	Nitrofurantoin	Mixed with PLA for HME	FDM (UP! Plus)	PLA	Sandler et al., 2014 [110]
Drug eluting product/filaments, pellets, catheters, discs, SR	Gentamicin or metho-trexate	Mixed with PLA for HME	FDM, MakerBot Replicator 2X (USA)	PLA	Weisman et al., 2015 [97,103,120]
Patch/SR (5 days), personalised & tailored drug delivery.	Tetracycline HCL	Drug mixed with polymer solution	EHD printing (not stated)	PCL, PVP & PVP-PCL composite	Wang et al., 2017 [118]
Patch/pancreatic cancer xenografts for cancer growth suppression	Fluorouracil	Mixed into molten paste of PCL/PLGA	PE, MHDS (not stated)	PLGA, PCL	Yi et al., 2016 [117]
Vascular stent/patient specific, bioresorbable, compressible & self-expanding.	Intrinsic antioxidant property	NA	MicroCLIP (custom made)	B-Ink™	Van Lith et al., 2016 [121]
Vascular stent/anthelmintic, nanocomposite	Niclosamide, inositol phosphate (IP6)	Mixed with PCL for HME or PCL-graphene composite	FDM (Airwolf HD)	PCL & graphene nanoplatelets	Misra et al., 2017 [122]
Hernia meshes/hernia repair, bioactive mesh	Gentamicin	Mixed with PLA for HME	FDM, (MakerBot Replicator 3D)	PLA	Ballard et al., 2017 [119]
Bioactive disc/antibacterial activity	Oleo-gum-resins of <i>Boswellia papyrifera</i> <i>Commiphora myrrha</i> & <i>Styrax benzoin</i>	Mixed gum resins and oxides for HME	FDM (Prusa Mendel-13)	Oleo Gum Resin & nanoparticles of TiO ₂ , P25, MoO ₃ , & Cu ₂ O	Horst et al., 2017 [123]

* FDM: Fused Deposition Modelling; CLIP: Continuous Liquid Interface Production; EHD: Electro Hydro Dynamic; MHDS: Multiple Head Deposition System; HME: Hot Melt Extrusion; PLA: Polylactic acid; PLGA: Polylactic co-glycolic acid; PVP: Polyvinylpyrrolidone; PCL: Polycaprolactone; B-Ink™: 52% mPDC, 2.2% Irgacure 819, 0.2% Sudan I & 46% diethyl fumarate

Table 9
AM drug eluting implants/scaffolds for bone regeneration & related infections.

Delivery device/features	Drug	Drug loading	3D printer	Material	Author
Drug eluting implant/slow release	INH	Mixed in binding solution	BJ (Fochif Mechatronics Technique Co. Ltd)	PLLA	Wu et al., 2014 [128]
Drug eluting implant/distinct bi-modal, or pulsed release profile	LFX	Mixed in binding solution	BJ (Fochif Mechatronics Technique Co. Ltd)	PLLA	Huang et al., 2007 [125]
Multi-drug implant/sustained & programmed drug release, multi drug, chronic osteomyelitis	LFX & tobramycin	Mixed in binding solution	BJ (Fochif Mechatronics Technique Co. Ltd)	PDLLA	Wu et al., 2016 [127]
Multi-drug implant/sustained & programmed drug release, multi drug, bone TB	INH & RFP	Mixed in binding solution	BJ (Fochif Mechatronics Technique Co. Ltd)	PDLLA	Wu et al., 2009 [8]
Multi-drug implant/controlled-release drug implant	LFX & RFP	Mixed in binding solution	BJ (Fochif Mechatronics Technique Co. Ltd)	PLLA	Wu et al., 2009 [126]
Titanium implants/potential drug releasing capabilities	NA	NA	SLM (ProX 200 Production 3DP)	Ti6Al4V	Gulati et al., 2016 [147]
Drug eluting implant/primary & secondary bone cancer, surface composed of nanotubes	Doxorubicin & Apo2L/TRAIL	Drug solution was loaded onto printed parts, under vacuum & later dried.	SLM (ProX 200 production 3DP)	Ti6Al4V	Maher et al., 2017 [148]
Drug eluting implant/bioresorbable, biofilm prevention, accelerated osteoblast cell differentiation	RFP	RFP & PLGA co-precipitate to form nano-composite in the printing solution	MJ (Dimatix Materials Printer, DMP2800)	TiAl6V4, PLGA, BCP nanoparticles	Gu et al., 2012 [149]
Composite scaffold/Guided regeneration	NA	NA	PE, multi-nozzle (custom made)	PCL/PLGA/ β -TCP	Shim et al., 2013 [130]
Composite scaffold/delayed release, bioabsorbable	Radio-labelled rhBMP-2	Printed scaffold soaked in rhBMP-2 loaded microspheres solution	SLA (Viper si2)	PPF/carbonate hydroxyapatite coating, PLGA microspheres	Parry et al. (2017) [132]
Composite scaffold/excellent osteogenesis in the goat.	rhBMP-2	Absorbed into printed scaffold under vacuum	PE, MHDS (TissForm™)	PLGA/TCP	Yu, D. et al., 2008 [131]
Composite scaffold/enhanced regeneration	rhBMP-2	Absorbed into printed scaffold with collagen/gelatin under vacuum	PE, multi-nozzle (custom made)	PCL/PLGA/gelatin or collagen	Shim et al., 2014 [129]
Composite scaffold/Guided regeneration, membrane like scaffold	rhBMP-2	Absorbed into printed scaffold with collagen under vacuum	PE, multi-nozzle (custom made)	PCL/PLGA/ β -TCP	Shim et al., 2014 [129]
Bio-porous scaffold/SR, enhanced osteogenic activity	rhBMP-2	Immobilized on scaffold surface	PE (Korea Institute of Machinery and Materials)	PCL, Dopamine HCl (coating)	Lee et al., 2016 [135]
Functionalised scaffold/peptide functionalized, enhanced osteogenic activity	N3-OGP &/Or N3-BMP-2	Immobilized on PEU using CuAAC click, subsequently HME to make filament	FDM, CartesioW	Propargyl functionalized PEU	Li et al., 2017 [136]
Functionalised scaffold/peptide functionalized, good osteoconductivity & osteointegration	BMP-2	Impregnated on printed scaffold	PE, multi-nozzle (BioScaffolder, GeSiM)	PCL	Jensen et al., 2014 [137]
Complex scaffold/bone defect healing	VEGF	Mixed with alginate or alginate gellan gum to form printing paste	PE, multi-nozzle (BioScaffolder, GeSiM)	CPC paste, alginate, gellan gum	Ahlfeld et al., 2017 [133]
Composite scaffold/chronic osteomyelitis	Tobramycin	Mixed with polymer and melt during printing	PE, multi-nozzle (custom made)	PCL/PLGA	Shim et al., 2015 [150]
Composite scaffold/proposed feasibility for bone repair therapeutics	NA	NA	PE, multi-nozzle (Nano-Plotter NP 2.1, GeSiM)	MBG coated with PHBHHx	Yang et al., 2014 [139]
Composite scaffold/SR, multi-functional, local anticancer & enhanced osteogenic activity, & magnetic hyperthermia	Doxorubicin	Mixed within material	PE, multi-nozzle (3D Bioplotter™ EnvisionTEC)	Fe ₃ O ₄ /MBG/PCL	Zhang et al., 2014 [144]
Composite scaffold/controlled ion release & drug delivery, enhanced mechanical strength	Dexa-methasone	Mixed within material	PE, multi-nozzle (3D Bioplotter™ EnvisionTEC)	Sr-MBG	Zhang et al., 2014 [145]
Composite scaffold/SR (12 week), multi-drug, osteoarticular tuberculosis, functionalized MBG	INH & RFP	Impregnated on printed scaffold	PE, multi-nozzle (3D Bioplotter™ EnvisionTEC)	MBG-COOH/MBG-CH ₃	Zhu et al., 2015 [141,143]
Composite scaffold/SR (12 week), multi-drug, osteoarticular tuberculosis, functionalized MBG	INH & RFP	Mixed within material	PE, multi-nozzle (3D Bioplotter™ EnvisionTEC)	MBG-COOH/MBG-CH ₃	Li et al., 2015 [143]
Composite scaffold/SR (4 week)	DMOG	Mixed within material	PE, multi-nozzle (3D Bioplotter™ EnvisionTEC)	MBG/PHBHHx	Min et al., 2015 [142]
Composite scaffold/controlled release	TGF β 3, small molecule drug Y27632	Embedded in printed scaffold, blended with HA	Low temperature FDM (custom made)	PU/HA	Hung et al., 2016 [134]

* BJ: Binder Jetting; SLM: Selective Laser Melting; MJ: Material Jetting; PE: Pneumatic Extrusion; SLA: Stereolithographic Apparatus; HME: Hot Melt Extrusion; MHDS: Multiple Head Deposition System; RFP: Rifampicin; INH: Isoniazid; LFX: Levofloxacin; Ti6Al4V: Titanium Alloy; PLGA: Poly Lactic Co-Glycolic Acid; BCP: Biphasic Calcium Phosphate; PLLA: Poly L-Lactic Acid; PDLLA: Poly D,L-lactic acid; CuAAC: Copper-Catalyzed Azide Alkyne Cycloaddition; rhBMP-2: Recombinant Bone Morphogenetic Protein-2; OGP: Osteogenic Growth Peptide; INH: Isoniazid; RFP: Rifampicin; DMOG: Dimethylallyl Glycine; MBG: Mesoporous Bioactive Glass; PCL: Polycaprolactone; PLGA: Poly(lactic co-glycolic acid); TCP: Tricalcium Phosphate; PEU: PolyEster Urea; PHBHHx: Poly (3-hydroxybutyrate-co-3-hydroxyhexanoate); Sr: Strontium; PU: Polyurethane; HA: Hyaluronic acid; PPF: Polypropylene Fumarate

also has the potential for other clinical applications such as drug eluting ear plugs. The design and preparation of suppositories has been briefly described in Fig. 7. In a similar approach, Tudela et al. developed a cerclage pessary for prevention of preterm birth [100]. Prenatal ultrasound was used to measure cervical length and radius to 3D print personalised pessaries. Pessary for women, with stress urinary incontinence, to prevent urinary leakage was also developed by a separate group of researchers [101]. In contrast, using a mould free approach, Tappa et al. has demonstrated the fabrication of personalised pessary made of biodegradable PCL and PLA. Various pessaries with different shapes were fabricated, together with IUS, subdermal rods, surgical mesh and discs to deliver hormones [102,103]. Genina, N. et al. and Hollander, J. et al. also demonstrated the fabrication of T-shaped IUS, subcutaneous rods and filaments as feed stock material to produce implants using FDM. Both ethylvinyl acetate (EVA) and PCL demonstrated the sustained release of indomethacin [104,105]. Hakim et al. also demonstrated the fabrication of vaginal stents for paediatric and adolescent population. The design customization was based on CT scan imaging to vary the lengths and widths of stents and dilators [106]. It has potential to deliver antibiotics or hormones, prevent bleeding, provide pain relief and prevent hematoma formation after surgery [107]. Jaklenec, A. et al. has developed a vaccine formulation which in general can be used for delivery through the mucosa either *via* vaginal, rectal, nasal, oral or pulmonary routes [108]. Pouliot, J. et al. has patented the alternative approach/treatment with patient specific drug delivery implants to treat cancer (mouth, anal, cervical, and vaginal) [109].

3.4. Drug delivery implants

Drug delivery implants may include but are not limited to the types of constructs for drug delivery or medical applications, such as composite scaffolds, bone cages, filaments, catheters, stents, intra-uterine devices, meshes and drug eluting devices. In general, currently commercially available implants lack the personalisation of the treatment and consideration of several issues, similar to vaginal delivery, such as anatomical differences, age, genders and disease condition. Moreover, it may compromise the safety and efficacy of therapy due to a lack of personalisation. The advances in AM technologies have promoted the use of drug laden implants (Tables 8, 9, 10).

3.4.1. Discs, filaments and surgical patches

Drug loaded disc implants and filaments are one of the simplest structures for medical applications. Nitrofurantoin loaded disc implants made of biodegradable polymers have been studied by several

researchers (Table 8) [110–112]. Boetker et al. demonstrated that rheology of the molten materials, undissolved particles and amount of methylcellulose can affect the drug release from the implant [111]. Water et al. demonstrated an 85% biofilm reduction over 18 h [110]. In addition, Sandler et al. also demonstrated the inhibition of biofilm colonization to treat recurrent infections [112]. Separately, Weisman has demonstrated the fabrication of drug eluting products, including disc and other implants [97,103,113].

Patches are delivery systems for drugs and cosmetics typically considered for skin and wound care. It could be of various types (Table 8) such as porous patches [114] and microneedle patches [115,116]. However, a surgical patch implant can be an important delivery system to treat internal organs. The patch in this regard can be designed with precise geometry and dose.

The surgical patch as demonstrated by Yi et al. was fabricated into patches of various shape, porosity and layers made from PCL and PLGA (Fig. 8), loaded with fluorouracil. The team demonstrated in a rabbit model that the surgical patch could significantly reduce the size of a pancreatic tumour [117]. Wang et al. also demonstrated the fabrication of biodegradable surgical patches. The tetracycline loaded patch demonstrated a sustained release of drug in *in vitro* conditions for 5 days. This can potentially provide sustained anti-inflammatory and anti-bacterial actions. The team also studied the effect of AM operation parameters such as collector speed, flow rate, working distance and applied voltage on diameter and morphology of fibres to optimize parameters including the patch shape, dimensions and drug release kinetics [118]. Ballard et al. demonstrated the fabrication of biodegradable meshes loaded with Gentamicin to repair hernia which can be tailored based on intraoperative measurements, thus eliminating waste and minimising the unwanted drug exposure to other parts of the body [119]. Tappa et al. fabricated a progesterone loaded surgical meshes for vaginal applications [102,103].

3.4.2. Stents

Stents are devices inserted into the lumen of vessels, such as artery, pulmonary tract, bile duct, etc., to keep the anatomical passage open. The dimensions of stent can drastically differ in different anatomical lumen and some disease conditions. The use of permanent stents, such as metal based stent increases the risk of mechanical damage, intimal hyperplasia and thrombosis [121]. While commercial drug-eluting stents can reduce the restenosis rates, the stent remains a source of inflammation. Furthermore, in cases of diffuse lesions, angiography-based estimation of plaque-free zones is difficult, resulting in an overestimation of vessel diameter, causing over-stenting. To avoid over-stenting

Table 10
AM bioceramics & bone cage for bone regeneration and related infections.

Delivery device/features	Drug	Drug loading	3D printer	Material	Author
Bioceramics/multi-drug, implant associated osteomyelitis	RFP & VNC	Mixed within material	BJ, (Modified ZPrinter® 450)	α-TCP & PMMA	Inzana et al., 2015 [153,154]
Bioceramics & biocomposite/Multi-drug, SR	VNC, ofloxacin & tetracycline	Immersion & vacuum impregnation	BJ, (Z-Corporation)	Hydroxyapatite, brushite, monetite & PLA/PGA	Gbureck et al., 2007 [155]
Bioceramics/controlled release	VNC, rhBMP-2, heparin	Mixed within material	BJ (Multi Jet, Z-Corporation)	Brushite, monetite, Unreacted α/β-TCP, chitosan, HPMC	Vorndran, E. et al. (2010) [152]
Bioceramics/antibacterial & osteogenic activity, nanocomposites	Silver nanoparticle	Mixed in binder solution for injectable paste	PE (custom made, Fraunhofer Institute for Materials Research and Beam Technology, Germany)	β-TCP, graphene oxide	Zhang, Y. et al. (2017) [159]
Combination of bone cage & nanofibrous patch/enhancement of tendon-bone healing	Collagen	Collagen loaded in PLGA solution for electrospinning into nanofibers	FDM (U-Maker) for bone cage; Electrospinning (not stated)	PLA cage & PLGA nanofibers	Chou et al., 2016 [158]
Combination of bone cage & nanofibrous membrane or patch	VNC & ceftazidime	Drug dissolved in PLGA solution before electrospinning	FDM (U-Maker) for bone cage; Electrospinning (not stated)	PLA cage & PLGA nanofibers	Chou et al., 2017 [124]

* BJ: Binder Jetting; PE: Pneumatic Extrusion; FDM: Fused Deposition Modelling; RFP: Rifampicin; VNC: Vancomycin; rhBMP-2: Recombinant Bone Morphogenetic Protein-2; α-TCP: Alpha Tri Calcium Phosphate; PMMA: Poly Methyl Methacrylate; PLA: Poly Lactic Acid; PLGA: Poly Lactic co-Glycolic Acid; HPMC: Hydroxypropyl Methyl Cellulose; PGA: Poly Glycolic Acid

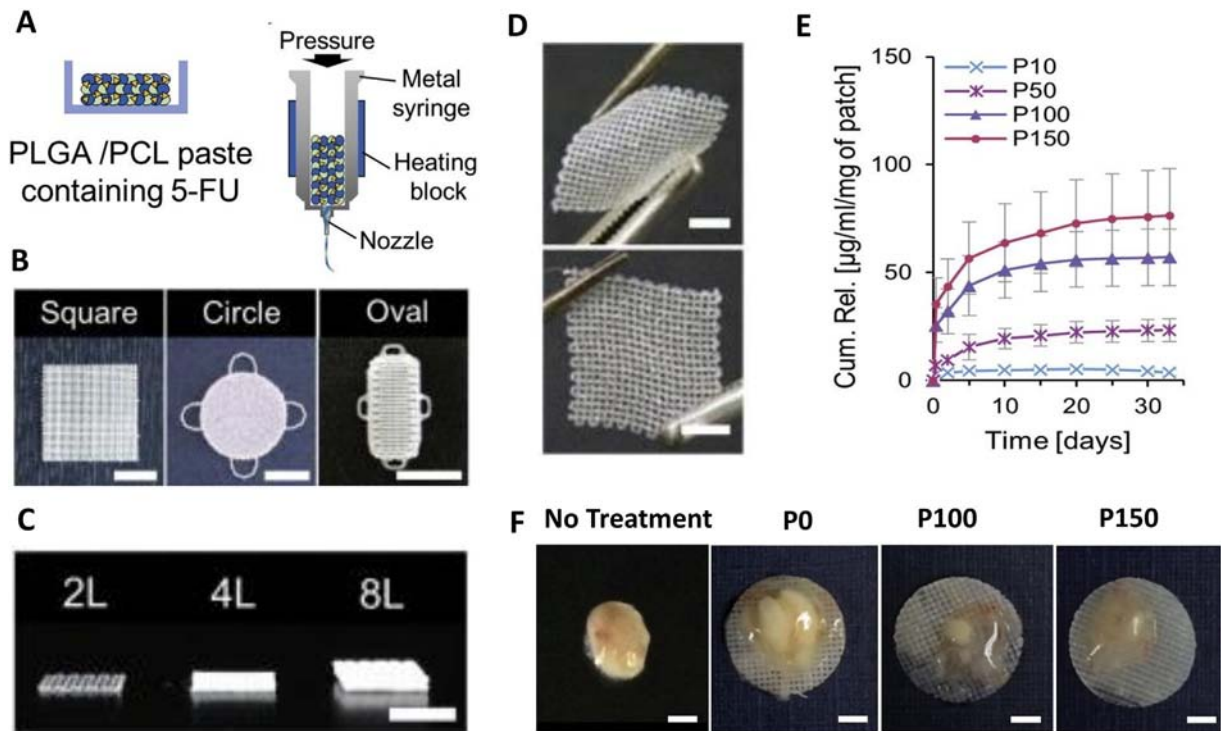


Fig. 8. A) Schematic of drug loaded polymer paste from 3D extrusion deposition system. B) Three shapes of the patches: square without loops; circle and oval shapes with loops on each side for suturing. Scale bar: 5 mm. C) Lattice patches layered 2, 4, and 8 times. Scale bar: 2 mm. D) Photographs presenting the flexible and stretchable properties of the patches. E) Cumulative release profile of patches with increasing drug loading. F) *In vivo* effect of drug loaded patch on pancreatic tumour. Photographs of the excised tumours and the patches at four weeks after implantation. Scale bar: 2 mm. Adapted from [117] with permission.

and provide personalised therapy, an ideal stent should have the following properties: personalised, bio-resorbable, compressible, flexible and drug eluting. Computed tomography imaging can provide a suitable and non-invasive approach to assess lumen anatomy for designing of the personalised stent (Fig. 9).

Van Lith et al. demonstrated the fabrication of a bio-resorbable vascular stent made from polydiolcitrate which shows intrinsic antioxidants property using the microCLIP technology (Table 8) [121]. The team customised AM stents which significantly increased the radial compression strength of pig artery *in vitro*. The stents were compressible and self-expanding *in vitro* within a clinically relevant time frame. Misra et al. also fabricated the vascular stents using PCL and graphene nanoplatelets loaded with niclosamide and inositol phosphate which

could inhibit cell growth (Table 8) [122]. The team demonstrated the feasibility of the customised vascular stent deployment in a porcine model.

3.4.3. Implants for bone regeneration

Each bone has its unique anatomy within the human body, with wide varieties of shape, size and mechanical strength. The size, shape and mechanical strength also differ within age and gender. The associated functional muscles and tendons are also unique for each bone. The treatment becomes further challenging due to anatomical complications in comminute fracture, bone defects and fractures caused by trauma, revision surgeries, infection and bone tumour, and high functional expectations. Therefore, an optimal treatment of bone fracture

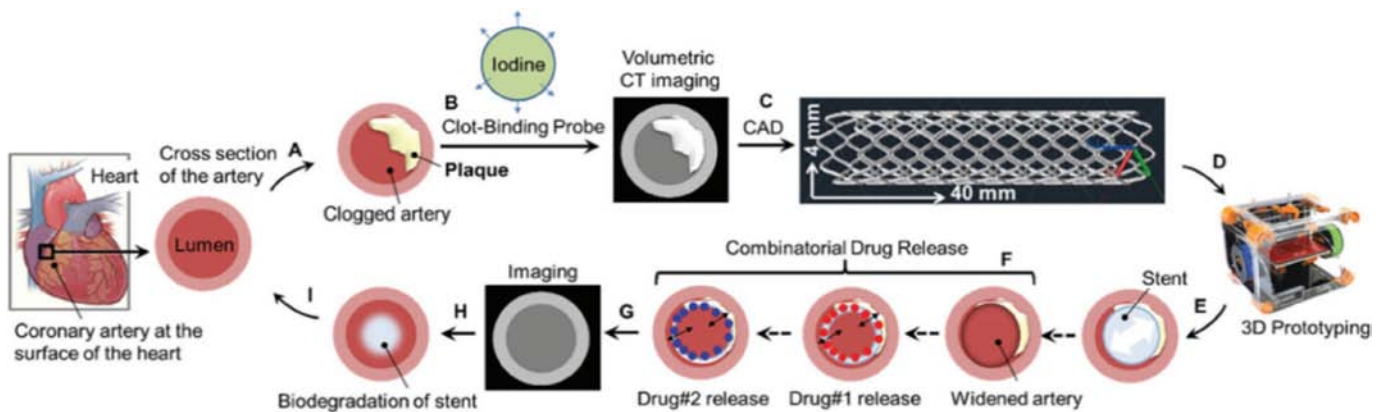


Fig. 9. Stepwise process for developing a personalised 3DP coronary stent. A) Cross-section of the artery shown at the surface of the heart, plaque build-up is shown inside the lumen due to various factors, e.g., aging, diet, genetics; B) a clot-binding probe, i.e., a fibrin targeted iodinated CT contrast probe is administered to locate the blood clot. At the same time, volumetric CT imaging helps to get accurate measurement of the blockage; C) imaging information is transferred to a CAD software to design a personalised stent; D) PCL-GR polymer composite is used for FDM in a 3DP; E) AM stent is placed inside the artery; F) the incorporation of two drugs for sequential release; G) monitoring of healing process by CT imaging; H and I) biodegrading of polymer inside a widened artery. Adapted from [122] with permission.

and bone defects should provide adequate protection to soft tissue, treat possible infections, support surface alignment and enhance bone healing [124].

Currently, bone defects and bone infections are separately treated. Moreover, the bone implants are not customised for each patient. In recent years, the development in AM technologies has facilitated the fabrication of implants with multifunctionalities. In general, recent AM implants for the bone regeneration are composite scaffolds, bioceramics, biocomposites, multidrug implants, bone cage, combination of bone cage and nanofibers membrane. These implants have been utilised to deliver various protein drugs and small molecules (Tables 9, 10).

3.4.3.1. Polymeric implants. Biodegradable polymers such as PCL, PLGA and PLA have been widely used to fabricate polymer implants (Table 9). These polymers typically provide good mechanical strength and aid in sustained drug release. The combinations of polymers, mesoporous bioactive glass (MBG), calcium phosphates, etc., have also been utilised to prepare composite scaffold with improved mechanical strength. In recent years, AM composite scaffolds loaded with antibiotics and proteins have been studied. The delivery of bioactive proteins through delivery device has been a key strategy for effective bone regeneration. However, the stability and integrity of such proteins are often a concern. Delivery of small molecules with specific reference to antibiotics is also necessary to treat infections associated with bones and adjacent soft tissues. However, several process parameters in AM, such as use of heat, organic solvent, or crosslinkers cause reduction in efficacy of the antibiotics. Furthermore, a controlled release of antibiotics is preferred to treat the infections completely, while avoiding side effects.

Huang et al. fabricated polymeric implants of PLLA loaded with levofloxacin (LFX) and demonstrated the *in vitro* bimodal, pulsatile and steady state release of LFX from the implants [125]. Wu et al. also demonstrated the fabrication of PLLA and poly D-lactic acid (PDLA) implants to deliver anti-tubercular and anti-cancer drugs. The team demonstrated the *in vivo* release of drug in rabbit model [8] and a programmed release

of LFX followed by RFP after 8 days for a total duration of 6 weeks [126]. In addition, the team demonstrated the capability of dual therapy, i.e., anti-cancer chemotherapy and pharmacotherapy for chronic osteomyelitis [127]. Besides, Wu et al. also demonstrated the fabrication of PLLA implants for drug delivery [128].

Shim et al. demonstrated the fabrication of rhBMP-2 laden scaffolds utilising a multi-head printer with layer by layer fabrication. This was done in two sequential steps: first polycaprolactone/poly(lactic co-glycolic acid)/beta tri-calcium phosphate (PCL/PLGA/ β -TCP) construct was printed at 135 °C using one head while one of other heads was used to load the rhBMP-2 by filling the gaps on printed layer at 20 °C (Fig. 10A–B) [129,130]. The team reported the enhanced and guided regeneration of the bone in rabbits in separate studies. Yu et al. fabricated a rhBMP-2 loaded composite scaffold made of PLGA/TCP using low temperature 3D printer [131]. The team demonstrated that the scaffold became an active artificial bone with combination of rhBMP-2 and exhibited excellent osteogenesis in goat.

Parry et al. also developed a composite scaffold for enhanced reconstruction of anterior cruciate ligament achieved by delaying the release of rhBMP-2. The scaffold demonstrated a decreased burst release and a delayed release of rhBMP-2 over 32 days. This was achieved through an additive effect of coating on the scaffold with calcium phosphate and loading of PLGA microspheres with encapsulated rhBMP-2 [132]. The team also demonstrated the suitability of graft fixation to maintain pull out strength in *ex vivo* rabbit model. Another composite scaffold was developed by Ahlfeld et al., using AM to plot CPC paste mixed with VEGF-loaded hydrogels. The main component of the scaffold was CPC which provided good mechanical strength and also mimics bone, while the hydrogel strands was important for VEGF delivery. [133]. Hung et al. has also demonstrated the fabrication of composite scaffold based on water-based 3D printable material, polyurethane (PU) and hyaluronic acid (HA). The team demonstrated a sustained and tuneable release of TGF β 3 *in vitro* for 9 days with significant improvement in cartilage repair in rabbit model [134].

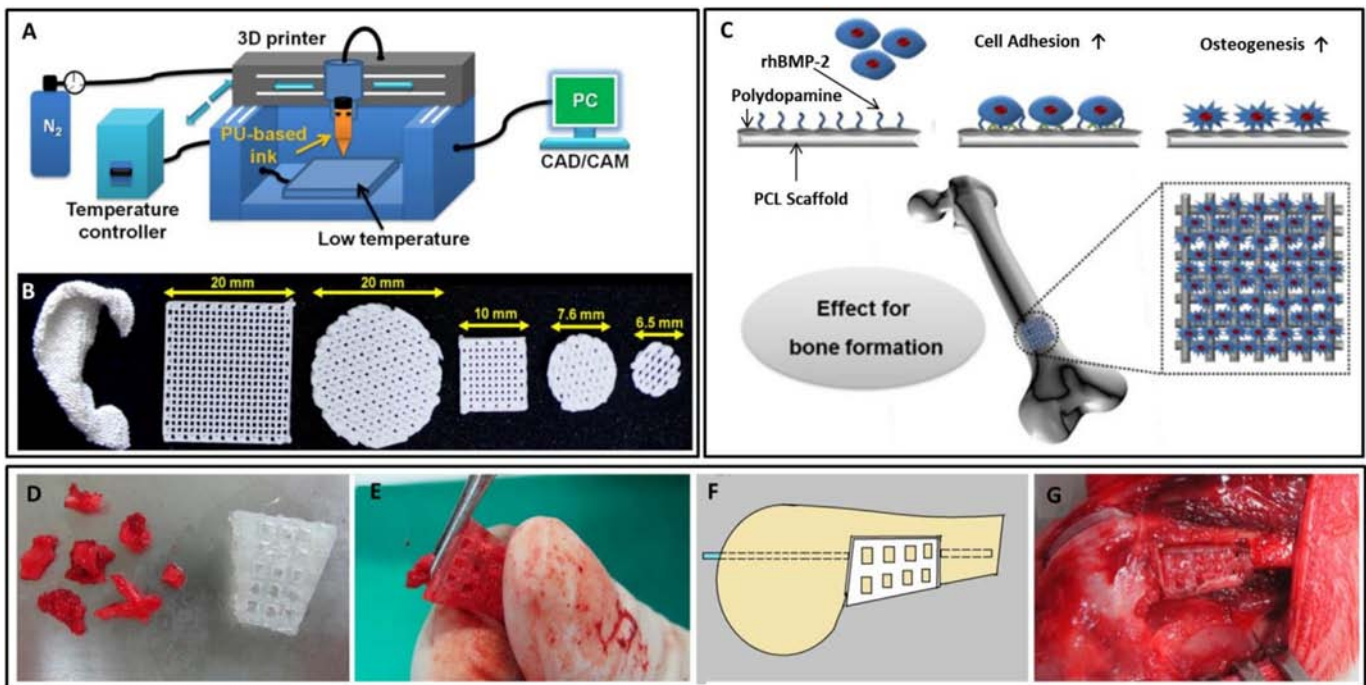


Fig. 10. A) Schematics of the low-temperature fused deposition manufacturing platform to prepare AM composite scaffold B) Composite scaffold of various shapes prepared with water based polyurethane materials. C) Schematic of functionalized scaffold showing the effect on osteogenesis. D) - G) Procedure of bone grafting with bone cage in rabbits. D) Preparation of morselized corticocancellous bone chips. E) Padding bone chips into the cage; F) Illustration of series connection of the composite graft with femoral shaft by the intramedullary K-wire; G) Photograph of the composite graft after fixation. Adapted from [134,135,138] with permission.

Peptide functionalised scaffolds are combination of scaffold materials and surface immobilized proteins to increase surface biocompatibility of the scaffolds. In general, surface functionalization of scaffold with bone morphogenetic protein 2 (BMP-2) could enhance cell adhesion and osteogenesis (Table 9). Lee et al. immobilised recombinant human BMP-2 (rhBMP-2) on dopamine coated PCL porous scaffold, which demonstrated good osteogenic activity *in vitro* (Fig. 10C). It also exhibited the sustained release with different mechanism as compared to other rhBMP-2 delivery devices [135]. Li et al. demonstrated that scaffolds based on polyester urea (PEU) with surface immobilized osteogenic growth peptide (OGP) or BMP-2 enhanced the osteogenic differentiation *in vitro* [136]. In contrast, Jensen et al. demonstrated, in porcine cranial bone defect model, that unmodified PCL scaffold was better in osteoconductivity and osseointegration as compared to BMP-2 treated PCL scaffolds [137].

Polymeric composite scaffolds based on biodegradable polymers PCL and PLGA have been reported by Shim et al. [130]. Tobramycin, one of the thermostable and most widely used antibiotics for bone infections was loaded into the composite scaffold. The team demonstrated a sustained release of tobramycin for up to 51 days *in vitro* from scaffold and a reduction in swelling in the defected rat femur. Hung et al. also demonstrated the delivery of small molecule drug loaded in composite scaffold, made from water-based PU and HA [134]. The team demonstrated the sustained and tuneable drug release *in vitro* and its potential to repair cartilage in a rabbit model.

MBG based scaffolds are silica mesoporous materials with pores of nanometres. MBG is brittle and fails to provide the mechanical strength required of clinical bone repair [139]. This urged the development of composite scaffold combining MBG and other materials for enhanced mechanical strength. Yang et al. fabricated a MBG scaffold coated with Poly (3-hydroxybutyrate-co-3-hydroxyhexanoate) (PHBHHx), in which PHBHHx has been shown to improve the mechanical strength of the scaffold without losing the porosity of scaffold. It can be potentially used for drug delivery as well. The team also demonstrated the improvement of cell attachment and viability, likely owing to the hydrophilic surface, nanostructures, release of calcium and silicon ions from the coating.

Zhu et al. fabricated composite scaffold to treat infections [140,141] and to improve angiogenesis and osteogenesis [142]. The team demonstrated the co-release of anti-tubercular drugs, namely, isonicotinyhydrazide (INH) and rifampicin (RFP), in a sustained manner over 84 days to kill bacilli without compromising liver and kidney functions. In addition, they also showed osteogenic capability of scaffold. In another study, the team demonstrated the sustained delivery of dimethylallyl glycine (DMOG) through the scaffold to induce hypoxic microenvironment which promotes blood vessels growth and subsequently bone healing. Li et al. also demonstrated the potential of INH and RFP delivery through MBG scaffold in treating bone defects using a rabbit model [143].

Another emerging technique is to use trace metals to improve the mechanical strength and add functionalities of the composite. Zhang et al. has fabricated composite scaffolds made of magnetic iron oxide, MBG and PCL loaded with doxorubicin [144]. The scaffold exhibited enhanced mechanical property, slow drug release and additional magnetic heating property, which can kill bone cancer cells. In another study, the team fabricated strontium based composite scaffold. Strontium is an innate trace metal found in bone and aids in bone formation. The addition of strontium in scaffold increased the mechanical strength by 170 times, with also controlled delivery of strontium to bone cells to promote the bone formation [145]. Qi et al. fabricated calcium sulphate and MBG based composite scaffolds, which demonstrated stimulated cell adhesion, proliferation, alkaline phosphatase activity and osteogenesis-related gene expressions *in vitro*. Similarly, the *in vivo* study demonstrated significant enhancement in new bone formation in calvarias defects in rats [146].

3.4.3.2. Metallic implants. Traditionally, metal implants are used as bone implant to provide mechanical support for bone healing and

regeneration. However, this use has been limited to sole mechanical support. The use of iron and strontium to improve mechanical strength and added functionality in composite scaffold has been discussed in previous sections. Recently, AM titanium alloy-based implant has demonstrated the capability of providing drug delivery, in addition to mechanical support (Table 9). Gulati et al. has demonstrated the fabrication of titanium implants using selective laser melting (SLM) machine. In addition, the printed implants, consisting of surface topography with micro and nano structure, demonstrated effective osteointegration property [147]. Later, Maher et al. also demonstrated the capability of similar titanium implants to deliver anti-cancer drugs and enhanced cell attachment, which supports its potential as chemotherapy treatment for bone cancer [48]. In another research, Yang et al. fabricated porous titanium dental implant for drug delivery [151]. Gu et al. also fabricated the micropatterns of calcium phosphates nanoparticles and PLGA nanocomposite on titanium and glass surface with the capability to deliver RFP [149].

3.4.3.3. Ceramic implants. Bioceramics are usually calcium-based materials for bone repair. These include calcium sulphates and calcium phosphates such as brushite, monetite, hydroxyapatite, dicalcium phosphate (DCP) and TCP. Vorndran et al. demonstrated the fabrication of bioceramics at low temperature with loading of proteins (rhBMP-2 and Heparin) and vancomycin (VNC) into the bioceramics during the process of fabrication (Table 10). The team also demonstrated a modified release of bioactive with the use of different calcium phosphates and binders [152]. Subsequently, Inzana et al. fabricated the bioceramic scaffold to simultaneously delivery RFP and VNC for implant associated bone infections. The team demonstrated that the sustained release of antibiotics can be achieved by coating the scaffold with PLGA which resulted in a 50% eradication of pathogen in an *in vivo* mice model [153,154]. Similarly, Gbureck et al. also demonstrated the fabrication of bioceramics and biocomposites at low temperature loaded with VNC, tetracycline and ofloxacin in several calcium phosphates [155]. The team also demonstrated that incorporation of PCL or PLGA matrix can delay the release of bioactive to provide sustained action. Zhang et al. proposed a hypothesis based on their preliminary study [156] that, biphasic articular spacer constituting personalised bioceramic sheath can reach the dual goal of infection control and bone regeneration in infected arthroplasty cases [157].

3.4.3.4. Bone cage and anchoring. Comminuted fractures are complicated for orthopaedic surgeon due to the number of bone fragments causing surgical complications. The personalised bone graft can potentially help to resolve this issue. Chou et al. demonstrated the fabrication of customised bone cage made of PLA and drug loaded PLGA nanofibers using the FDM 3DP. The bone cage can be filled with the fragments of bones from comminuted fracture (Fig. 10D–G, Table 10). This structured bone graft strategy could help in faster bone regeneration while avail both the osteoconductive / mechanical properties and avoiding the graft resource limitation. In addition, the combination of PLGA nanofibrous membrane loaded with drugs can provide the sustained anti-infective therapy [124,138]. In another study, the team demonstrated the fabrication of bone anchoring bolt combined with nanofibrous membrane blended with collagen for enhanced tendon bone healing which is otherwise challenging [158].

3.4.4. Custom brachytherapy applicator

Conventional brachytherapy applicators are not customised to conform with the unique human anatomy. This results in normal body parts getting unwanted exposure of radiation causing medical complications. Custom brachytherapy applicators have been demonstrated to significantly minimise exposure to other non-affected body parts [160–164]. Sethi et al. has demonstrated the use of custom applicators for patients with post-surgical anatomy to provide customised radiation exposure with effective target coverage and avoidance of unwanted exposure [163]. Ricotti et al. has also

Table 11
AM *in-vitro* drug testing systems.

Application of AM model	Drugs tested	3D printer	Material	Author
(Ocular) Drug release from contact lenses	Ciprofloxacin, moxifloxacin, fluconazole	Not stated	ABS	Bajgrowicz et al., 2015 [182]
(Ocular) Drug release from contact lenses	Fluconazole	Not stated	ABS	Phan et al., 2015 [187]
(Nasal) Drug dissolution/permeation through the mucosa in the nasal cavity	Budesonide	FDM (Dimension Elite)	ABS	Pozzoli et al., 2016 [191]
(Nasal) Visualization of drug deposition patterns	Nasal sprays: apotex, astelin, miaoling, and nasonex	MJ (Polyjet, Objet30 Pro)	PP	Xi et al., 2015 [198]
(Respiratory) Drug deposition into infant upper airway	Budesonide	MJ (Polyjet, Objet Eden 330)	PolyJet FullCure 720 (Objet Geometries)	Minocchieri et al., 2008 [202]
(Cardiovascular) Drug effects on cardiomyocyte contractility	Verapamil, isoproterenol	MJ (Polyjet, Aerotech/0)	Dextran, PDMS, Thermoplastic PU, ABS, PLA	Lind et al., 2016 [211]
(Chemotherapy) Drug effect on breast cancer bone metastasis	Fluorouracil	SLA (Printrobot)	PEG, PEGDA	Zhu et al., 2015 [225]
(Drug transport) Drug transport across polycarbonate membrane	Levofloxacin, linezolid	MJ (Polyjet, Objet Connex 350 printer)	Objet Vero White Plus Proprietary resin	Anderson et al., 2013 [232]
(Anti-microbial therapy) Antibiotic efficacy against <i>E. Coli</i> (<i>Escherichia coli</i>)	Kanamycin, tetracycline	FDM (RepRap)	PLA	Glatzel et al., 2016 [234]

* FDM: Fused Deposition Modelling; MJ: Material Jetting; SLA: Stereolithography Apparatus; ABS: Acrylonitrile Butadiene Styrene; PDMS: Polydimethylsiloxane; PU: Polyurethane; PLA: Poly Lactic Acid; PEG: Polyethylene Glycol; PEGDA: Polyethylene Glycol Diacrylate. Bolded text refers to the various classes of AM for *in vitro* drug testing systems.

demonstrated the fabrication of high-dose cylindrical (for vaginal) and flat (for superficial lesion) applicators [162]. Sim et al. fabricated an insert to treat eye plaque [165]. Similarly, other custom brachytherapy applicators were also developed for skin [166], breast [167] and nose [168,169].

4. AM for drug testing systems

Other than drug delivery systems, AM has been used in many areas of healthcare and scientific research, including clinical training, surgical planning and medical imaging research [170]. The increase in accessibility to 3D printers, its scalability and affordability have provided an inexpensive modality for rapid design and prototyping of constructs for a variety of applications [171,172]. 3D printable models are created with computer aided design (CAD) package or *via* 3D scanner of an object or *via* medical imaging data – such as Centralised Tomography (CT) or Magnetic Resonance Imaging (MRI). This data is then converted to a printable file format before reconstruction using a 3D printer. Increasingly, improvements in AM technology allow anatomically accurate models to be printed. Scanned medical images of a patient can now be printed and studied in 3D. Moving a step further, many AM constructs became the basis for *in-vitro* drug tests. This section explores mainly the use of AM on physical models (without the incorporation of cells in the ink matrix) for *in-vitro* drug testing (Table 11), and only briefly on bio-printed models, which are already extensively reviewed in other excellent articles.

4.1. Ocular

Contact lenses (CLs) have been used as a promising approach to deliver drugs to the cornea [173]. Since 1965, CLs were proposed as potential drug carriers and considerable research were conducted to develop a commercial product [174–176]. However, previous *in-vitro* models to predict drug release rates have failed to reflect the physical characteristics of an ocular environment. Drug release experiments were typically performed by immersing lenses into vials containing 2 to 5 mL Phosphate Buffer Saline (PBS), with no form of fluid exchange [177–179]. However, the tear volume on the actual corneal surface is significantly smaller in amount (approximately $7 \pm 2 \mu\text{L}$) and undergoes a rate of tear exchange at approximately 0.95 to 1.55 $\mu\text{L}/\text{min}$ [180,181]. The large volumes used *in*

vitro resulted in rapid elution of drugs, which may differ greatly from *in vivo* drug release profiles from CLs on the ocular surface.

To overcome these problems, Bajgrowicz et al. demonstrated the use of AM to fabricate a mould for an *in vitro* eye model to study the release kinetics of ciprofloxacin and moxifloxacin from commercially available daily disposables CLs [182]. The 3D printed polycarbonate-acrylonitrile-butadiene-styrene mould comprised of a “corneal/scleral” section and an “eye lid” piece and these eye models were connected to a microfluidic syringe pump to simulate tear flow and volume adjustment (Fig. 11A and B). CLs were soaked in ciprofloxacin and moxifloxacin solutions, respectively, before being placed into the eye model. Flow-through fluid was collected at specific time intervals to determine the concentrations of drug using UV–Vis Spectrophotometer. Drug release was sustained throughout the 24-h observation period for the eye model ($P < 0.05$) while the drugs were released rapidly within the first hour for the conventional method, which was consistent with previous reports. Comparable results have been observed from other studies that have examined drug release from CLs in microfluidic systems [183–186]. In addition, a study conducted by Phan et al. [187] using the same parameters for studying the release kinetics of fluconazole as a potential ocular antifungal agent for fungal keratitis also yielded similar findings. Using an eye mould, therefore, allows better simulation of the *in vivo* conditions.

4.2. Nasal

Nasal drug delivery has been known to be safer than most traditional routes of drug administration [188]. The expanding role of aerosols in nasal drug delivery exploits the large surface area of the nasal mucosa, therefore allowing many drugs such as peptides, vitamins, macromolecules, opioids and also antimigraine drugs to be delivered directly into the systemic circulation [189]. It was reported that the efficacy of a nasal drug would rely on its site of deposition in the nasal cavity [190]. Systemic delivery is also improved with increased drug exposure to the respiratory zone of the nasal cavity, the septum and nasal floor around the turbinates, owing to their high degree of vascularization [189]. Currently, intranasal drug deposition *in vivo* can be measured using gamma camera imaging. However, the increased risk of exposure to radiation and ethical considerations have discouraged the use of this modality for studying nasal drug deposition. Existing *in vitro* models to investigate nasal drug deposition have met with many limitations.

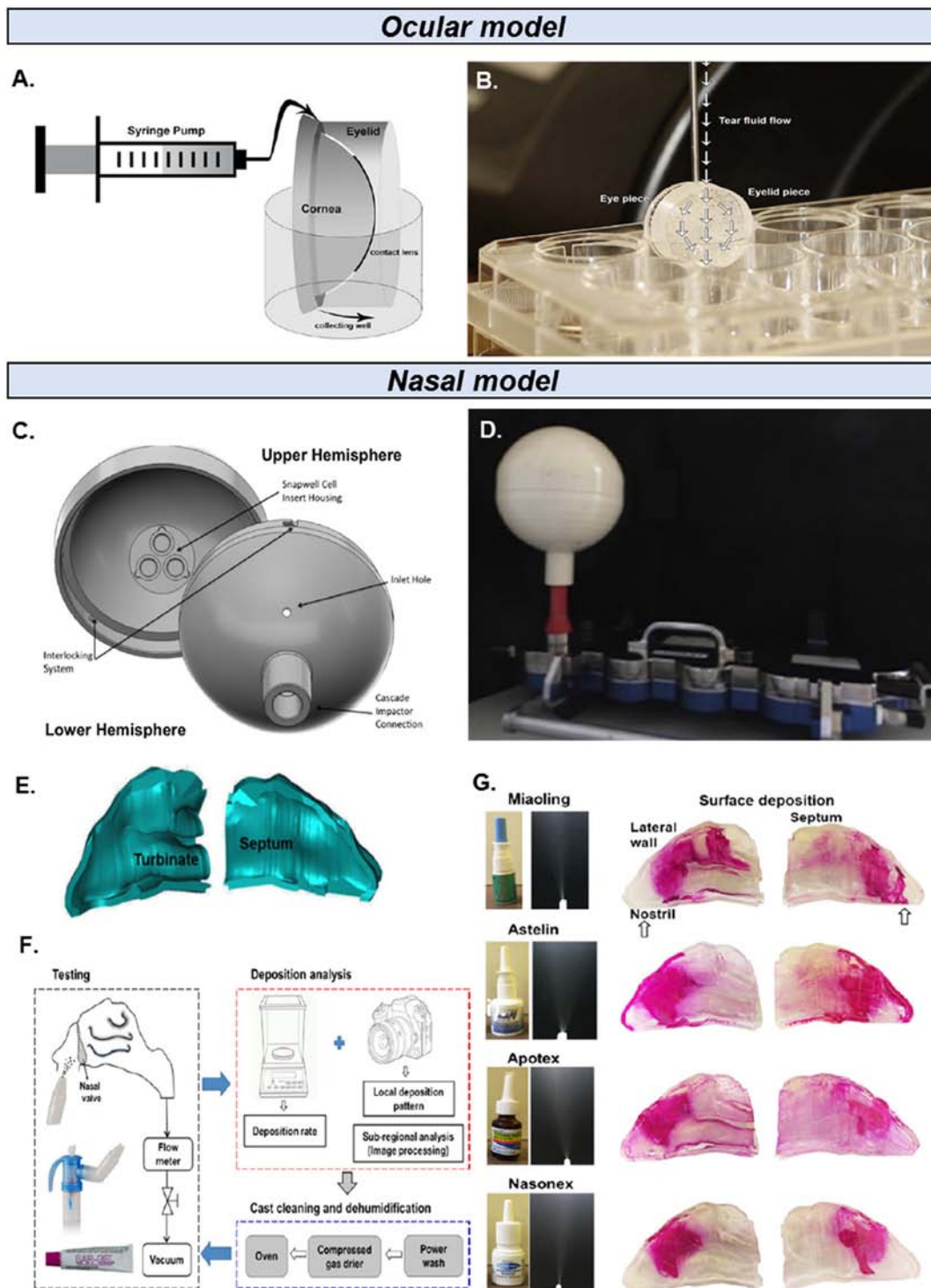


Fig. 11. AM ocular and nasal *in-vitro* drug testing models. A) Schematic of the final set up with a microfluidic pump and a collecting well plate. B) A front-view photograph of the eye model. C) 3D drawing of the modified expansion chamber. D) British Pharmacopoeia Apparatus E equipped with modified expansion chamber. E) The schematic of the cast cut open to visualize and measure the location depositions inside the nose. F) Schematic diagram of intranasal deposition test. There are three steps: drug delivery testing, deposition rate and deposition pattern analysis, and cast cleaning dehumidification. G) Deposition pattern and quantification in the nose with four nasal spray products: Miaoling, Astelin, Apotex, and Nasonex. Adapted from [182,191] with permission.

Cascade impactors (CI) alone are unable to provide information on drug dissolution or permeation through the mucosa in the nasal cavity.

To overcome these limitations, Pozzoli et al. [191] developed a custom-made expansion chamber (MEC) using FDM printing (Dimension Elite) and the ABS material. RPMI 2650 nasal cell epithelia on Snapwell cell inserts were incorporated into the MEC, which was attached to a cascade impactor for the testing of drug deposition and permeation by using a commercially available budesonide nasal spray, Rhinocort®.

The inclusion of RPMI 2650 nasal cell epithelia allows better representation of the mucosal surface present in the nose. Fig. 11C and D illustrates the 3D drawing of the MEC and the cascade impactor fitted with the MEC respectively. A total dose of 96 µg of budesonide was delivered into the chamber using a Rhinocort®. The cell inserts were then removed from the modified chamber and transferred into a 6-well plate containing Hank's Buffered Salt Solution (HBSS). At the end of 4 h, it was discovered that only about 17% of Budesonide remained on the

surface and inside the cells, suggesting the relatively low binding affinity of budesonide for human nasal tissue, a trend in congruence with data previously published by Baumann et al. [192].

Alternatively, anatomical models such as cadaver heads [193,194], nasal cavity replicas [195,196] or nasal casts using FDM or stereolithography (e.g., the SLA, Viper or SAINT models) [197] have been developed to study nasal drug deposition. However, validated modalities to visualize and quantify regional or local deposition of drug fractions are rare. Xi et al. [198] developed a nasal cast model using MRI scans for assessing the deposition patterns of four commercially available nasal spray pumps (Apotex, Astelin, Miaoling, and Nasonex). The models were printed with MJ printing (Polyjet, Objet30 Pro) and PP was used as the base material. Fig. 11E depicts the schematic of the nasal cast and Fig. 11F shows the schematic diagram of the intranasal deposition test which comprised of three steps: (1) drug delivery testing, (2) deposition rate and deposition pattern analysis, and (3) cast cleaning dehumidification. Sar-Gel, a water-indicating paste which changes colour from white to purple upon contact with water was used to visualize the drug droplet deposition patterns. Fig. 11G shows the nasal deposition pattern for Miaoling, Astelin, Apotex, and Nasonex nasal sprays.

4.3. Respiratory

Differences in infant airway anatomy and physiology from older children and adults have reduced the effectiveness of existing models for studying drug deposition among infants. This is due to the changes in

the airway morphometrics, breathing patterns, airway resistance, and lung volume, which happens during the first months of life. [199] Therefore, these factors would affect the drug deposition inside the lungs. [200] It was reported that only <1% of the nominal dose was delivered to the lungs of ventilated infants as compared to 8–22% in adults [201].

To overcome this limitation, Minocchieri et al. [202] used AM to construct a premature infant nose throat-model (PrINT-Model), which corresponds to a premature infant of 32-wk gestational age (Fig. 12A). This work was based on the predecessor model, known as the Sophia Anatomical Infant Nose-Throat (SAINT) model, which is an upper airway model of a 9-mo-old infant, derived from a CT scan and reconstructed using stereolithography as described by Janssens et al. [197]. Fig. 12B shows the classical experimental set-up used to measure the distribution of liquid aerosol generated by the IPI nebulizer within the upper and lower airways of the SAINT model. The PrINT-Model was constructed from slices obtained from three-planar magnetic resonance imaging scan. Two separate models were constructed using photopolymer resin with one showing the entire head's surface (Fig. 12Ai) and the other, a reduced laboratory model (Fig. 12Aii–iv) which comprised of the face and air conducting parts for subsequent tests. The model was printed using MJ printing technique (Polyjet, Objet Eden 330) and proprietary PolyJet FullCure 720 material. The model was connected to a cascade impactor to assess the lung dose, at an airflow of 1, 5 and 10 L/min to simulate constant inspiration. It was reported that increasing the constant inspiratory flow led to a reduction in lung dose. The trend of reciprocal dependency between inspiratory flow and lung dose was likely due to higher inertial

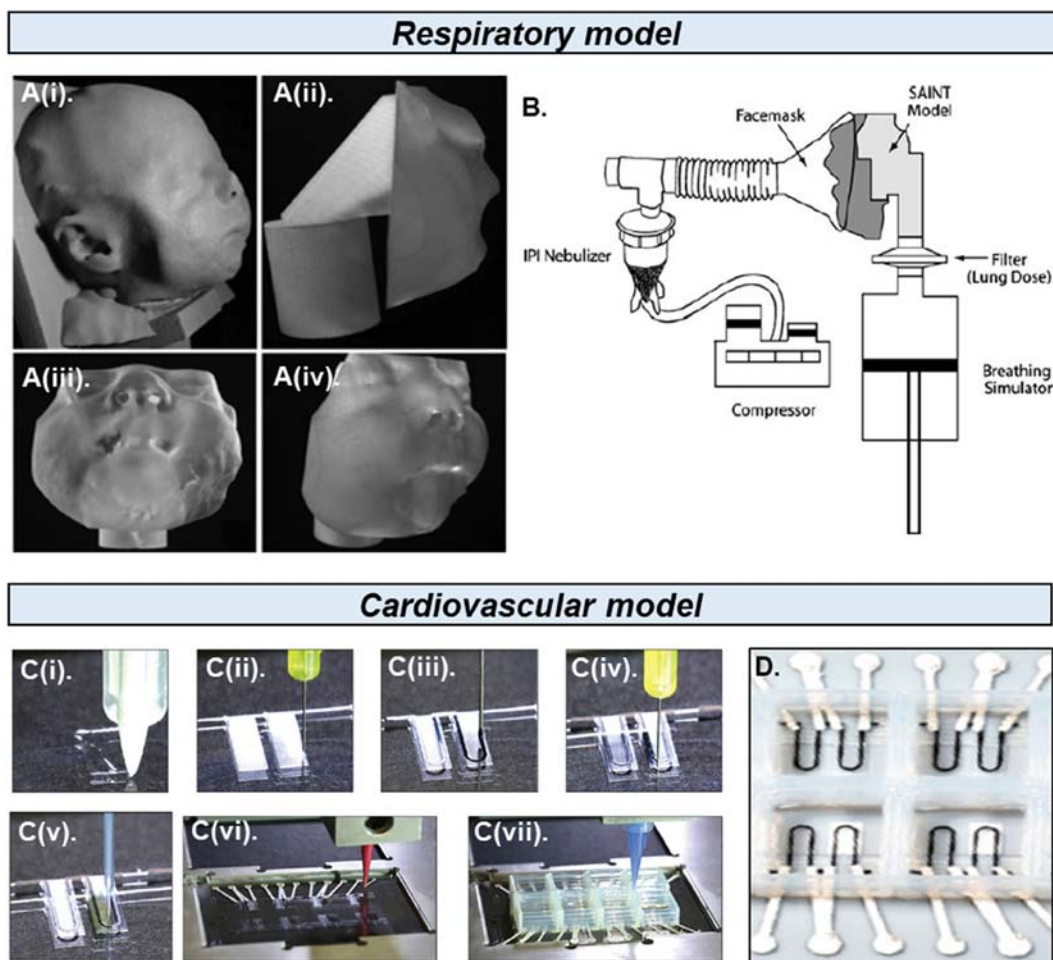


Fig. 12. AM respiratory and cardiovascular *in vitro* drug testing models. Ai) Side view of the complete upper airway model; Aii – iv) show a lateral, up-front and side view of the reduced laboratory model (face and air conducting parts), all built in FullCure 720. B) Experimental set-up used to measure the distribution of liquid aerosol generated by the IPI nebulizer within the upper and lower airways of the SAINT model. Ci – vii) Automated printing of the device on a 2 × 3 in. glass slide substrate in seven sequential steps. For each step, a corresponding still image from the printing procedure is displayed. D) A section of the fully printed final device. Adapted from [202,211,220] with permission.

impaction of aerosol particles in the upper airways, thus, the lesser aerosol penetration to the lower airways and other studies using upper airway cast models have yielded similar results [197,203,204]. The infant nose throat-model presents a more realistic and accurate prediction of aerosol deposition in premature infants, which would be difficult or impossible to obtain *in vivo*.

4.4. Cardiovascular

Microphysiological systems (MPS), also known as organs-on-chips, capable of replicating both structure and function of native tissues *in vitro*, have served as attractive alternatives to conventional cell cultures and animal studies for drug testing [205]. These systems, however, fall short in their capacity to be integrated with sensors and their production often entails soft material lithographic processes, which requires multiple steps, masks and dedicated tools – all of these may diminish its qualities of rapid prototyping and customization [206–210].

Lind et al. [211] fabricated a cardiac MPS, allowing for the integration of soft strain gauge sensors within micro-architectures that promoted self-assembly of cardiomyocytes to form laminar cardiac tissues. The capability of multi-material AM allowed a variety of viscoelastic inks to be printed, thereby enabling a wide range of functional, structural, and biological materials to be patterned and integrated in a single programmable manufacturing step [212–215]. Some of the materials used in the printing include Dextran, PDMS, Thermoplastic PU, ABS and PLA. Fig. 12Ci–vii documents the various stages of automated microscale 3D-printing procedure of constructing the cardiac MPS. Highly diluted polymer-based inks with low solid content were used to ensure patterning of thin individual layers to match the stress generated by laminar cardiac tissues [208,209,216,217]. Fig. 12D shows a series of grooved microstructures of varying spacing between curved filaments printed onto soft PDMS substrate to recapitulate the highly organised, structurally and electrically anisotropic layers of the heart musculature [218]. The device works *via* the contraction of an anisotropic engineered cardiac tissue which deflects a cantilever substrate thereby stretching a soft strain gauge embedded in the cantilever. This generates a resistance change proportional to the contractile stress of the tissue. A dilution series of 2 different drugs - L-type calcium channel blocker verapamil and the β -adrenergic agonist isoproterenol – in media were added to the cardiac tissues (cardiomyocytes were seeded and self-assembled on the device) and incubated for 10 mins for each dose prior to recording. For every dose, at least 30 s were recorded in each channel. The cardiac MPS showed negative inotropic response to verapamil, while negative chronotropic effect was observed for spontaneously beating tissues which was supported by prior studies on isolated postnatal whole rat hearts [219]. An expected effect was also observed for isoproterenol, with a positive chronotropic response to spontaneously beating laminar tissues, similar to previous studies of engineered Neonatal rat ventricular myocytes (NRVM) micro-tissues [207].

4.5. Chemotherapy

Cancer chemosensitivity is most commonly studied in 2D cell culture and *in vivo* animal models. Despite the convenience and the affordability of 2D cell cultures, they are generally known for their poor resemblance to the tumour microenvironment alluding to the loss of biological, chemical and mechanical cues [221]. Cells cultured in 2D presents different morphologies and levels of gene expression, compared to 3D tissue cultures [222].

Several AM matrices have been reported [223,224] to simulate cancer microenvironments. Zhu et al. developed a stereolithography-based technique to create a biomimetic and tuneable 3D bone matrix to study breast cancer bone invasion and chemosensitivity *in-vitro* [225]. The 3D bone matrix contained hydroxyapatite nanoparticles (an essential mineral component in the human bone) mixed with printable poly(ethylene) glycol diacrylate resin. MDA-MB-231, a type of breast cancer cells

with a high metastatic potential, were seeded on top of the bone matrix. After incubation for 24 h, an anti-cancer drug 5-Fluorouracil was added and incubated for another 72 h. While apoptosis was observed in both the 3D matrix and 2D culture, less cytotoxicity was observed in the 3D matrix as compared to 2D culture. The 2D cell monolayer cultures are prone to undergo enhanced drug penetration, and therefore showed less drug resistance than tumour–drug interactions *in vivo*. Cells grown on the 3D matrix preserved the characteristics essential for tumour growth, hence exhibited greater chemo-resistance [226,227]. This phenomenon may be explained by improved cell–matrix interactions which altered the transporter expression and reduced drug diffusion [228,229]. This bone scaffold serves as a promising model for the study the of breast cancer bone invasion and the evaluation of future chemotherapies.

4.6. Drug transport

Microfluidic devices utilised for assays in most laboratories are generally prepared using conventional and soft lithography [230,231]. However, there is currently no device made using one-step rapid production possible of incorporating the flow of samples for subsequent detection of analytes of interest.

Anderson et al. [232] reported the use of a reusable, high throughput, fluidic device incorporating a membrane above the channels for studying drug transport. MJ (Polyjet, Objet Connex 350 printer) printing technique and the Objet Vero White Plus Proprietary resin were used in the production of the fluidic device. The device of 8 parallel channels was each incorporated with a porous polycarbonate membrane to study drug transport across the membrane (Fig. 13A–C). Bovine pulmonary artery endothelial cells were seeded on the cell culture inserts containing a polycarbonate membrane above the channels and allowed to grow until confluency for 24 h. Two antibiotics, levofloxacin and linezolid, with concentrations between 100 and 2000 nM were administered through these channels and the samples were analysed with LC/MS/MS. It was observed that the drug transport across the membrane increased with drug concentration. These findings suggest the usefulness of this fluidic device for studying the effects of molecular transport of drugs on cells.

4.7. Antimicrobial

The increasing resistance among bacteria towards broad-spectrum antibiotics in recent years has led to the need for selective use of antibiotics [233]. However, this method entails a series of efficient, affordable, and fast diagnostic tests to recognize the most effective drug, or a combination, to ensure optimal therapy.

Glatzel et al. [234] developed a portable device for antimicrobial testing, using FDM technology. The device provided an improved ease of use and reusability. In addition, the device was intrinsically sterile due to the high operating temperature of 180–350 °C [235]. Polylactic acid (PLA) was used because of its affordability, printability by FDM and high fidelity. The device comprised of four chambers, with each connected to the same inlet. The deposition of the bacteria growth medium and antibiotics into the chambers were realized with automation. Fig. 13D details the sequence of testing. The four chambers allow for three varying concentrations of the same antibiotic or three different antibiotics with a blank for testing. A strain of bioluminescent *E. coli* was injected through the inlet port Fig. 13E to demonstrate the inhibition effect of tetracycline and kanamycin, as determined by the distance which was cleared of bioluminescence upon incubation with *E. coli*. The test results exhibited conformity within the margin of error of commercially available antibiotic test discs.

4.8. Bioprinting for *in vitro* drug testing

The abovementioned have demonstrated the capacity and competency of AM to create physical (non-cellular) models, which are

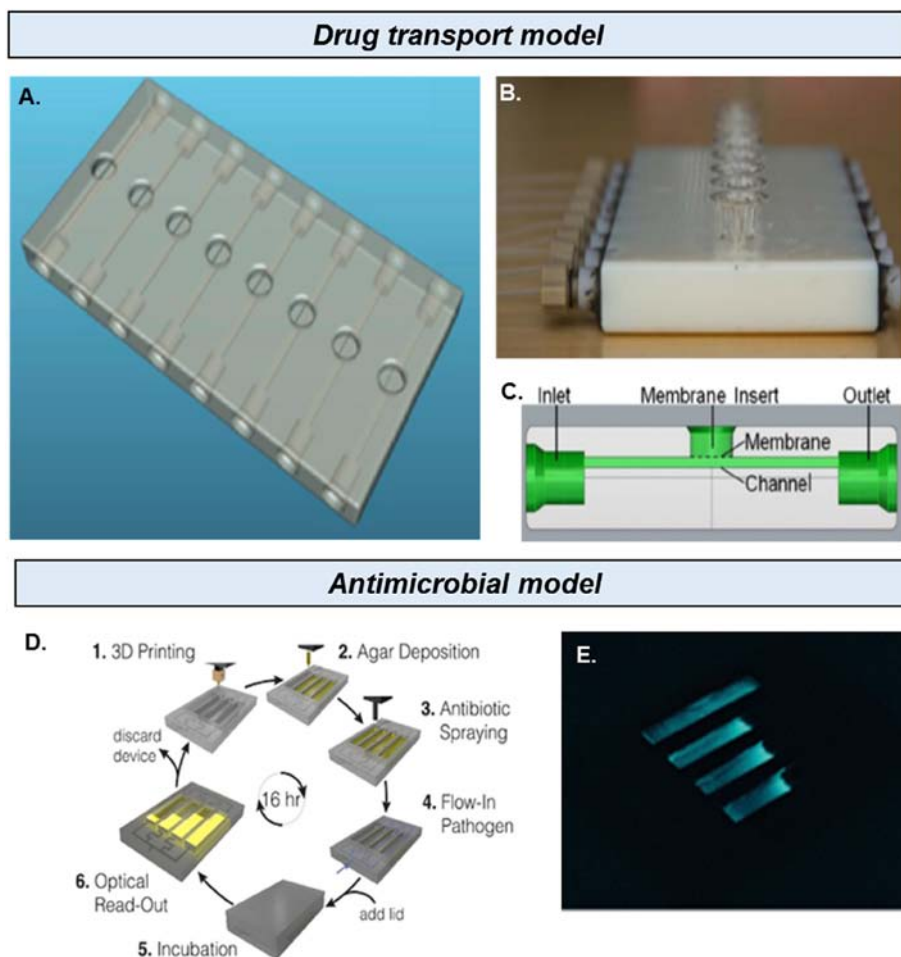


Fig. 13. AM drug transport and antimicrobial *in vitro* drug testing models. A) Design of the AM microfluidic device. B) AM microfluidic device, containing adapters for syringe-based pumps, channels, membrane insertion port, and outlets. C) Side view schematic of the device shows how the inlet addresses the channel and allows fluid to flow under the membrane. The membrane is part of a commercially available membrane insert that is manually inserted into the port on top of the device. Finally, there is an outlet to allow fluid to leave the device. D) Diagram illustrating the steps involved in the production of the device. E) The device in the dark with bioluminescent bacteria. Adapted from [232,234] with permission.

anatomically accurate and functional – for predicting effects of drug action and delivery. In terms of cellular models, there has been a movement towards a reduction in animal testing to determine the efficacy and toxicity of a drug candidate on the human body, partially due to erroneous pharmacokinetic predictions arising from species differences [236,237]. This resulted in an increase in pressure to improve current *in vitro* human-derived cellular models as suitable alternatives to animal

testing. Advances in the field of bioprinting can be leveraged to create physiologically relevant tissue constructs, tissue models, tissues, organs and organ-on-a-chip (OoC) models for modern medicine and pharmaceuticals [238]. Bioprinting is defined as the simultaneous writing of living cells and biomaterials with a prescribed layer-by-layer stacking organization using a computer-aided transfer process for fabrication of bioengineered constructs [239].

Table 12
Bioprinted OoC models for *in-vitro* drug testing

Application of bioprinted OoC	Drugs tested	3D printer	3DP material	Author
(Liver) Drug metabolism in HepG2 human hepatocarcinoma cells	7-ethoxy-4-trifluoromethyl coumarin	PE	Alginate solution	Chang et al., 2010 [251]
(Liver) Prodrug metabolism and radioprotective effects on human hepatic carcinoma cells of the cell line HepG2 and human mammary epithelial of the cell line M10	Amifostine	PE	Matrigel	Snyder et al., 2011 [252]
(Liver) Drug toxicity on HepG2/C3A human hepatocarcinoma cells	Acetaminophen	PE (Organovo NovoGen MMX bioprinter™)	GelMA with 0.5% photoinitiator	Knowlton et al., 2016 [249]
(Cardiovascular) Drug toxicity on neonatal rat cardiomyocytes and human umbilical vein endothelial cells (HUVECs)	Doxorubicin	PE (Organovo, NovoGen MMX bioprinter™)	Alginate, GelMA, and photoinitiator	Zhang et al., 2016 [253]
(Kidney) Drug toxicity on human immortalized renal proximal tubule epithelial cell (RPTEC/TERT1)	Cyclosporine A	PE (Custom-designed, multimaterial 3D bioprinter)	Fibrinogen-gelatin-CaCl ₂ -transglutaminase solution	Homan et al., 2016 [254]

* PE: Paste Extrusion; GelMA: Gelatin Methacryloyl. Bolded text refers to the various classes of bioprinted OoC models for *in vitro* drug testing.

In this section, we will provide brief summaries of two emerging technologies within the field of bioprinting for *in-vitro* drug testing, namely, OoC and cell-laden models.

4.8.1. Bioprinted organ-on-a-chip models for *in vitro* drug testing

An OoC model is a multi-channel microfluidic cell culture device that allows continuous perfusion of chambers containing live cells organised in a fashion to simulate tissue and/or organ physiology [240]. As such, these models provide more physiologically relevant *in vivo* conditions through the inclusion of multicellular features, tightly regulated micro-environments and vascular perfusion, which are unattainable in conventional cell cultures. To date, there have been several OoC models developed, ranging from individual OoC such as gut-on-a-chip, lung-on-a-chip, blood vessel-on-a-chip, cancer-on-a-chip, bone marrow-on-a-chip, and kidney-on-a-chip, to multiple OoC models such as liver-tumour-bone marrow-on-a-chip or liver-skin-intestine-kidney-on-a-chip [237,241–247].

The complexity in design of the OoC can be overcome with bioprinting, which offers great advantages over traditional scaffolding methods in patterning and precisely positioning multiple cell types to fabricate intricate hetero-cellular microenvironments mimicking native tissues [238]. In addition, bioprinting for fabricating OoC offers flexibility over size and architecture of device, co-culture ability and low-risk of cross-contamination [238]. As such, these models have become increasingly essential in pharmaceuticals, especially in drug toxicology and high-throughput screening [248]. Among the various bioprinted OoC models, the liver models have been the primary focus in pharmaceuticals. Drug-induced liver injury is a major concern in pharmaceutical development and is by far the most common cause for discontinuing clinical trials and withdrawal of approved drugs during the post-market surveillance stage [249]. The liver also plays a vital role in the metabolism of xenobiotics, of which the effects of their related metabolites on other organs may be significant [250]. As such, evaluating drug metabolism and toxicities on liver OoC models were implemented [249,251,252]. Other bioprinted OoC models requiring prominent levels of perfusion such as cardiovascular and renal models were also developed to render similarities in their functional *in vivo* characteristics and were evaluated on

possible drug toxicities [253,254]. In the light of progressive understanding on these MPS, their biology and tissue characterization, the transition into bioprinted OoC models remains a few but growing trend. Table 12 below summarizes some developments in bioprinted OoC models for *in-vitro* drug testing.

4.8.2. Bioprinted cell-laden models for *in vitro* drug testing

Cells are encapsulated in suitable matrices to mimic its native 3D microenvironments. It has been shown that cells respond to these matrices and exhibit more *in vivo* like characteristics, in terms of cell morphology and expression of key *in-vivo* protein markers [255]. Within the human body, extracellular matrix (ECM) comprising of proteins, proteoglycans and glycosaminoglycans are dispersed among cells arranged in complex 3D spaces. The ECM plays several functions, such as providing an adhesive substrate, conferring macroscopic shape and microscope architecture, sequestering and presenting growth factors, and sensing and transducing mechanical signals to cells [256]. Therefore, the highly dynamic nature of ECM directs tissue morphogenesis and development. Beyond just serving as an inert supporting structure, matrices have been designed to make it biologically active to direct the development of bioengineered tissues, to produce a functionally regenerated tissue equivalent [257].

Hydrogels has been a popular choice for ECM in tissue engineering. Its hydrophilicity allows the encapsulation of cells and bioactive molecules in aqueous media and then manipulated using physical or chemical bonding through environmental changes (such as pH, temperature, and ionic concentration), enzymatic initiation, or photopolymerization to form insoluble, cross-linked meshwork, resulting in a cell-laden hydrogel [258]. In addition, hydrogels are biocompatible, with good porosity for diffusion of oxygen, nutrients, and metabolites, can be processed under mild cell-friendly conditions and produce little to no irritation [257]. The polymers that constitute the backbone of a hydrogel can be divided into naturally derived proteins such as collagen, gelatin, fibrin, hyaluronic acid, alginate and agarose or synthetic polymers such as poly(ethylene glycol) (PEG) and poloxamers (Pluronic® and Lutrol®).

In the light of these feasible characteristics of hydrogels as ECM alternatives, “bioinks” were developed through the deposition of cells and other biomaterials for the fabrication of volumetric tissue constructs in

Table 13
Bioprinted cell laden models for *in-vitro* drug testing

Application of bioprinted cell laden model	Drugs tested	3D printer	Material	Author
(Brain) Drug effect on calcium response, and gamma-aminobutyric acid (GABA) expression on human neural stem cells (hNSCs)	Bicuculline	PE (3D-Bioplotter System, EnvisionTEC,GmbH)	Alginate,agarose, CMC	Gu et al., 2016 [262]
(Liver) Cell toxicity of drug on human liver cancer cell line (Hep G2) and HUVECs	Troglitazone (Rezulin)	BJ/ DeskViewer TM (Cluster technology, Osaka, Japan)	Fibronectin, gelatin	Matsusaki et al.,2013 [260]
(Liver) Drug effect on LDH, albumin, and ATP levels on bioprinted liver tissue (Human hepatocytes, hepatic stellate cells, HUVECs)	Trovafloracin, levofloxacin	PE (NovoGen Bioprinter)	NovoGel 2.0 hydrogel	Nguyen et al., 2016 [259]
(Liver) Cell toxicity of drug on biomimetic human iPSC-derived hepatic model [human-induced pluripotent stem cell-derived hepatic progenitor cells (hiPSC-HPCs), HUVECs and adipose-derived stem cell (ADSC)]	Rifampicin	DLP (Custom built DMD system)	GelMA, glycidial methacrylate-hyaluronic acid	Ma et al., 2016 [250]
(Uterus) Evaluation of tocolytic agents on uterine contractions using AM hollow rings of magnetized human uterine smooth muscle cells (HUTSMCs)	Ibuprofen, indomethacin, nifedipine	Magnetic 3D bioprinting	Not stated	Souza et al., 2017 [263]
(Cancer) Chemotherapeutic response between 2D versus 3D bioprinted breast cancer model (Human breast cancer cell and Breast stroma cells: adipocyte, mammary fibroblast, and endothelial cell)	Tamoxifen	PE (NovoGen Bioprinter)	Not stated	King et al., 2013 [261]
(Cancer) Chemotherapeutic response on human cervical cancer cell (Hela)	Paclitaxel	PE (Custom-designed, 3D bioprinter)	Gelatin-alginate-fibrinogen Solution	Zhao et al., 2014 [223]
(Cancer) Chemotherapeutic response on human glioma cells	Temozolomide (TMZ)	PE (3D multi-nozzle bioprinter, Tissform III)	Gelatin-alginate-fibrinogen solution	Dai et al., 2016 [255]

*PE: Paste Extrusion; BJ: Binder Jetting; DLP: Digital Light Processing; DMD: Digital Micromirror Device; CMC: CarboxyMethyl Chitosan; GelMA: Gelatin methacryloyl. Bolded text refers to the various classes of bioprinted cell laden models for *in vitro* drug testing.

3D bioprinting, recapitulating tightly regulated microenvironments. Only with the restoration of cells to its native *in vivo* conditions will the results of *in vitro* drug testing be reliable and translatable to actual clinical outcomes. It was also reported that 3D bioprinted models were considered superior to simpler 3D *in vitro* models such as spheroid cultures [24]. As a result, multiple bioprinted liver and cancer cell-laden models were developed for predicting hepatotoxicity and chemotherapeutic responses [223,250,255,259–261]. Other bioprinted cell-laden models used for *in vitro* drug testing included the neural and uterine cell-laden models [262,263]. Table 13 below summarises the developments in bioprinted cell-laden models used for *in vitro* drug testing.

5. Future directions and challenges

Excitement about AM has accelerated steadily over the past decade. One of the contributing factors to this excitement is the highly promising note for manufacturing personalised drug dosage forms; special characteristics dosage forms, e.g., zero order drug release; or improved drug testing devices. However, there are several technical and regulatory challenges that need to be overcome before it can move on to widespread pharmaceutical applications and public acceptance. Here, the authors provide some of our opinions on the challenges and future directions for AM, especially on pharmaceutical applications.

5.1. Material/safety

As with all medical devices such as implants or pharmaceutical dosage forms, such as tablets or skin patch, the goal of AM drug delivery or testing system is for effective and safe human usage or consumption. Therefore, the materials used, or at least the final form of the materials, must be biocompatible. While aseptic manufacturing can be practised throughout the manufacturing process, terminal sterilisation often gives an additional assurance to the final product, hence often the practice in the pharmaceutical industries.

Based on CDC guidelines for disinfection and sterilisation in healthcare facilities, 4 of the most common means of sterilisation include high temperature wet sterilisation using steam (autoclave); low temperature sterilisation techniques such as ethylene oxide gas, hydrogen peroxide gas plasma and gamma radiation [264]. Traditional metal surgical tools or implants had been sterilised *via* autoclave. However, many 3D printable materials, such as plastics or polymers, may not be suitable for this method as the material may melt or warp under high heat. The choice of sterilisation is further complicated by the presence of drug moiety which may be heat or moisture sensitive. As such, pharmaceutical companies often employ low temperature sterilisation techniques for this purpose. To ensure successful sterilisation, the sterilant such as ethylene oxide gas, hydrogen peroxide gas or gamma rays must be able to penetrate the interior of the AM product and can penetrate common packaging materials. It should also have no significant effect in the appearance or function of the AM products. Other characteristics of an ideal low temperature sterilisation techniques include high efficacy, rapid activity, non-toxicity, adaptability, monitoring capability and cost effectiveness. Till this date, the various sterilant have only been tested for materials used in current medical devices or pharmaceutical dosage forms. As more materials become 3D printable, it is important that corresponding research be conducted to test for compatibility of new material with current sterilisation techniques.

Biocompatibility of 3D printable material is another aspect critical for safe human usage or consumption. Yet, biocompatibility may not be inherent for all printable materials [265]. The starting liquid resins for vat polymerisation are often extremely toxic acrylates. While the final printed parts are biocompatible, large molecular weight polymers, there is a risk of residual monomers leaching from the AM products [202]. In addition, harsh post-print processing is often applied to render these printed products safe and biocompatible. These harsh processing may cause damage or degradation to the drug moiety encapsulated

within the printed product. Furthermore, the process of AM often involves free radical polymerisation, strong heat, high laser sintering or other conditions. These process parameters may have effects on the nature of the drug, especially for biomolecules such as peptides or proteins. More research will need to be conducted to assess the effects of process parameters on drug moiety. These concerns over safety of AM products may have contributed to the low rate of clinical trials for AM implants, especially AM dosage forms for drug delivery. A quick search on clinicaltrials.gov reveals a low rate of 37 ongoing and completed clinical trials involving the use of AM products for education, implants or surgical aids. None of these trials involve the use of drug moiety.

Other than safety concerns for the material usage in AM, in general, as compared to traditional powder compaction for manufacturing pharmaceutical tablets, AM offers relatively limited choice for material, colours and surface finishes [21]. For vat polymerisation-based AM, the materials are confined to those with a photocurable functional group. For heat-based extrusions like FDM, it is important to include thermoplastic polymers to fabricate the 3D object. Each of the different AM technologies have different advantages and limitations to the choice of material. It is therefore, important to understand the fundamentals for each technology, for proper application of these AM technologies in pharmaceutical applications.

5.2. Scalability of AM technology

The ability for upscaling into industrial scale is often critical for any manufacturing technology, in its path for adoption into mainstream. AM was initially developed for rapid prototyping. While there has been tremendous improvement in its speed, precision and accuracy since its inception in the 80's, AM is mainly used in production of small quantities such as in personalised dosage forms or other specialised products.

AM companies are spending much of their efforts to manufacture production grade printers for large scale manufacturing. Other than increasing the size of printers to accommodate more volume for each print job, companies are also actively improving on the speed of production. One good example is that of Carbon3D, with their innovative CLIP technology that eliminates that need for repeated up's and down's of the build platform, thus improving on the speed of production [266]. 3D Systems' fab-grade 3D printer also showed promises in high speed manufacturing by surpassing the injection molding [267].

Compared to AM, traditional manufacturers of pharmaceutical dosage forms like tablets, can produce up to 1.6 million tablets per hour, a number that far exceeds what a 3D printer can currently do. The true purpose of AM of pharmaceutical dosage forms is to create products with unique functionalities that cannot be achieved by high-speed powder compaction tableting or other traditional manufacturing technologies. Therefore, the focus of AM pharmaceutical dosage forms should be on the unique functionalities of the product, rather than a way to replace traditional manufacturing of standard tablets.

5.3. AM ecosystem

AM has been showing great promise for many years. This is demonstrated through its use in prototyping, design iteration and small-scale production. These benefits are already significant, bringing us to the cusp of changing discrete manufacturing forever. As these fundamentals of AM (speed, quality and material) improve rapidly, new opportunities will arise that take AM ever closer to mass production. To do so, the role of public / governmental support, educated workforce and consumer acceptance may be the 3 main pillars not to be neglected.

To increase the adoption of AM by manufacturing industries, several countries have either established a national body for the coordinating efforts or developed a master plan for the adoption and promotion of AM. For example, a National AM Innovation Cluster (NAMIC) was set up in Singapore, October 2015, to nurture promising AM technologies

and start-ups, and to accelerate translational R&D from public sector funded institutions with a focus on commercial applications. NAMIC seeds and enables public-private cross-collaboration, acting as a connector between industry, research performers and public agencies. It also assists companies seeking capital injection either through project joint-funding or leveraging on its investor networks [268]. Other national level AM body or associations include AM Association of Taiwan [269] and Australian Research Council Research Hub for Transforming Australia's Manufacturing Industry through High Value AM [270]. AM has also been highlighted in the recent policies of several countries such as China, Germany, Japan, South Korea and United States [264].

Other than public support, it is also important to have a steady supply of suitably skilled workforce to support AM industries and its adoption to pharmaceutical or other manufacturing industries. Academic institutes such as the National University of Singapore has recently introduced a Masters' Degree Programme in Mechanical Engineering with a specialisation in AM. Similarly, there are programs offered by others including the Penn State University, University of Maryland and University of Texas at El Paso [271–273].

Finally, for AM to become widely adopted, there must be a demand for it. In terms of pharmaceutical industries, it means that patients or consumers must first be receptive to the idea of AM medicine. In a study by Goyanes et al. [274], it showed that while AM is able to fabricate differing shapes of tablets such as torus, sphere, disc, capsule and tilted diamond shapes, not all the shapes are acceptable by patient's standard. Out of which, the torus shape has a highest patient acceptability score which indicate that FDM AM technology may be a promising fabrication method towards increasing patient's acceptability of solid oral medicines. Therefore, it is important to promote the public awareness and acceptability of AM drug delivery systems, as part of the effort to improve adoption of AM.

5.4. Regulatory challenges

In 2015, the world's first AM oral dispersible medication SPRITAM® was approved by FDA. It was thought of as a major milestone for AM and the current regulatory bodies with its accompanying legal framework. However, upon closer examination, it is apparent that the approval was more for a new mass production of equivalent product, rather than that of a personalised pharmaceutical dosage form [275]. Furthermore, the ZipDose® technology used is most similar to traditional powder compaction for mass manufacturing of pharmaceutical tablets, as compared to other AM methods. Since then, no other AM pharmaceutical dosage form has been approved by FDA.

The path to meeting current regulatory requirements of FDA is an uphill task that can impede the introduction of AM pharmaceutical dosage forms to the market. As of current, there are no fixed guidelines for the regulation of AM pharmaceutical dosage forms. Several key questions need to be clarified when setting out the regulatory requirement for AM pharmaceutical dosage forms. 1) Will the regulation include the initial “pharmaceutical ink”, 3D printer and final product? If so, some of the initial inks may be toxic to humans, but the product is not, as in the case of vat polymerisation AM pharmaceutical dosage forms. 2) Will all the different AM technologies be regulated by FDA? This may be tedious to include all various technologies as materials used by each technology can be quite distinct from the other. 3) Will the regulatory approval require human results from clinical trials such as the typical Phase I to Phase 3 clinical trials for current pharmaceutical products? Typical clinical trials require 20 to 100 healthy volunteers, up to several hundred people with diseases/conditions and 300 to 3000 volunteers with disease/condition for the phase 1, 2 and 3 respectively [276]. However, in many cases of personalised pharmaceutical dosage forms, each product has only 1 single subject. It will be important to determine a fundamentally new method of fulfilling this requirement.

Beyond these fundamental questions for setting up a traditional regulatory framework, it may be possible to also draw experiences from the

FDA approval of AM medical devices, for the purpose in AM pharmaceutical dosage forms. Approximately eighty-five AM medical devices such as prosthetics and implants have gained FDA approval [277]. Most of the devices have received FDA approval through either the 510(k) or emergency use pathways. In the 510(k) pathway, AM product is demonstrated to be substantially equivalent to a legally marketed device. Such a regulatory approach can also be implemented for pharmaceutical products by approving an AM dosage form as a bioequivalent product to approved ones. It is unlikely that AM pharmaceutical dosage forms can be approved through the emergency use pathway, since during emergencies, the drug moiety would have been administered intravenously, instead of using a dosage form such as tablet. However, this emergency use pathway may be a viable route for AM drug eluting implants that are personalised to the human anatomy. Unfortunately, based on the above 2 mentioned pathways, it also means that AM pharmaceutical dosage forms can only at best, be complementary to traditional manufacturing, as every approval of AM pharmaceutical dosage forms is tagged on to a legally marketed dosage forms made from traditional manufacturing. Any new entity or drug moiety will then face additional regulatory requirement should it be AM as compared to traditional manufacturing. Therefore, it is vital that traditional FDA approval routes be clearly thought through for the approval of AM pharmaceutical dosage forms.

5.5. Cost effectiveness

The use of AM has increased significantly in recent years, with its applications in various industry sectors such as automotive, consumer electronics and healthcare (or medical) industries [2]. In many instances, the cost of fabricating a product using AM exceeds that of traditional manufacturing.

Current research, based on a compilation from the US Department of Commerce, reveals that AM in general, is cost effective for manufacturing small batches with continued centralised manufacturing [278]. The bulk of the cost for AM comes from the material used, but with the increasing adoption of AM, it may lead to a further reduction in raw material cost through economies of scale. This reduction in cost may further promote the usage of AM. The hardware for AM, also a key component of the cost, has been on a decline with a reduction in cost of 51% from year 2001 to 2011, after adjusting for inflation [278].

In terms of the utilisation of final product, AM allows the fabrication of products that were previously impossible using traditional manufacturing, such as a multi drug personalised tablet. Yet, these potential advantages may not always be obvious in different situations. Ill-structured cost, or hidden cost [279] such as the time cost spent on designing and fabricating the drug delivery system may erode away the much expected advantage of AM of drug delivery systems. In emergency situations, the advantage of AM may be negligible due to the time constraint imposed by the patient's or user's condition. In these cases, a traditionally manufactured tablet may be more advantageous as compared to AM. However, it is often difficult to measure the ill-structured cost and this difficulty may also be a culprit to the slow adoption of AM for pharmaceutical applications.

6. Conclusion

The rapidly expanding and evolving AM technologies, together with emergence of 3D printable materials embedded with drug moieties have huge potential in dosage form personalisation required by patients. Unique functionalities, such as sustained zero order drug kinetics tablet or personalised microneedle patch and drug eluting implants, never achievable by mass manufacturing, are now possible with the use of AM. This can revolutionize the manufacture of dosage forms and providing more relevant, effective and safe dose to the patient.

Several AM technologies have been employed to fabricate drug delivery and testing systems. Out of which, FDM and BJ have emerged

in recent years to be spearheading the fabrication of AM oral solid dosage forms. Other photo-polymerisation based 3D printers with high resolution have also been pivotal in developing drug testing systems.

Despite making massive achievements in other manufacturing industries, such as aerospace and automobile, AM of drug delivery and testing systems is still at its infancy. Several technical and regulatory challenges need to be overcome before mainstream adoption in the pharmaceutical industry. However, with the speed of development and the unique functionalities that AM brings to personalised dosage forms, it is without doubt in our opinion that AM will become a mainstream manufacturing tool in the future for pharmaceutical applications.

References

- [1] L.K. Prasad, H. Smyth, 3D printing technologies for drug delivery: a review, *Drug Dev. Ind. Pharm.* 42 (2016) 1019–1031.
- [2] C.Y. Liaw, M. Guvendiren, Current and emerging applications of 3D printing in medicine, *Biofabrication* 9 (2017), 024102.
- [3] B.H. Daniel Günther, Johannes Franz Günther and Ingo Ederer, continuous 3D-printing for additive manufacturing, *Rapid Prototyp. J.* 20 (2014) 320–327.
- [4] Spritam—a new formulation of levetiracetam for epilepsy, *Med. Lett. Drugs Ther.* 58 (2016) 78–79.
- [5] M. Palo, J. Hollander, J. Suominen, J. Yliruusi, N. Sandler, 3D printed drug delivery devices: perspectives and technical challenges, *Expert Rev. Med. Devices* 14 (2017) 685–696.
- [6] J. Norman, R.D. Madurawe, C.M. Moore, M.A. Khan, A. Khairuzzaman, A new chapter in pharmaceutical manufacturing: 3D-printed drug products, *Adv. Drug Deliv. Rev.* 108 (2017) 39–50.
- [7] K. Park, 3D printing of 5-drug poly pill, *J. Control. Release* 217 (2015) 352.
- [8] W. Wu, Q. Zheng, X. Guo, J. Sun, Y. Liu, A programmed release multi-drug implant fabricated by three-dimensional printing technology for bone tuberculosis therapy, *Biomed. Mater.* 4 (2009), 065005.
- [9] H. Vakili, R. Kolakovic, N. Genina, M. Marmion, H. Salo, P. Ihalainen, J. Peltonen, N. Sandler, Hyperspectral imaging in quality control of inkjet printed personalised dosage forms, *Int. J. Pharm.* 483 (2015) 244–249.
- [10] S.H. Lim, S.M. Chia, L. Kang, K.Y. Yap, Three-dimensional printing of carbamazepine sustained-release scaffold, *J. Pharm. Sci.* 105 (2016) 2155–2163.
- [11] Y.E. Choonara, L.C. du Toit, P. Kumar, P.P. Kondiah, V. Pillay, 3D-printing and the effect on medical costs: a new era? *Expert Rev. Pharmacoecon. Outcomes Res.* 16 (2016) 23–32.
- [12] M.S. Stephanie, B.W. Stephen, The future of three-dimensional printing: intellectual property or intellectual confinement? *New Media Soc.* 18 (2014) 138–155.
- [13] Hype cycle for 3D printing, <https://www.gartner.com/doc/3759564/hype-cycle-d-printing-2017>, Accessed date: 4 April 2018.
- [14] W.K. Hsiao, B. Lorber, H. Reitsamer, J. Khinast, 3D printing of oral drugs: a new reality or hype? *Expert Opin. Drug Deliv.* (2017) 1–4.
- [15] N. Sandler, M. Preis, Printed drug-delivery systems for improved patient treatment, *Trends Pharmacol. Sci.* 37 (2016) 1070–1080.
- [16] L. Zema, A. Melocchi, A. Maroni, A. Gazzaniga, Three-dimensional printing of medicinal products and the challenge of personalized therapy, *J. Pharm. Sci.* 106 (2017) 1697–1705.
- [17] U.S. FDA, 3D Printing of Medical Devices, U.S. Food & Drug Administration, 2018 <https://www.fda.gov/downloads/MedicalDevices/DeviceRegulationandGuidance/GuidanceDocuments/UCM499809.pdf>, Accessed date: 21 March 2018.
- [18] I. Gibson, D. Rosen, B. Stucker, *Additive Manufacturing Technologies*, Second ed. Springer-Verlag, New York, 2015.
- [19] A. Marino, J. Barsotti, G. de Vito, C. Filippeschi, B. Mazzolai, V. Piazza, M. Labardi, V. Mattoli, G. Ciofani, Two-photon lithography of 3D nanocomposite piezoelectric scaffolds for cell stimulation, *ACS Appl. Mater. Interfaces* 7 (2015) 25574–25579.
- [20] H. Stratesteffen, M. Kopf, F. Kreimendahl, A. Blaeser, S. Jockenhoel, H. Fischer, GelMA-collagen blends enable drop-on-demand 3D printability and promote angiogenesis, *Biofabrication* 9 (2017), 045002.
- [21] M.A. Alhnan, T.C. Okwuosa, M. Sadia, K.W. Wan, W. Ahmed, B. Arafat, Emergence of 3D printed dosage forms: opportunities and challenges, *Pharm. Res.* 33 (2016) 1817–1832.
- [22] J. Goole, K. Amighi, 3D printing in pharmaceuticals: a new tool for designing customized drug delivery systems, *Int. J. Pharm.* 499 (2016) 376–394.
- [23] U.K. Roopavath, D.M. Kalaskar, 1 - Introduction to 3D Printing in Medicine, 3D Printing in Medicine, Woodhead Publishing, 2017 1–20.
- [24] A. Goyanes, M. Kobayashi, R. Martinez-Pacheco, S. Gaisford, A.W. Basit, Fused-filament 3D printing of drug products: microstructure analysis and drug release characteristics of PVA-based caplets, *Int. J. Pharm.* 514 (2016) 290–295.
- [25] Y. Sun, S. Soh, Printing tablets with fully customizable release profiles for personalized medicine, *Adv. Mater.* 27 (2015) 7847–7853.
- [26] C.W. Rowe, W.E. Katstra, R.D. Palazzolo, B. Giritlioglu, P. Teung, M.J. Cima, Multimechanism oral dosage forms fabricated by three dimensional printing, *J. Control. Release* 66 (2000) 11–17.
- [27] G.F. Acosta-Velez, C.S. Linsley, M.C. Craig, B.M. Wu, Photocurable bioink for the inkjet 3D pharming of hydrophilic drugs, *Bioengineering (Basel)* 4 (2017).
- [28] E.A. Clark, M.R. Alexander, D.J. Irvine, C.J. Roberts, M.J. Wallace, S. Sharpe, J. Yoo, R.J. M. Hague, C.J. Tuck, R.D. Wildman, 3D printing of tablets using inkjet with UV photoinitiation, *Int. J. Pharm.* 529 (2017) 523–530.
- [29] A. Goyanes, P. Robles Martinez, A. Buanz, A.W. Basit, S. Gaisford, Effect of geometry on drug release from 3D printed tablets, *Int. J. Pharm.* 494 (2015) 657–663.
- [30] T. Tagami, K. Fukushige, E. Ogawa, N. Hayashi, T. Ozeki, 3D printing factors important for the fabrication of polyvinylalcohol filament-based tablets, *Biol. Pharm. Bull.* 40 (2017) 357–364.
- [31] A. Goyanes, A.B. Buanz, A.W. Basit, S. Gaisford, Fused-filament 3D printing (3DP) for fabrication of tablets, *Int. J. Pharm.* 476 (2014) 88–92.
- [32] N. Sandler, A. Maattanen, P. Ihalainen, L. Kronberg, A. Meierjohann, T. Viitala, J. Peltonen, Inkjet printing of drug substances and use of porous substrates-towards individualized dosing, *J. Pharm. Sci.* 100 (2011) 3386–3395.
- [33] K. Park, I.C. Kwon, K. Park, Oral protein delivery: current status and future prospect, *React. Funct. Polym.* 71 (2011) 280–287.
- [34] B.F. Choonara, Y.E. Choonara, P. Kumar, D. Bijukumar, L.C. du Toit, V. Pillay, A review of advanced oral drug delivery technologies facilitating the protection and absorption of protein and peptide molecules, *Biotechnol. Adv.* 32 (2014) 1269–1282.
- [35] N. Ramadhani, M. Shabir, C. McConville, Preparation and characterisation of Kolliphor(R) P 188 and P 237 solid dispersion oral tablets containing the poorly water soluble drug disulfiram, *Int. J. Pharm.* 475 (2014) 514–522.
- [36] B. Darpo, H. Xue, N. Adetoro, B.G. Matthews, H.S. Pentikis, Thorough QT/QTc evaluation of the cardiac safety of secnidazole at therapeutic and supratherapeutic doses in healthy individuals, *J. Clin. Pharmacol.* 58 (3) (2018) 286–293.
- [37] D. Stepanova, R.G. Beran, The benefits of antiepileptic drug (AED) blood level monitoring to complement clinical management of people with epilepsy, *Epilepsy Behav.* 42 (2015) 7–9.
- [38] A. Hoffman, D. Stepensky, E. Lavy, S. Eyal, E. Klausner, M. Friedman, Pharmacokinetic and pharmacodynamic aspects of gastroretentive dosage forms, *Int. J. Pharm.* 277 (2004) 141–153.
- [39] C.M. Lopes, C. Bettencourt, A. Rossi, F. Buttini, P. Barata, Overview on gastroretentive drug delivery systems for improving drug bioavailability, *Int. J. Pharm.* 510 (2016) 144–158.
- [40] X. Chai, H. Chai, X. Wang, J. Yang, J. Li, Y. Zhao, W. Cai, T. Tao, X. Xiang, Fused deposition modeling (FDM) 3D printed tablets for intragastric floating delivery of domperidone, *Sci. Rep.* 7 (2017) 2829.
- [41] A.D. Miller, G.L. Krauss, F.M. Hamzeh, Improved CNS tolerability following conversion from immediate- to extended-release carbamazepine, *Acta Neurol. Scand.* 109 (2004) 374–377.
- [42] J.P. Pelletier, J. Martel-Pelletier, F. Rannou, C. Cooper, Efficacy and safety of oral NSAIDs and analgesics in the management of osteoarthritis: evidence from real-life setting trials and surveys, *Semin. Arthritis Rheum.* 45 (2016) S22–27.
- [43] D.G. Yu, C. Branford-White, Z.H. Ma, L.M. Zhu, X.Y. Li, X.L. Yang, Novel drug delivery devices for providing linear release profiles fabricated by 3DP, *Int. J. Pharm.* 370 (2009) 160–166.
- [44] J. Wang, A. Goyanes, S. Gaisford, A.W. Basit, Stereolithographic (SLA) 3D printing of oral modified-release dosage forms, *Int. J. Pharm.* 503 (2016) 207–212.
- [45] D.G. Yu, X.L. Yang, W.D. Huang, J. Liu, Y.G. Wang, H. Xu, Tablets with material gradients fabricated by three-dimensional printing, *J. Pharm. Sci.* 96 (2007) 2446–2456.
- [46] H.Y. Hsu, S. Toth, G.J. Simpson, M.T. Harris, Drop printing of pharmaceuticals: effect of molecular weight on PEG coated-naproxen/PEG3350 solid dispersions, *AIChE J.* 61 (2015) 4502–4508.
- [47] J. Skowrya, K. Pietrzak, M.A. Alhnan, Fabrication of extended-release patient-tailored prednisolone tablets via fused deposition modelling (FDM) 3D printing, *Eur. J. Pharm. Sci.* 68 (2015) 11–17.
- [48] M. Kyobula, A. Adediji, M.R. Alexander, E. Saleh, R. Wildman, I. Ashcroft, P.R. Gellert, C.J. Roberts, 3D inkjet printing of tablets exploiting bespoke complex geometries for controlled and tuneable drug release, *J. Control. Release* 261 (2017) 207–215.
- [49] J. Zhang, X. Feng, H. Patil, R.V. Tiwari, M.A. Repka, Coupling 3D printing with hot-melt extrusion to produce controlled-release tablets, *Int. J. Pharm.* 519 (2017) 186–197.
- [50] A. Goyanes, A.B. Buanz, G.B. Hatton, S. Gaisford, A.W. Basit, 3D printing of modified-release aminosaliclylate (4-ASA and 5-ASA) tablets, *Eur. J. Pharm. Biopharm.* 89 (2015) 157–162.
- [51] F. Fina, A. Goyanes, S. Gaisford, A.W. Basit, Selective laser sintering (SLS) 3D printing of medicines, *Int. J. Pharm.* 529 (2017) 285–293.
- [52] T.C. Okwuosa, D. Stefaniak, B. Arafat, A. Isreb, K.W. Wan, M.A. Alhnan, A lower temperature FDM 3D printing for the manufacture of patient-specific immediate release tablets, *Pharm. Res.* 33 (2016) 2704–2712.
- [53] M. Sadia, A. Sosnicka, B. Arafat, A. Isreb, W. Ahmed, A. Kelaraks, M.A. Alhnan, Adaptation of pharmaceutical excipients to FDM 3D printing for the fabrication of patient-tailored immediate release tablets, *Int. J. Pharm.* 513 (2016) 659–668.
- [54] A. Goyanes, H. Chang, D. Sedough, G.B. Hatton, J. Wang, A. Buanz, S. Gaisford, A.W. Basit, Fabrication of controlled-release budesonide tablets via desktop (FDM) 3D printing, *Int. J. Pharm.* 496 (2015) 414–420.
- [55] A. Goyanes, F. Fina, A. Martorana, D. Sedough, S. Gaisford, A.W. Basit, Development of modified release 3D printed tablets (printlets) with pharmaceutical excipients using additive manufacturing, *Int. J. Pharm.* 527 (2017) 21–30.
- [56] T.C. Okwuosa, B.C. Pereira, B. Arafat, M. Cieszyńska, A. Isreb, M.A. Alhnan, Fabricating a shell-core delayed release tablet using dual FDM 3D printing for patient-centred therapy, *Pharm. Res.* 34 (2017) 427–437.

- [57] T. Pascual, M. Apellaniz-Ruiz, C. Pernaut, C. Cueto-Felgueroso, P. Villalba, C. Alvarez, L. Manso, L. Inglada-Perez, M. Robledo, C. Rodriguez-Antona, E. Ciruelos, Polymorphisms associated with everolimus pharmacokinetics, toxicity and survival in metastatic breast cancer, *PLoS One* 12 (2017), e0180192.
- [58] N. Scoutaris, M.R. Alexander, P.R. Gellert, C.J. Roberts, Inkjet printing as a novel medicine formulation technique, *J. Control. Release* 156 (2011) 179–185.
- [59] S.A. Khaled, J.C. Burley, M.R. Alexander, J. Yang, C.J. Roberts, 3D printing of five-in-one dose combination polypill with defined immediate and sustained release profiles, *J. Control. Release* 217 (2015) 308–314.
- [60] S.A. Khaled, J.C. Burley, M.R. Alexander, C.J. Roberts, Desktop 3D printing of controlled release pharmaceutical bilayer tablets, *Int. J. Pharm.* 461 (2014) 105–111.
- [61] A. Goyanes, J. Wang, A. Buanz, R. Martinez-Pacheco, R. Telford, S. Gaisford, A.W. Basit, 3D printing of medicines: engineering novel oral devices with unique design and drug release characteristics, *Mol. Pharm.* 12 (2015) 4077–4084.
- [62] Q. Li, H. Wen, D. Jia, X. Guan, H. Pan, Y. Yang, S. Yu, Z. Zhu, R. Xiang, W. Pan, Preparation and investigation of controlled-release glipizide novel oral device with three-dimensional printing, *Int. J. Pharm.* 525 (2017) 5–11.
- [63] R.C.R. Beck, P.S. Chaves, A. Goyanes, B. Vukosavljevic, A. Buanz, M. Windbergs, A.W. Basit, S. Gaisford, 3D printed tablets loaded with polymeric nanocapsules: an innovative approach to produce customized drug delivery systems, *Int. J. Pharm.* 528 (2017) 268–279.
- [64] S.A. Khaled, J.C. Burley, M.R. Alexander, J. Yang, C.J. Roberts, 3D printing of tablets containing multiple drugs with defined release profiles, *Int. J. Pharm.* 494 (2015) 643–650.
- [65] F. Liu, A. Ghaffur, J. Bains, S. Hamdy, Acceptability of oral solid medicines in older adults with and without dysphagia: a nested pilot validation questionnaire based observational study, *Int. J. Pharm.* 512 (2016) 374–381.
- [66] .M. Jagani, H. Legay, S.R. Ranmal, J. Bertrand, K. Ooi, C. Tuleu, Can a flavored spray (pill glide) help children swallow their medicines? A pilot study, *Pediatrics* 138 (2016).
- [67] J. Levin, H. Maibach, Interindividual variation in transdermal and oral drug deliveries, *J. Pharm. Sci.* 101 (2012) 4293–4307.
- [68] A.A. Konta, M. García-Piña, R.D. Serrano, Personalised 3D printed medicines: which techniques and polymers are more successful? *Bioengineering (Basel)* 4 (2017).
- [69] S. Boudriau, C. Hanzel, J. Massicotte, L. Sayegh, J. Wang, M. Lefebvre, Randomized comparative bioavailability of a novel three-dimensional printed fast-melt formulation of levetiracetam following the administration of a single 1000-mg dose to healthy human volunteers under fasting and fed conditions, *Drugs R D* 16 (2016) 229–238.
- [70] D.G. Yu, X.X. Shen, C. Branford-White, L.M. Zhu, K. White, X.L. Yang, Novel oral fast-disintegrating drug delivery devices with predefined inner structure fabricated by three-dimensional printing, *J. Pharm. Pharmacol.* 61 (2009) 323–329.
- [71] W. Jamróz, M. Kurek, E. Lyszczarz, J. Szafraniec, J. Knapik-Kowalczyk, K. Syrek, M. Paluch, R. Jachowicz, 3D printed orodispersible films with aripiprazole, *Int. J. Pharm.* 533 (2) (2017) 413–420.
- [72] K. Pietrzak, A. Isreb, M.A. Alhnan, A flexible-dose dispenser for immediate and extended release 3D printed tablets, *Eur. J. Pharm. Biopharm.* 96 (2015) 380–387.
- [73] A.B. Overgaard, J. Hojsted, R. Hansen, J. Moller-Sonnergaard, L.L. Christrup, Patients' evaluation of shape, size and colour of solid dosage forms, *Pharm. World Sci.* 23 (2001) 185–188.
- [74] M.R. Prausnitz, R. Langer, Transdermal drug delivery, *Nat. Biotechnol.* 26 (2008) 1261–1268.
- [75] M.P. Ratnaparkhi, Ashvini S. Kadam, Shilpa P. Chaudhary, Transdermal drug delivery: an overview, *Int. J. Res. Dev. Pharm. I Sci.* 3 (2014) 1042–1053.
- [76] P.P. Ajit Kumar Vishwakarma, Navneet Kumar Verma, Dhaneshwar Kumar Vishwakarma, Jai Narayan Mishra, An overview of transdermal patches, *Int. J. Pharm. Rev. Res.* 7 (2017) 17–23.
- [77] A. Goyanes, U. Det-Amornrat, J. Wang, A.W. Basit, S. Gaisford, 3D scanning and 3D printing as innovative technologies for fabricating personalized topical drug delivery systems, *J. Control. Release* 234 (2016) 41–48.
- [78] Z. Muwaffak, A. Goyanes, V. Clark, A.W. Basit, S.T. Hilton, S. Gaisford, Patient-specific 3D scanned and 3D printed antimicrobial polycaprolactone wound dressings, *Int. J. Pharm.* 527 (2017) 161–170.
- [79] M.H. Ling, M.C. Chen, Dissolving polymer microneedle patches for rapid and efficient transdermal delivery of insulin to diabetic rats, *Acta Biomater.* 9 (2013) 8952–8961.
- [80] S. Liu, M.N. Jin, Y.S. Quan, F. Kamiyama, H. Katsumi, T. Sakane, A. Yamamoto, The development and characteristics of novel microneedle arrays fabricated from hyaluronic acid, and their application in the transdermal delivery of insulin, *J. Control. Release* 161 (2012) 933–941.
- [81] Y. Ito, E. Hagiwara, A. Saeki, N. Sugioka, K. Takada, Feasibility of microneedles for percutaneous absorption of insulin, *Eur. J. Pharm. Sci.* 29 (2006) 82–88.
- [82] Y.H. Mohammed, M. Yamada, L.L. Lin, J.E. Grice, M.S. Roberts, A.P. Raphael, H.A. Benson, T.W. Prow, Microneedle enhanced delivery of cosmetically relevant peptides in human skin, *PLoS One* 9 (2014), e101956.
- [83] K. van der Maaden, W. Jiskoot, J. Bouwstra, Microneedle technologies for (trans) dermal drug and vaccine delivery, *J. Control. Release* 161 (2012) 645–655.
- [84] R.F. Donnelly, T.R. Raj Singh, A.D. Woolfson, Microneedle-based drug delivery systems: microfabrication, drug delivery, and safety, *Drug Deliv.* 17 (2010) 187–207.
- [85] C.K. Choi, J.B. Kim, E.H. Jang, Y.N. Youn, W.H. Ryu, Curved biodegradable microneedles for vascular drug delivery, *Small* 8 (2012) 2483–2488.
- [86] Z. Zhu, H. Luo, W. Lu, H. Luan, Y. Wu, J. Luo, Y. Wang, J. Pi, C.Y. Lim, H. Wang, Rapidly dissolvable microneedle patches for transdermal delivery of exenatide, *Pharm. Res.* 31 (2014) 3348–3360.
- [87] S.H. Lim, J.Y. Ng, L. Kang, Three-dimensional printing of a microneedle array on personalized curved surfaces for dual-pronged treatment of trigger finger, *Biofabrication* 9 (2017), 015101.
- [88] Z. Ali, E.B. Türeyen, Y. Karpat, M. Çakmakçı, Fabrication of polymer microneedles for transdermal drug delivery system using DLP based projection stereo-lithography, *Procedia CIRP* 42 (2016) 87–90.
- [89] A.R. Johnson, C.L. Caudill, J.R. Tumbleston, C.J. Bloomquist, K.A. Moga, A. Ermoshkin, D. Shirvanyants, S.J. Mecham, J.C. Luft, J.M. DeSimone, Single-step fabrication of computationally designed microneedles by continuous liquid interface production, *PLoS One* 11 (2016), e0162518.
- [90] Y. Chen, B.Z. Chen, Q.L. Wang, X. Jin, X.D. Guo, Fabrication of coated polymer microneedles for transdermal drug delivery, *J. Control. Release* 265 (2017) 14–21.
- [91] M.J. Uddin, N. Scoutaris, P. Klepetsanis, B. Chowdhry, M.R. Prausnitz, D. Douroumis, Inkjet printing of transdermal microneedles for the delivery of anticancer agents, *Int. J. Pharm.* 494 (2015) 593–602.
- [92] S.D. Gittard, A. Ovsianikov, N.A. Monteiro-Riviere, J. Lusk, P. Morel, P. Minghetti, C. Lenardi, B.N. Chichkov, R.J. Narayan, Fabrication of polymer microneedles using a two-photon polymerization and micromolding process, *J. Diabetes Sci. Technol.* 3 (2009) 304–311.
- [93] S.D. Gittard, A. Ovsianikov, H. Akar, B. Chichkov, N.A. Monteiro-Riviere, S. Stafslie, B. Chisholm, C.C. Shin, C.M. Shih, S.J. Lin, Y.Y. Su, R.J. Narayan, Two photon polymerization-micromolding of polyethylene glycol-gentamicin sulfate microneedles, *Adv. Eng. Mater.* 12 (2010) B77–B82.
- [94] A. Doraiswamy, C. Jin, R.J. Narayan, P. Mageswaran, P. Mente, R. Modi, R. Auyeung, D.B. Chrisey, A. Ovsianikov, B. Chichkov, Two photon induced polymerization of organic-inorganic hybrid biomaterials for microstructured medical devices, *Acta Biomater.* 2 (2006) 267–275.
- [95] C. Chiappini, E. De Rosa, J.O. Martinez, X. Liu, J. Steele, M.M. Stevens, E. Tasciotti, Biodegradable silicon nanoneedles delivering nucleic acids intracellularly induce localized *in vivo* neovascularization, *Nat. Mater.* 14 (2015) 532–539.
- [96] S.D. Gittard, P.R. Miller, C. Jin, T.N. Martin, R.D. Boehm, B.J. Chisholm, S.J. Stafslie, J. W. Daniels, N. Cilz, N.A. Monteiro-Riviere, A. Nasir, R.J. Narayan, Deposition of antimicrobial coatings on microstereolithography-fabricated microneedles, *JOM* 63 (2011) 59–68.
- [97] J. Weisman, N. Kaskas, A. Green, D. Ballard, J. Ambrose, L. Sun, D. Mills, Three-dimensional printing of chemotherapeutic and antibiotic eluting fibers, seeds, and discs for localized drug delivery in cutaneous disease, 2015 Annual Meeting of the Society for Investigative Dermatology, May 2015, p. S92, Albuquerque, New Mexico, Abstract number 536.
- [98] E. Espey, T. Ogburn, Long-acting reversible contraceptives: intrauterine devices and the contraceptive implant, *Obstet. Gynecol.* 117 (2011) 705–719.
- [99] Y. Sun, X. Ruan, H. Li, H. Kathuria, G. Du, L. Kang, Fabrication of non-dissolving analgesic suppositories using 3D printed moulds, *Int. J. Pharm.* 513 (2016) 717–724.
- [100] F. Tudela, R. Kelley, C. Ascher-Walsh, J.L. Stone, Low cost 3D printing for the creation of cervical cerclage pessary used to prevent preterm birth, *Obstet. Gynecol.* 127 (2016) 154S.
- [101] J.P. Mufaddal, L. F. Thomas, L. Annela, S. Gloria, An innovative pessary, SLIP, and the molds used to print the pessary, USA, <https://www.engr.wisc.edu/students-develop-innovative-devices-through-biomedical-engineering-design/> 2015, Accessed date: 15 October 2017.
- [102] K. Tappa, U. Jammalamadaka, D.H. Ballard, T. Bruno, M.R. Israel, H. Vemula, J.M. Meacham, D.K. Mills, P.K. Woodard, J.A. Weisman, Medication eluting devices for the field of OBGYN (MEDOBYGN): 3D printed biodegradable hormone eluting constructs, a proof of concept study, *PLoS One* 12 (2017), e0182929.
- [103] J.A. Weisman, C. Nicholson, D. Mills, Methods and devices for three-dimensional printing or additive manufacturing of bioactive medical devices, Google Patents, 2016.
- [104] N. Genina, J. Hollander, H. Jukarainen, E. Makila, J. Salonen, N. Sandler, Ethylene vinyl acetate (EVA) as a new drug carrier for 3D printed medical drug delivery devices, *Eur. J. Pharm. Sci.* 90 (2016) 53–63.
- [105] J. Hollander, N. Genina, H. Jukarainen, M. Khajeheian, A. Rosling, E. Makila, N. Sandler, Three-dimensional printed PCL-based implantable prototypes of medical devices for controlled drug delivery, *J. Pharm. Sci.* 105 (2016) 2665–2676.
- [106] J. Hakim, J.E. Dietrich, P.A. Smith, C. Buskmiller, Vaginal stents, vaginal dilators, and methods of fabricating the same, Google Patents, 2016.
- [107] N.M. Elman, C.A. Apostolis, Stent devices for support, controlled drug delivery and pain management after vaginal surgery, Google Patents, 2013.
- [108] A. Jaklencic, W. Gates, P.A. Eckhoff, B. Nikolic, L.L. Wood, Jr., R.S. Langer, Micromolded or 3-D printed pulsatile release vaccine formulations, Google Patents, USA 2015, pp. 42pp.
- [109] J. Pouliot, K. Goldberg, I.C. Hsu, J.A.M. Chnha, A. Garg, S. Patel, P. Abbeel, T. Siau, Patient-specific temporary implants for accurately guiding local means of tumor control along patient-specific internal channels to treat cancer, Google Patents, USA, 2016, pp. 70pp.
- [110] N. Sandler, I. Salmela, A. Fallarero, A. Rosling, M. Khajeheian, R. Kolakovic, N. Genina, J. Nyman, P. Vuorela, Towards fabrication of 3D printed medical devices to prevent biofilm formation, *Int. J. Pharm.* 459 (2014) 62–64.
- [111] J. Boetker, J.J. Water, J. Aho, L. Arnfast, A. Bohr, J. Rantanen, Modifying release characteristics from 3D printed drug-eluting products, *Eur. J. Pharm. Sci.* 90 (2016) 47–52.
- [112] J.J. Water, A. Bohr, J. Boetker, J. Aho, N. Sandler, H.M. Nielsen, J. Rantanen, Three-dimensional printing of drug-eluting implants: preparation of an antimicrobial poly lactide feedstock material, *J. Pharm. Sci.* 104 (2015) 1099–1107.
- [113] J.A. Weisman, J.C. Nicholson, K. Tappa, U. Jammalamadaka, C.G. Wilson, D.K. Mills, Antibiotic and chemotherapeutic enhanced three-dimensional printer filaments and constructs for biomedical applications, *Int. J. Nanomedicine* 10 (2015) 357–370.
- [114] K.L. Fujimoto, J. Guan, H. Oshima, T. Sakai, W.R. Wagner, *In vivo* evaluation of a porous, elastic, biodegradable patch for reconstructive cardiac procedures, *Ann. Thorac. Surg.* 83 (2007) 648–654.

- [115] H. Kathuria, H. Li, J. Pan, S.H. Lim, J.S. Kochhar, C. Wu, L. Kang, Large size microneedle patch to deliver lidocaine through skin, *Pharm. Res.* 33 (2016) 2653–2667.
- [116] H. Kathuria, J.S. Kochhar, M.H. Fong, M. Hashimoto, C. Iliescu, H. Yu, L. Kang, Polymeric microneedle array fabrication by photolithography, *J. Vis. Exp.* 105 (2015), 52914. <https://doi.org/10.3791/52914>.
- [117] H.G. Yi, Y.J. Choi, K.S. Kang, J.M. Hong, R.G. Pati, M.N. Park, I.K. Shim, C.M. Lee, S.C. Kim, D.W. Cho, A 3D-printed local drug delivery patch for pancreatic cancer growth suppression, *J. Control. Release* 238 (2016) 231–241.
- [118] J.C. Wang, H. Zheng, M.W. Chang, Z. Ahmad, J.S. Li, Preparation of active 3D film patches via aligned fiber electrohydrodynamic (EHD) printing, *Sci. Rep.* 7 (2017) 43924.
- [119] D.H. Ballard, J.A. Weisman, U. Jammalamadaka, K. Tappa, J.S. Alexander, F.D. Griffen, Three-dimensional printing of bioactive hernia meshes: *in vitro* proof of principle, *Surgery* 161 (2017) 1479–1481.
- [120] J.A. Weisman, U. Jammalamadaka, K. Tappa, J.C. Nicholson, D.H. Ballard, C.G. Wilson, H. D'Agostino, D.K. Mills, 3D printing antibiotic and chemotherapeutic eluting catheters and constructs, *J. Vasc. Interv. Radiol.* 26 (2015) S12.
- [121] R. van Lith, E. Baker, H. Ware, J. Yang, A.C. Farshed, C. Sun, G. Ameer, 3D-printing strong high-resolution antioxidant bioresorbable vascular stents, *Adv. Mater. Technol.* 1 (2016) 1600138.
- [122] S.K. Misra, F. Ostadhosseini, R. Babu, J. Kus, D. Tankasala, A. Sutrisno, K.A. Walsh, C.R. Bromfield, D. Pan, 3D-printed multidrug-eluting stent from graphene-nanoplatelet-doped biodegradable polymer composite, *Adv. Healthc. Mater.* 6 (2017).
- [123] D.J. Horst, S.M. Tebcherani, E.T. Kubaski, R. de Almeida Vieira, Bioactive potential of 3D-printed oleo-gum-resin disks: *B. papyrifera*, *C. myrrha*, and *S. benzoin* loading nanooxides-TiO₂, P25, Cu₂O, and MoO₃, *Bioinorg. Chem. Appl.* 2017 (2017) 6398167.
- [124] Y.C. Chou, D. Lee, T.M. Chang, Y.H. Hsu, Y.H. Yu, E.C. Chan, S.J. Liu, Combination of a biodegradable three-dimensional (3D) - printed cage for mechanical support and nanofibrous membranes for sustainable release of antimicrobial agents for treating the femoral metaphyseal comminuted fracture, *J. Mech. Behav. Biomed. Mater.* 72 (2017) 209–218.
- [125] W. Huang, Q. Zheng, W. Sun, H. Xu, X. Yang, Levofloxacin implants with predefined microstructure fabricated by three-dimensional printing technique, *Int. J. Pharm.* 339 (2007) 33–38.
- [126] W. Wu, Q. Zheng, X. Guo, W. Huang, The controlled-releasing drug implant based on the three dimensional printing technology: fabrication and properties of drug releasing *in vivo*, *J. Wuhan Univ. Technol. Mat. Sci. Ed.* 24 (2009) 977–981.
- [127] W. Wu, C. Ye, Q. Zheng, G. Wu, Z. Cheng, A therapeutic delivery system for chronic osteomyelitis via a multi-drug implant based on three-dimensional printing technology, *J. Biomater. Appl.* 31 (2016) 250–260.
- [128] G. Wu, W. Wu, Q. Zheng, J. Li, J. Zhou, Z. Hu, Experimental study of PLLA/INH slow release implant fabricated by three dimensional printing technique and drug release characteristics *in vitro*, *Biomed. Eng. Online* 13 (2014) 97.
- [129] J.H. Shim, S.E. Kim, J.Y. Park, J. Kundu, S.W. Kim, S.S. Kang, D.W. Cho, Three-dimensional printing of rhBMP-2-loaded scaffolds with long-term delivery for enhanced bone regeneration in a rabbit diaphyseal defect, *Tissue Eng. A* 20 (2014) 1980–1992.
- [130] J.H. Shim, J.B. Huh, J.Y. Park, Y.C. Jeon, S.S. Kang, J.Y. Kim, J.W. Rhie, D.W. Cho, Fabrication of blended polycaprolactone/poly(lactic-co-glycolic acid)/beta-tricalcium phosphate thin membrane using solid freeform fabrication technology for guided bone regeneration, *Tissue Eng. A* 19 (2013) 317–328.
- [131] D. Yu, Q. Li, X. Mu, T. Chang, Z. Xiong, Bone regeneration of critical calvarial defect in goat model by PLGA/TCP/rhBMP-2 scaffolds prepared by low-temperature rapid-prototyping technology, *Int. J. Oral Maxillofac. Surg.* 37 (2008) 929–934.
- [132] J.A. Parry, M.G. Olthof, K.L. Shogren, M. Dadsetan, A. Van Wijnen, M. Yaszemski, S. Kakar, Three-dimension-printed porous poly(propylene fumarate) scaffolds with delayed rhBMP-2 release for anterior cruciate ligament graft fixation, *Tissue Eng. A* 23 (2017) 359–365.
- [133] T. Ahlfeld, A.R. Akkineni, Y. Forster, T. Kohler, S. Knaack, M. Gelinsky, A. Lode, Design and fabrication of complex scaffolds for bone defect healing: combined 3D plotting of a calcium phosphate cement and a growth factor-loaded hydrogel, *Ann. Biomed. Eng.* 45 (2017) 224–236.
- [134] K.C. Hung, C.S. Tseng, L.G. Dai, S.H. Hsu, Water-based polyurethane 3D printed scaffolds with controlled release function for customized cartilage tissue engineering, *Biomaterials* 83 (2016) 156–168.
- [135] S.J. Lee, D. Lee, T.R. Yoon, H.K. Kim, H.H. Jo, J.S. Park, J.H. Lee, W.D. Kim, I.K. Kwon, S. A. Park, Surface modification of 3D-printed porous scaffolds via mussel-inspired polydopamine and effective immobilization of rhBMP-2 to promote osteogenic differentiation for bone tissue engineering, *Acta Biomater.* 40 (2016) 182–191.
- [136] S. Li, Y. Xu, J. Yu, M.L. Becker, Enhanced osteogenic activity of poly(ester urea) scaffolds using facile post-3D printing peptide functionalization strategies, *Biomaterials* 141 (2017) 176–187.
- [137] J. Jensen, J.H. Rolfing, D.Q. Le, A.A. Kristiansen, J.V. Nygaard, L.B. Hokland, M. Bendtsen, M. Kassem, H. Lysdahl, C.E. Bungler, Surface-modified functionalized polycaprolactone scaffolds for bone repair: *in vitro* and *in vivo* experiments, *J. Biomed. Mater. Res. A* 102 (2014) 2993–3003.
- [138] Y.C. Chou, D. Lee, T.M. Chang, Y.H. Hsu, Y.H. Yu, S.J. Liu, S.W. Ueng, Development of a three-dimensional (3D) printed biodegradable cage to convert morselized corticocancellous bone chips into a structured cortical bone graft, *Int. J. Mol. Sci.* 17 (2016).
- [139] S. Yang, J. Wang, L. Tang, H. Ao, H. Tan, T. Tang, C. Liu, Mesoporous bioactive glass doped-poly (3-hydroxybutyrate-co-3-hydroxyhexanoate) composite scaffolds with 3-dimensionally hierarchical pore networks for bone regeneration, *Colloids Surf. B: Biointerfaces* 116 (2014) 72–80.
- [140] M. Zhu, K. Li, Y. Zhu, J. Zhang, X. Ye, 3D-printed hierarchical scaffold for localized isoniazid/rifampin drug delivery and osteoarticular tuberculosis therapy, *Acta Biomater.* 16 (2015) 145–155.
- [141] M. Zhu, H. Wang, J. Liu, H. He, X. Hua, Q. He, L. Zhang, X. Ye, J. Shi, A mesoporous silica nanoparticle/beta-TCP/BG composite drug delivery system for osteoarticular tuberculosis therapy, *Biomaterials* 32 (2011) 1986–1995.
- [142] Z. Min, Z. Shichang, X. Chen, Z. Yufang, Z. Changqing, 3D-printed dimethylallyl glycine delivery scaffolds to improve angiogenesis and osteogenesis, *Biomater. Sci.* 3 (2015) 1236–1244.
- [143] K. Li, M. Zhu, P. Xu, Y. Xi, Z. Cheng, Y. Zhu, X. Ye, Three-dimensionally plotted MBG/PHBHHx composite scaffold for antitubercular drug delivery and tissue regeneration, *J. Mater. Sci. Mater. Med.* 26 (2015) 102.
- [144] J. Zhang, S. Zhao, M. Zhu, Y. Zhu, Y. Zhang, Z. Liu, C. Zhang, 3D-printed magnetic Fe₃O₄/MBG/PCL composite scaffolds with multifunctionality of bone regeneration, local anti-cancer drug delivery and hyperthermia, *J. Mater. Chem. B* 2 (2014) 7583–7595.
- [145] J. Zhang, S. Zhao, Y. Zhu, Y. Huang, M. Zhu, C. Tao, C. Zhang, Three-dimensional printing of strontium-containing mesoporous bioactive glass scaffolds for bone regeneration, *Acta Biomater.* 10 (2014) 2269–2281.
- [146] X. Qi, P. Pei, M. Zhu, X. Du, C. Xin, S. Zhao, X. Li, Y. Zhu, Three dimensional printing of calcium sulfate and mesoporous bioactive glass scaffolds for improving bone regeneration *in vitro* and *in vivo*, *Sci. Rep.* 7 (2017) 42556.
- [147] K. Gulati, M. Prideaux, M. Kogawa, L. Lima-Marques, G.J. Atkins, D.M. Findlay, D. Losic, Anodized 3D-printed titanium implants with dual micro- and nano-scale topography promote interaction with human osteoblasts and osteocyte-like cells, *J. Tissue Eng. Regen. Med.* 11 (12) (2017) 3313–3325.
- [148] S. Maher, G. Kaur, L. Lima-Marques, A. Evdokiou, D. Losic, Engineering of micro- to nanostructured 3D-printed drug-releasing titanium implants for enhanced osseointegration and localized delivery of anticancer drugs, *ACS Appl. Mater. Interfaces* 9 (2017) 29562–29570.
- [149] Y. Gu, X. Chen, J.H. Lee, D.A. Monteiro, H. Wang, W.Y. Lee, Inkjet printed antibiotic and calcium-eluting bioresorbable nanocomposite micropatterns for orthopedic implants, *Acta Biomater.* 8 (2012) 424–431.
- [150] J.-H. Shim, M.-J. Kim, J.Y. Park, R.G. Pati, Y.-P. Yun, S.E. Kim, H.-R. Song, D.-W. Cho, Three-dimensional printing of antibiotics-loaded poly-ε-caprolactone/poly(lactic-co-glycolic acid) scaffolds for treatment of chronic osteomyelitis, *Tissue Eng. Regen. Med.* 12 (2015) 283–293.
- [151] F. Yang, C. Chen, Q. Zhou, Y. Gong, R. Li, C. Li, F. Klampfl, S. Freund, X. Wu, Y. Sun, X. Li, M. Schmidt, D. Ma, Y. Yu, Laser beam melting 3D printing of Ti6Al4V based porous structured dental implants: fabrication, biocompatibility analysis and photoelastic study, *Sci. Rep.* 7 (2017) 45360.
- [152] E. Vorndran, U. Klammert, A. Ewald, J.E. Barralet, U. Gbureck, Simultaneous immobilization of bioactives during 3D powder printing of bioceramic drug-release matrices, *Adv. Funct. Mater.* 20 (2010) 1585–1591.
- [153] J.A. Inzana, Three-Dimensional Printing of Antibiotic-Laden Calcium Phosphates for Treatment of Orthopaedic Implant-Associated Bone Infections, Department of Biomedical Engineering, University of Rochester, USA, 2015.
- [154] J.A. Inzana, R.P. Trombetta, E.M. Schwarz, S.L. Kates, H.A. Awad, 3D printed bioceramics for dual antibiotic delivery to treat implant-associated bone infection, *Eur. Cell. Mater.* 30 (2015) 232–247.
- [155] U. Gbureck, E. Vorndran, F.A. Muller, J.E. Barralet, Low temperature direct 3D printed bioceramics and biocomposites as drug release matrices, *J. Control. Release* 122 (2007) 173–180.
- [156] U. Klammert, U. Gbureck, E. Vorndran, J. Rodiger, P. Meyer-Marcotty, A.C. Kubler, 3D powder printed calcium phosphate implants for reconstruction of cranial and maxillofacial defects, *J. Craniomaxillofac. Surg.* 38 (2010) 565–570.
- [157] Y. Zhang, J. Zhu, Z. Wang, Y. Zhou, X. Zhang, Constructing a 3D-printable, bioceramic sheathed articular spacer assembly for infected hip arthroplasty, *J. Med. Hypotheses Ideas* 9 (2015) 13–19.
- [158] Y.C. Chou, W.L. Yeh, C.L. Chao, Y.H. Hsu, Y.H. Yu, J.K. Chen, S.J. Liu, Enhancement of tendon-bone healing via the combination of biodegradable collagen-loaded nanofibrous membranes and a three-dimensional printed bone-anchoring bolt, *Int. J. Nanomedicine* 11 (2016) 4173–4186.
- [159] Y. Zhang, D. Zhai, M. Xu, Q. Yao, H. Zhu, J. Chang, C. Wu, 3D-printed bioceramic scaffolds with antibacterial and osteogenic activity, *Biofabrication* 9 (2017), 025037.
- [160] S.W. Kim, C. Jeong, K.H. Chang, Y.S. Ji, B. Cho, D. Lee, Y.S. Kim, S.Y. Song, S.W. Lee, J. Kwak, Development of 3D printed applicator in brachytherapy for gynecologic cancer, *Int. J. Radiat. Oncol. Biol. Phys.* 99 (2017), E678.
- [161] J.A. Cunha, K. Mellis, R. Sethi, T. Siau, A. Sudhyadhom, A. Garg, K. Goldberg, I.C. Hsu, J. Pouliot, Evaluation of PC-ISO for customized, 3D printed, gynecologic 192-Ir HDR brachytherapy applicators, *J. Appl. Clin. Med. Phys.* 16 (2015) 5168.
- [162] R. Ricotti, A. Vavassori, A. Bazani, D. Ciardo, F. Pansini, R. Spoto, V. Sammarco, F. Cattani, G. Baroni, R. Orecchia, B.A. Jereczek-Fossa, 3D-printed applicators for high dose rate brachytherapy: dosimetric assessment at different infill percentage, *Phys. Med. Biol.* 32 (2016) 1698–1706.
- [163] R. Sethi, A. Cunha, K. Mellis, T. Siau, C. Diederich, J. Pouliot, I.C. Hsu, Clinical applications of custom-made vaginal cylinders constructed using three-dimensional printing technology, *J. Contemp. Brachytherapy* 8 (2016) 208–214.
- [164] L. Vitzthum, D. Sterling, K.E. Dusenbery, E. Ehler, 3D printed composite copper-plastic bolus for radiation therapy, *Int. J. Radiat. Oncol. Biol. Phys.* 93 (2015) S166–S167.
- [165] L. Sim, Novel application of 3D printing in brachytherapy using MED610 3D printed insert for I-125 ROPES eye plaque, *Australas. Phys. Eng. Sci. Med.* 39 (2016) 863–870.
- [166] E.L. Jones, A. Tonino Baldion, C. Thomas, T. Burrows, N. Byrne, V. Newton, S. Aldridge, Introduction of novel 3D-printed superficial applicators for high-dose-rate skin brachytherapy, *Brachytherapy* 16 (2017) 409–414.

- [167] J.M. Walker, D.A. Elliott, C.D. Kubicky, C.R. Thomas Jr., A.M. Naik, Manufacture and evaluation of 3-dimensional printed sizing tools for use during intraoperative breast brachytherapy, *Adv. Radiat. Oncol.* 1 (2016) 132–135.
- [168] S. Clarke, M. Yewondwossen, J. Robar, Brachytherapy: 3D printed surface applicators for high dose rate brachytherapy, *Med. Phys.* 43 (2016) 4934–4935.
- [169] J.R., Applications of 3D Printing in Radiation Oncology, Canada, 2016 (Accessed on: 30 Oct 2017).
- [170] T.M. Bucking, E.R. Hill, J.L. Robertson, E. Maneas, A.A. Plumb, D.I. Nikitichev, From medical imaging data to 3D printed anatomical models, *PLoS One* 12 (2017), e0178540.
- [171] F. Rengier, A. Mehndiratta, H. von Tengge-Kobligk, C.M. Zechmann, R. Unterhinninghofen, H.U. Kauczor, F.L. Giesel, 3D printing based on imaging data: review of medical applications, *Int. J. Comput. Assist. Radiol. Surg.* 5 (2010) 335–341.
- [172] A.P. Trace, D. Ortiz, A. Deal, M. Retrouvey, C. Elzie, C. Goodmurphy, J. Morey, C.M. Hawkins, Radiology's emerging role in 3-D printing: applications in health care, *J. Am. Coll. Radiol.* 13 (2016) 856–862 (e854).
- [173] E.M. Hehl, R. Beck, K. Luthard, R. Guthoff, B. Drewelow, Improved penetration of aminoglycosides and fluoroquinolones into the aqueous humour of patients by means of Acuvue contact lenses, *Eur. J. Clin. Pharmacol.* 55 (1999) 317–323.
- [174] M.R. Jain, Drug delivery through soft contact lenses, *Br. J. Ophthalmol.* 72 (1988) 150–154.
- [175] L. Xinming, C. Yingde, A.W. Lloyd, S.V. Mikhailovsky, S.R. Sandeman, C.A. Howel, L. Liewen, Polymeric hydrogels for novel contact lens-based ophthalmic drug delivery systems: a review, *Cont. Lens Anterior Eye* 31 (2008) 57–64.
- [176] A.J. Hyatt, M.S. Rajan, K. Burling, M.J. Ellington, A. Tassoni, K.R. Martin, Release of vancomycin and gentamicin from a contact lens versus a fibrin coating applied to a contact lens, *Invest. Ophthalmol. Vis. Sci.* 53 (2012) 1946–1952.
- [177] A. Hui, A. Boone, L. Jones, Uptake and release of ciprofloxacin-HCl from conventional and silicone hydrogel contact lens materials, *Eye Contact Lens* 34 (2008) 266–271.
- [178] C.C. Peng, J. Kim, A. Chauhan, Extended delivery of hydrophilic drugs from silicone-hydrogel contact lenses containing vitamin E diffusion barriers, *Biomaterials* 31 (2010) 4032–4047.
- [179] A. Boone, A. Hui, L. Jones, Uptake and release of dexamethasone phosphate from silicone hydrogel and group I, II, and IV hydrogel contact lenses, *Eye Contact Lens* 35 (2009) 260–267.
- [180] S. Mishima, A. Gasset, S.D. Klyce Jr., J.L. Baum, Determination of tear volume and tear flow, *Investig. Ophthalmol.* 5 (1966) 264–276.
- [181] R.E. Furukawa, K.A. Polse, Changes in tear flow accompanying aging, *Am. J. Optom. Physiol. Optic* 55 (1978) 69–74.
- [182] M. Bajgrowicz, C.M. Phan, L.N. Subbaraman, L. Jones, Release of ciprofloxacin and moxifloxacin from daily disposable contact lenses from an *in vitro* eye model, *Invest. Ophthalmol. Vis. Sci.* 56 (2015) 2234–2242.
- [183] A. Tieppo, K.M. Pate, M.E. Byrne, *In vitro* controlled release of an anti-inflammatory from daily disposable therapeutic contact lenses under physiological ocular tear flow, *Eur. J. Pharm. Biopharm.* 81 (2012) 170–177.
- [184] M. Ali, S. Horikawa, S. Venkatesh, J. Saha, J.W. Hong, M.E. Byrne, Zero-order therapeutic release from imprinted hydrogel contact lenses within *in vitro* physiological ocular tear flow, *J. Control. Release* 124 (2007) 154–162.
- [185] C.J. White, M.K. McBride, K.M. Pate, A. Tieppo, M.E. Byrne, Extended release of high molecular weight hydroxypropyl methylcellulose from molecularly imprinted, extended wear silicone hydrogel contact lenses, *Biomaterials* 32 (2011) 5698–5705.
- [186] J.C. Kaczmarek, A. Tieppo, C.J. White, M.E. Byrne, Adjusting biomaterial composition to achieve controlled multiple-day release of dexamethasone from an extended-wear silicone hydrogel contact lens, *J. Biomater. Sci. Polym. Ed.* 25 (2014) 88–100.
- [187] C.M. Phan, M. Bajgrowicz, H. Gao, L.N. Subbaraman, L.W. Jones, Release of fluconazole from contact lenses using a novel *in vitro* eye model, *Optom. Vis. Sci.* 93 (2016) 387–394.
- [188] B.L. Laube, The expanding role of aerosols in systemic drug delivery, gene therapy, and vaccination, *Respir. Care* 50 (2005) 1161–1176.
- [189] S. Grassin-Delye, A. Buenestado, E. Naline, C. Faisy, S. Blouquit-Laye, L.J. Couderc, M. Le Guen, M. Fischler, P. Devillier, Intranasal drug delivery: an efficient and non-invasive route for systemic administration: focus on opioids, *Pharmacol. Ther.* 134 (2012) 366–379.
- [190] B.L. Laube, Devices for aerosol delivery to treat sinusitis, *J. Aerosol Med.* 20 (Suppl. 1) (2007) S5–17 (discussion S17–18).
- [191] M. Pozzoli, H.X. Ong, L. Morgan, M. Sukkar, D. Traini, P.M. Young, F. Sonvico, Application of RPMI 2650 nasal cell model to a 3D printed apparatus for the testing of drug deposition and permeation of nasal products, *Eur. J. Pharm. Biopharm.* 107 (2016) 223–233.
- [192] D. Baumann, C. Bachert, P. Hogger, Development of a novel model for comparative evaluation of intranasal pharmacokinetics and effects of anti-allergic nasal sprays, *Eur. J. Pharm. Biopharm.* 80 (2012) 156–163.
- [193] R. Valentine, T. Athanasiadis, M. Thwin, D. Singhal, E.K. Weitzel, P.J. Wormald, A prospective controlled trial of pulsed nasal nebulizer in maximally dissected cadavers, *Am. J. Rhinol.* 22 (2008) 390–394.
- [194] M. Durand, J. Pourchez, B. Louis, J.F. Pouget, D. Isabey, A. Coste, J.M. Prades, P. Rusch, M. Cottier, Platinated nasal model: a new concept of anatomically realistic cast, *Rhinology* 49 (2011) 30–36.
- [195] W. Moller, U. Schuschnig, G. Meyer, H. Mentzel, M. Keller, Ventilation and drug delivery to the paranasal sinuses: studies in a nasal cast using pulsating airflow, *Rhinology* 46 (2008) 213–220.
- [196] V. Kundoor, R.N. Dalby, Assessment of nasal spray deposition pattern in a silicone human nose model using a color-based method, *Pharm. Res.* 27 (2010) 30–36.
- [197] H.M. Janssens, J.C. de Jongste, W.J. Fokkens, S.G. Robben, K. Wouters, H.A. Tiddens, The Sophia anatomical infant nose-throat (saint) model: a valuable tool to study aerosol deposition in infants, *J. Aerosol Med.* 14 (2001) 433–441.
- [198] J. Xi, J.E. Yuan, Y. Zhang, D. Nevroski, Z. Wang, Y. Zhou, Visualization and quantification of nasal and olfactory deposition in a sectional adult nasal airway cast, *Pharm. Res.* 33 (2016) 1527–1541.
- [199] M.T. Laine-Alava, U.K. Minkinen, Variation of nasal respiratory pattern with age during growth and development, *Laryngoscope* 107 (1997) 386–390.
- [200] A.P. Roth, C.F. Lange, W.H. Finlay, The effect of breathing pattern on nebulizer drug delivery, *J. Aerosol Med.* 16 (2003) 325–339.
- [201] B.K. Rubin, J.B. Fink, Aerosol therapy for children, *Respir. Care Clin. N. Am.* 7 (2001) 175–213 (v).
- [202] S. Minocchieri, J.M. Burren, M.A. Bachmann, G. Stern, J. Wildhaber, S. Buob, R. Schindel, R. Kraemer, U.P. Frey, M. Nelle, Development of the premature infant nose throat-model (PrINt-model): an upper airway replica of a premature neonate for the study of aerosol delivery, *Pediatr. Res.* 64 (2008) 141–146.
- [203] K.G. Schuepp, J. Jauernig, H.M. Janssens, H.A. Tiddens, D.A. Straub, R. Stangl, M. Keller, J.H. Wildhaber, *In vitro* determination of the optimal particle size for nebulized aerosol delivery to infants, *J. Aerosol Med.* 18 (2005) 225–235.
- [204] H.M. Janssens, J.C. De Jongste, W.C. Hop, H.A. Tiddens, Extra-fine particles improve lung delivery of inhaled steroids in infants: a study in an upper airway model, *Chest* 123 (2003) 2083–2088.
- [205] N.A. Ashammakhi, A. Elzagheid, Organ-on-a-chip: new tool for personalized medicine, *J. Craniofac. Surg.* (2018). <https://doi.org/10.1097/SCS.00000000000004604> (Epub ahead of print).
- [206] A. Mammoto, T. Mammoto, M. Kanapathipillai, C. Wing Yung, E. Jiang, A. Jiang, K. Lofgren, E.P. Gee, D.E. Ingber, Control of lung vascular permeability and endotoxin-induced pulmonary oedema by changes in extracellular matrix mechanics, *Nat. Commun.* 4 (2013) 1759.
- [207] T. Boudou, W.R. Legant, A. Mu, M.A. Borochin, N. Thavandiran, M. Radisic, P.W. Zandstra, J.A. Epstein, K.B. Margulies, C.S. Chen, A microfabricated platform to measure and manipulate the mechanics of engineered cardiac microtissues, *Tissue Eng. A* 18 (2012) 910–919.
- [208] A. Agarwal, Y. Farouz, A.P. Nesmith, L.F. Deravi, M.L. McCain, K.K. Parker, Micropatterning alginate substrates for *in vitro* cardiovascular muscle on a chip, *Adv. Funct. Mater.* 23 (2013) 3738–3746.
- [209] A. Grosberg, P.W. Alford, M.L. McCain, K.K. Parker, Ensembles of engineered cardiac tissues for physiological and pharmacological study: heart on a chip, *Lab Chip* 11 (2011) 4165–4173.
- [210] S.J. Park, M. Gazzola, K.S. Park, S. Park, V. Di Santo, E.L. Blevins, J.U. Lind, P.H. Campbell, S. Dauth, A.K. Capulli, F.S. Pasqualini, S. Ahn, A. Cho, H. Yuan, B.M. Maoz, R. Vijaykumar, J.W. Choi, K. Deisseroth, G.V. Lauder, L. Mahadevan, K.K. Parker, Phototactic guidance of a tissue-engineered soft-robotic ray, *Science* 353 (2016) 158–162.
- [211] J.U. Lind, T.A. Busbee, A.D. Valentine, F.S. Pasqualini, H. Yuan, M. Yadid, S.J. Park, A. Kotikian, A.P. Nesmith, P.H. Campbell, J.J. Vlassak, J.A. Lewis, K.K. Parker, Instrumented cardiac microphysiological devices via multimaterial three-dimensional printing, *Nat. Mater.* 16 (2017) 303–308.
- [212] J.O. Hardin, T.J. Ober, A.D. Valentine, J.A. Lewis, Microfluidic printheads for multimaterial 3D printing of viscoelastic inks, *Adv. Mater.* 27 (2015) 3279–3284.
- [213] K. Sun, T.S. Wei, B.Y. Ahn, J.Y. Seo, S.J. Dillon, J.A. Lewis, 3D printing of interdigitated Li-ion microbattery architectures, *Adv. Mater.* 25 (2013) 4539–4543.
- [214] J.S. Miller, K.R. Stevens, M.T. Yang, B.M. Baker, D.H. Nguyen, D.M. Cohen, E. Toro, A. Chen, P.A. Galie, X. Yu, R. Chaturvedi, S.N. Bhatia, C.S. Chen, Rapid casting of patterned vascular networks for perfusable engineered three-dimensional tissues, *Nat. Mater.* 11 (2012) 768–774.
- [215] D.B. Kolesky, K.A. Homan, M.A. Skylar-Scott, J.A. Lewis, Three-dimensional bioprinting of thick vascularized tissues, *Proc. Natl. Acad. Sci. U. S. A.* 113 (2016) 3179–3184.
- [216] G. Wang, M.L. McCain, L. Yang, A. He, F.S. Pasqualini, A. Agarwal, H. Yuan, D. Jiang, D. Zhang, L. Zangi, J. Geva, A.E. Roberts, Q. Ma, J. Ding, J. Chen, D.Z. Wang, K. Li, J. Wang, R.J. Wanders, W. Kulik, F.M. Vaz, M.A. Laflamme, C.E. Murray, K.R. Chien, R. I. Kelley, G.M. Church, K.K. Parker, W.T. Pu, Modeling the mitochondrial cardiomyopathy of Barth syndrome with induced pluripotent stem cell and heart-on-chip technologies, *Nat. Med.* 20 (2014) 616–623.
- [217] J.T. Hinson, A. Chopra, N. Nafissi, W.J. Polacheck, C.C. Benson, S. Swist, J. Gorham, L. Yang, S. Schafer, C.C. Sheng, A. Haghighi, J. Homsy, N. Hubner, G. Church, S.A. Cook, W.A. Linke, C.S. Chen, J.G. Seidman, C.E. Seidman, Heart disease: titin mutations in iPSC cells define sarcomere insufficiency as a cause of dilated cardiomyopathy, *Science* 349 (2015) 982–986.
- [218] A.G. Kleber, Y. Rudy, Basic mechanisms of cardiac impulse propagation and associated arrhythmias, *Physiol. Rev.* 84 (2004) 431–488.
- [219] I. Ostadalova, F. Kolar, B. Ostadal, V. Rohlicek, J. Rohlicek, J. Prochazka, Early postnatal development of contractile performance and responsiveness to Ca²⁺, verapamil and ryanodine in the isolated rat heart, *J. Mol. Cell. Cardiol.* 25 (1993) 733–740.
- [220] B.L. Laube, G. Sharpless, C. Shermer, O. Nasir, V. Sullivan, K. Powell, Deposition of albuterol aerosol generated by pneumatic nebulizer in the Sophia Anatomical Infant Nose-Throat (SAINT) model, *Pharm. Res.* 27 (2010) 1722–1729.
- [221] F. Pampaloni, E.G. Reynaud, E.H. Stelzer, The third dimension bridges the gap between cell culture and live tissue, *Nat. Rev. Mol. Cell Biol.* 8 (2007) 839–845.
- [222] P.A. Kenny, G.Y. Lee, C.A. Myers, R.M. Neve, J.R. Semeiks, P.T. Spellman, K. Lorenz, E. H. Lee, M.H. Barcellos-Hoff, O.W. Petersen, J.W. Gray, M.J. Bissell, The morphologies of breast cancer cell lines in three-dimensional assays correlate with their profiles of gene expression, *Mol. Oncol.* 1 (2007) 84–96.

- [223] Y. Zhao, R. Yao, L. Ouyang, H. Ding, T. Zhang, K. Zhang, S. Cheng, W. Sun, Three-dimensional printing of Hela cells for cervical tumor model *in vitro*, *Biofabrication* 6 (2014), 035001.
- [224] F. Xu, J. Celli, I. Rizvi, S. Moon, T. Hasan, U. Demirci, A three-dimensional *in vitro* ovarian cancer coculture model using a high-throughput cell patterning platform, *Biotechnol. J.* 6 (2011) 204–212.
- [225] W. Zhu, B. Holmes, R.L. Glazer, L.G. Zhang, 3D printed nanocomposite matrix for the study of breast cancer bone metastasis, *Nanomedicine* 12 (2016) 69–79.
- [226] B. Desoize, J. Jardillier, Multicellular resistance: a paradigm for clinical resistance? *Crit. Rev. Oncol. Hematol.* 36 (2000) 193–207.
- [227] L.W. Dunne, Z. Huang, W. Meng, X. Fan, N. Zhang, Q. Zhang, Z. An, Human decellularized adipose tissue scaffold as a model for breast cancer cell growth and drug treatments, *Biomaterials* 35 (2014) 4940–4949.
- [228] M.M. Gottesman, T. Fojo, S.E. Bates, Multidrug resistance in cancer: role of ATP-dependent transporters, *Nat. Rev. Cancer* 2 (2002) 48–58.
- [229] B. Weigelt, M.J. Bissell, Unraveling the microenvironmental influences on the normal mammary gland and breast cancer, *Semin. Cancer Biol.* 18 (2008) 311–321.
- [230] D.C. Duffy, J.C. McDonald, O.J. Schueller, G.M. Whitesides, Rapid prototyping of microfluidic systems in poly(dimethylsiloxane), *Anal. Chem.* 70 (1998) 4974–4984.
- [231] J.C. McDonald, D.C. Duffy, J.R. Anderson, D.T. Chiu, H. Wu, O.J. Schueller, G.M. Whitesides, Fabrication of microfluidic systems in poly(dimethylsiloxane), *Electrophoresis* 21 (2000) 27–40.
- [232] K.B. Anderson, S.Y. Lockwood, R.S. Martin, D.M. Spence, A 3D printed fluidic device that enables integrated features, *Anal. Chem.* 85 (2013) 5622–5626.
- [233] H.W. Boucher, G.H. Talbot, J.S. Bradley, J.E. Edwards, D. Gilbert, L.B. Rice, M. Scheld, B. Spellberg, J. Bartlett, Bad bugs, no drugs: no ESKAPE! An update from the infectious diseases society of america, *Clin. Infect. Dis.* 48 (2009) 1–12.
- [234] S. Glatzel, M. Hezwani, P.J. Kitson, P.S. Gromski, S. Schürer, L. Cronin, A portable 3D printer system for the diagnosis and treatment of multidrug-resistant bacteria, *Chem* 1 (2016) 494–504.
- [235] D.R. Ian Gibson, Brent Stucker, additive manufacturing technologies: 3D printing, rapid prototyping, and direct digital manufacturing, 2nd edition, Johns. Matthey Technol. Rev. 59 (2015) 193–198.
- [236] J.H. Lin, Species similarities and differences in pharmacokinetics, *Drug Metab. Dispos.* 23 (1995) 1008–1021.
- [237] H. Kimura, T. Yamamoto, H. Sakai, Y. Sakai, T. Fujii, An integrated microfluidic system for long-term perfusion culture and on-line monitoring of intestinal tissue models, *Lab Chip* 8 (2008) 741.
- [238] I.T. Ozbolat, W. Peng, V. Ozbolat, Application areas of 3D bioprinting, *Drug Discov. Today* 21 (2016) 1257–1271.
- [239] I.T. Ozbolat, Scaffold-based or scaffold-free bioprinting: competing or complementing approaches? *J. Nanotechnol. Eng. Med.* 6 (2015), 024701.
- [240] S.N. Bhatia, D.E. Ingber, Microfluidic organs-on-chips, *Nat. Biotechnol.* 32 (2014) 760–772.
- [241] D. Huh, B.D. Matthews, A. Mammoto, M. Montoya-Zavala, H.Y. Hsin, D.E. Ingber, Reconstituting organ-level lung functions on a chip, *Science* 328 (2010) 1662–1668.
- [242] M. Tsai, A. Kita, J. Leach, R. Rounsevell, J.N. Huang, J. Moake, R.E. Ware, D.A. Fletcher, W.A. Lam, *In vitro* modeling of the microvascular occlusion and thrombosis that occur in hematologic diseases using microfluidic technology, *J. Clin. Investig.* 122 (2012) 408–418.
- [243] C.L. Walsh, B.M. Babin, R.W. Kasinskas, J.A. Foster, M.J. McGarry, N.S. Forbes, A multipurpose microfluidic device designed to mimic microenvironment gradients and develop targeted cancer therapeutics, *Lab Chip* 9 (2009) 545–554.
- [244] K.-Y. Jang, K.-Y. Suh, A multi-layer microfluidic device for efficient culture and analysis of renal tubular cells, *Lab Chip* 10 (2010) 36–42.
- [245] J.H. Sung, C. Kam, M.L. Shuler, A microfluidic device for a pharmacokinetic–pharmacodynamic (PK–PD) model on a chip, *Lab Chip* 10 (2010) 446.
- [246] I. Maschmeyer, A.K. Lorenz, K. Schimek, T. Hasenberger, A.P. Ramme, J. Hübner, M. Lindner, C. Drewell, S. Bauer, A. Thomas, N.S. Sambo, F. Sonntag, R. Lauster, U. Marx, A four-organ-chip for interconnected long-term co-culture of human intestine, liver, skin and kidney equivalents, *Lab Chip* 15 (2015) 2688–2699.
- [247] Y.-s. Torisawa, C.S. Spina, T. Mammoto, A. Mammoto, J.C. Weaver, T. Tat, J.J. Collins, D.E. Ingber, Bone marrow-on-a-chip replicates hematopoietic niche physiology *in vitro*, *Nat. Methods* 11 (2014) 663–669.
- [248] I.T. Ozbolat, M. Hospodiuk, Current advances and future perspectives in extrusion-based bioprinting, *Biomaterials* 76 (2016) 321–343.
- [249] S. Knowlton, S. Tasoglu, A bioprinted liver-on-a-chip for drug screening applications, *Trends Biotechnol.* 34 (2016) 681–682.
- [250] X. Ma, X. Qu, W. Zhu, Y.-S. Li, S. Yuan, H. Zhang, J. Liu, P. Wang, C.S.E. Lai, F. Zanella, G.-S. Feng, F. Sheikh, S. Chien, S. Chen, Deterministically patterned biomimetic human iPSC-derived hepatic model *via* rapid 3D bioprinting, *Proc. Natl. Acad. Sci.* 113 (2016) 2206–2211.
- [251] R. Chang, K. Emami, H. Wu, W. Sun, Biofabrication of a three-dimensional liver micro-organ as an *in vitro* drug metabolism model, *Biofabrication* 2 (2010), 045004.
- [252] J.E. Snyder, Q. Hamid, C. Wang, R. Chang, K. Emami, H. Wu, W. Sun, Bioprinting cell-laden matrigel for radioprotection study of liver by pro-drug conversion in a dual-tissue microfluidic chip, *Biofabrication* 3 (2011), 034112.
- [253] Y.S. Zhang, A. Arneri, S. Bersini, S.-R. Shin, K. Zhu, Z. Goli-Malekabadi, J. Aleman, C. Colosi, F. Busignani, V. Dell’Erba, C. Bishop, T. Shupe, D. Demarchi, M. Moretti, M. Rasponi, M.R. Dokmeci, A. Atala, A. Khademhosseini, Bioprinting 3D microfibrillar scaffolds for engineering endothelialized myocardium and heart-on-a-chip, *Biomaterials* 110 (2016) 45–59.
- [254] K.A. Homan, D.B. Kolesky, M.A. Skylar-Scott, J. Herrmann, H. Obuobi, A. Moisan, J.A. Lewis, Bioprinting of 3D convoluted renal proximal tubules on perfusable chips, *Sci. Rep.* 6 (2016).
- [255] X. Dai, C. Ma, Q. Lan, T. Xu, 3D bioprinted glioma stem cells for brain tumor model and applications of drug susceptibility, *Biofabrication* 8 (2016) 045005.
- [256] T. Rozario, D.W. DeSimone, The extracellular matrix in development and morphogenesis: a dynamic view, *Dev. Biol.* 341 (2010) 126–140.
- [257] T.K. Merceron, S.V. Murphy, Hydrogels for 3D bioprinting applications, *Essentials of 3D Biofabrication and Translation*, Elsevier 2015, pp. 249–270.
- [258] J. Malda, J. Visser, F.P. Melchels, T. Jüngst, W.E. Hennink, W.J.A. Dhert, J. Groll, D.W. Huttmacher, 25th anniversary article: engineering hydrogels for biofabrication, *Adv. Mater.* 25 (2013) 5011–5028.
- [259] D.G. Nguyen, J. Funk, J.B. Robbins, C. Crogan-Grundy, S.C. Presnell, T. Singer, A.B. Roth, Bioprinted 3D primary liver tissues allow assessment of organ-level response to clinical drug induced toxicity *in vitro*, *PLoS One* 11 (2016), e0158674.
- [260] M. Matsusaki, K. Sakae, K. Kadowaki, M. Akashi, Three-dimensional human tissue chips fabricated by rapid and automatic inkjet cell printing, *Adv. Healthc. Mater.* 2 (2013) 534–539.
- [261] S.M. King, S.C. Presnell, D.G. Nguyen, Abstract 2034: development of 3D bioprinted human breast cancer for *in vitro* drug screening, *Proceedings: AACR Annual Meeting 2014*, 74, April 5–9, 2014, p. 2034, San Diego, CA.
- [262] Q. Gu, E. Tomaskovic-Crook, R. Lozano, Y. Chen, R.M. Kapsa, Q. Zhou, G.G. Wallace, J. M. Crook, Functional 3D neural mini-tissues from printed gel-based bioink and human neural stem cells, *Adv. Healthc. Mater.* 5 (2016) 1429–1438.
- [263] G. Souza, H. Tseng, J. Gage, A. Mani, P. Desai, F. Leonard, A. Liao, M. Longo, J. Refuerzo, B. Godin, Magnetically bioprinted human myometrial 3D cell rings as a model for uterine contractility, *Int. J. Mol. Sci.* 18 (2017) 683.
- [264] CDC, Disinfection & sterilization guidelines | guidelines library | infection control | CDC, <https://www.cdc.gov/infectioncontrol/guidelines/disinfection/index.html> 2017, Accessed date: 20 November 2017.
- [265] K.P. Valente, S. Khetani, A.R. Kolahchi, A. Sanati-Nezhad, A. Suleman, M. Akbari, Microfluidic technologies for anticancer drug studies, *Drug Discov. Today* 22 (11) (2017) 1654–1670.
- [266] J.R. Tumbleston, D. Shirvanyants, N. Ermoshkin, R. Januszewicz, A.R. Johnson, D. Kelly, K. Chen, R. Pinschmidt, J.P. Rolland, A. Ermoshkin, E.T. Samulski, J.M. DeSimone, Continuous liquid interface production of 3D objects, *Science* 347 (2015) 1349–1352.
- [267] 3DS, 3D systems’ Fab-grade 3D printers break the speed barrier surpassing traditional injection molding | 3D Systems, @3dsystems, (Accessed on) <https://www.3dsystems.com/press-releases/3d-systems-fab-grade-3d-printers-break-speed-barrier-surpassing-traditional-injection> 2017.
- [268] NAMIC, Welcome to NAMIC | NAMIC, <http://namic.sg/> 2018, Accessed date: 20 November 2017.
- [269] AMAT, Additive manufacturing association of Taiwan (AMAT), <http://www.3dp.org.tw/> 2017, Accessed date: 20 November 2017.
- [270] ARC Research Hub to transform manufacturing through 3D metal printing | Australian Research Council, <http://www.arc.gov.au/news-media/media-releases/arc-research-hub-transform-manufacturing-through-3d-metal-printing> 2014, Accessed date: 20 November 2017.
- [271] Additive manufacturing | Department of Materials Science and Engineering, <http://www.matse.psu.edu/research-topics/additive-manufacturing> 2018, Accessed date: 4 April 2017.
- [272] Additive manufacturing | Office of Advanced Engineering Education, <https://advancedengineering.umd.edu/additive-manufacturing> 2018, Accessed date: 4 April 2018.
- [273] W.M. Keck Center for 3D Innovation, <http://keck.utep.edu> 2018, Accessed date: 4 April 2018.
- [274] A. Goyanes, M. Scarpa, M. Kamlow, S. Gaisford, A.W. Basit, M. Orlu, Patient acceptability of 3D printed medicines, *Int. J. Pharm.* 530 (2017) 71–78.
- [275] APRECI, Why choose SPRITAM, <https://www.spritam.com/#/hcp/about-spritam/why-choose-spritam> 2017, Accessed date: 12 October 2017.
- [276] FDA, The drug development process - step 3: clinical research, FDA - Office of the Commissioner, (Accessed on) https://www.fda.gov/ForPatients/Approvals/Drugs/ucm405622.htm#Clinical_Research_Phase_Studies 2017.
- [277] UK national strategy for additive manufacturing/3D Printing, <http://www.amnationalstrategy.uk/wp-content/uploads/2015/2005/UK-AM-National-Strategy-Update-Report-2013-v2012.pdf> 2017, Accessed date: 20 November 2017.
- [278] Costs and cost effectiveness of additive manufacturing, U. S. Department of Commerce <https://www.nist.gov/publications/costs-and-cost-effectiveness-additive-manufacturing> 2014, Accessed date: 23 March 2018.
- [279] Y.K. Son, A cost estimation model for advanced manufacturing systems, *Int. J. Prod. Res.* 29 (1991) 441–452.